ORNL/NRC/LTR-99/27

Contract Program or Project Title:	Heavy-Section Steel Technology (HSST) Program Engineering Technology Division
Subject of this Document:	Technical Basis for Statistical Models of Extended K_{Ic} and K_{Ia} Fracture Toughness Databases for RPV Steels
Type of Document:	Letter Report
Authors:	K. O. Bowman P. T. Williams
Date of Document:	February 2000
Responsible NRC Individual and NRC Office or Division	S. N. M. Malik Division of Engineering Technology Office of Nuclear Regulatory Research

Prepared for the
U. S. Nuclear Regulatory Commission
Washington, D.C. 20555-0001
Under Interagency Agreement DOE 1886-N011-9B
NRC JCN No. B0119

OAK RIDGE NATIONAL LABORATORY
Oak Ridge, Tennessee 37831-8056
managed by
LOCKHEED MARTIN ENERGY RESEARCH CORPORATION
for the
U. S. DEPARTMENT OF ENERGY
under Contract No. DE-AC05-96OR22464

ORNL/NRC/LTR-99/27

Technical Basis for Statistical Models of Extended K_{Ic} and K_{Ia} Fracture Toughness Databases for RPV Steels

K. O. Bowman

Computer Science and Mathematics Division

P. T. Williams

Computational Physics and Engineering Division

Oak Ridge National Laboratory
Oak Ridge, Tennessee

Manuscript Completed – November 1999
Date Published – February 2000

Prepared for the
U.S. Nuclear Regulatory Commission
Office of Nuclear Regulatory Research
Under Interagency Agreement DOE 1886-N011-9B

NRC JCN No. B0119

OAK RIDGE NATIONAL LABORATORY
Oak Ridge, Tennessee 37831-8056
managed by
LOCKHEED MARTIN ENERGY RESEARCH CORPORATION
for the
U.S. DEPARTMENT OF ENERGY
under Contract No. DE-AC05-96OR22464

NOMENCLATURE

a	location parameter of Weibull distribution
b	scale parameter of Weibull distribution
c	shape parameter of Weibull distribution
$(\hat{a},\hat{b},\hat{c})$	maximum-likelihood estimators
(a_3^*,b_3^*,c_3^*)	moment estimators for a 3-parameter Weibull distribution
(a_2^*,b_2^*)	moment estimators for a 2-parameter Weibull distribution
(a_2^{**},b_2^{**})	almost unbiased moment estimators for a 2-parameter Weibull distribution
$\sqrt{b_1}$	sample moment coefficient of skewness
K_{Ia}	plane-strain crack-arrest fracture toughness
K_{Ic}	plane-strain static-initiation fracture toughness
K_I	applied Mode I stress-intensity factor
m_1'	1st crude moment of the sample = sample mean, $\bar{x}$
m_2	2nd central moment of the sample about the sample mean
n, N	sample size
p	probability level
RT_{NDT}	nil-ductility-transition temperature
T	test temperature
$\bar{T}$	$(\overline{T-RT_{NDT}})$ = mean normalized temperature of dataset
ΔT	$(T-RT_{NDT})$ = normalized temperature
$t(\underline{m})$	moment function
w	Weibull density
$x_{0.5}$	median K_{Ia} or K_{Ic} at 50% cumulative probability of failure
x_p	K_{Ia} or K_{Ic} at $p^{th}\times 100\%$ cumulative probability of failure
$\bar{x}$	sample mean
$\sqrt{\beta_1}$	moment coefficient of skewness
β_2	moment coefficient of kurtosis
Γ	Euler's gamma function
λ_1	$=\Gamma(1+1/c)$
λ_2	$=\Gamma(1+2/c)$
μ_1'	1st central moment of the population = population mean
μ_2	2nd central moment of the population = population variance
μ_3	3rd central moment of the population
μ_4	4th central moment of the population
π_s^*/π_s	Padé sequences
π_s^*,π_s	polynomials in N of degrees s-1 and s , respectively
σ,σ^2	standard deviation and variance of the population
ζ	Riemann zeta function

Technical Basis for Statistical Models of Extended K_{Ic} and K_{Ia} Fracture Toughness Databases for RPV Steels

K. O. Bowman

Computer Science and Mathematics Division
Oak Ridge National Laboratory
P. O. Box 2008
Oak Ridge, TN 37831-6367

P. T. Williams

Computational Physics and Engineering Division
Oak Ridge National Laboratory
P. O. Box 2009
Oak Ridge, TN, 37831-8056

ABSTRACT: This report presents the technical basis for new statistical representations of extended fracture toughness K_{Ic} and K_{Ia} databases. This effort was performed by the Heavy Section Steel Technology (HSST) program at ORNL in the context of a probabilistic methodology appropriate for use in an effort by the Nuclear Regulatory Commission (NRC) to update its regulatory guidance for pressurized-thermal-shock (PTS) transients. The representations for K_{Ic} and K_{Ia} were developed through rigorous statistical procedures applied to extended fracture toughness databases for reactor pressure vessel (RPV) steels. A 2-parameter Weibull distribution, with the parameters calculated by the *Method of Moments* point-estimation technique, forms the basis for the new statistical models. Results of these analyses are reported in both graphical and equation form.

1. INTRODUCTION

The Heavy-Section Steel Technology (HSST) Program at ORNL has produced new statistical representations for the two properties, the plane-strain static initiation toughness K_{Ic} and the plane-strain crack-arrest toughness K_{Ia}, used to characterize the fracture toughness of reactor pressure vessel (RPV) steels. This effort was performed in the context of a probabilistic methodology appropriate for use in an overall effort by the Nuclear Regulatory Commission (NRC) to update its regulatory guidance for pressurized-thermal-shock (PTS) transients. These new representations for K_{Ic} and K_{Ia} were developed through the application of rigorous statistical procedures applied to an extended fracture toughness database for RPV steels.

Developments of the extended database and the new statistical representations for K_{Ic} and K_{Ia} have been accomplished through the following steps:

1. A survey was conducted to identify available K_{Ic} data from pressure vessel steels that could augment the amended database of EPRI NP-719-SR [1] published by Nanstad et al. [2]. The EPRI report [1] includes the data used for construction of the original K_{Ic} fracture toughness curve given in Appendix A, Section XI, of the ASME Boiler and Pressure Vessel Code [3]. The candidate K_{Ic} data were evaluated using specific requirements that included the following: (a) satisfaction of validity requirements given in ASTM Standard E 399 [4], (b) availability in tabular form and (c) availability of the reference nil-ductility transition temperature (RT_{NDT}) determined according to ASME Code requirements [5].

2. A similar survey was carried out to compile an extended K_{Ia} database that would include those data given in the EPRI report [1]. Because the ASTM Standard E 1221 [6] for K_{Ia} is relatively new, many of the existing data were generated prior to adoption of the standard. Thus, it was agreed that candidate K_{Ia} data would be evaluated in a more general context, including engineering judgment of acknowledged experts and general acceptance by the nuclear technology community.

3. Analytical tools (computer codes, etc.) were assembled to implement statistical approaches for interpreting the K_{Ic} and K_{Ia} data. Expert professional statisticians were brought into the study to ensure that suitable methods were being applied to the data.

4. Statistical analyses of the K_{Ic} and K_{Ia} data were performed to establish trend and confidence curves. Results of these analyses were reported in both graphical and equation form.

This report presents the technical basis for new statistical representations of the extended K_{Ic} and K_{Ia} databases. The results of Steps 1 and 2 of the study are given in Section 2 with a description of the extended K_{Ic} and K_{Ia} databases. In Section 3, the analytical approach to developing the statistical representation of the K_{Ic} and K_{Ia} databases is discussed, followed in Section 4 by a summary of its application to K_{Ic} and K_{Ia} where the resulting statistical models are presented in both graphical and analytical form. Conclusions are summarized in Section

5. A complete tabulation of the extended K_{Ic} and K_{Ia} databases is given in Appendix A, and the results of a preliminary regression analysis of the original EPRI K_{Ic} database are described in Appendix B.

A companion HSST report [7] describes an implementation of the K_{Ic} and K_{Ia} statistical models into the FAVOR probabilistic fracture mechanics program [8]. The FAVOR implementation of the new models provides a statistically-derived alternative to current PTS assessment methodology. (The latter methodology utilizes a fracture toughness model that defines the "mean minus 2σ" curve as the ASME K_{Ic} curve [8]). In ref. [7], results obtained from applying the new FAVOR implementation to PTS assessments of selected RPVs are compared to those generated using the current methodology.

2. EXTENDED K_{Ic} AND K_{Ia} DATABASES

2.1 K_{Ic} Database

In 1978, the ASME Section XI Task Group on Flaw Evaluation published an EPRI Special Report [1], which includes the experimental fracture toughness data used in the construction of the ASME K_{Ic} and K_{Ia} curves. In 1993, Nanstad et al. [2] at ORNL carried out a study to review the technical bases applied in the establishment of the ASME K_{Ic} curve. That study compared the data reported in refs. [1, 9 - 11] to the graphical plots in the EPRI report and in Appendix A of Section XI of the ASME code [3]. Errors were found in the EPRI NP-719-SR tabular data that were corrected, and an amended database was generated and reported in ref. [2].

The EPRI database (consisting of 171 K_{Ic} data points) includes data from 11 materials using compact tension C(T) and wedge-open-loading (WOL) test specimens ranging in size from 1T to 11T as summarized in Table 1. Figure 1 (as adapted from ref. [12]) gives a visual indication of the range of C(T) specimen sizes employed in constructing the database, and Fig. 2 shows how the specimen sizes are distributed across the normalized temperature range of $-385°F = (T - RT_{NDT}) = 50°F$. All 171 K_{Ic} data points are plotted in Fig. 3a as a function of test temperature. A frequency histogram and cumulative frequency plot of the data points distributed across the test temperature range are shown in Figs. 3b and 3c, respectively. The same data in Fig. 3 is replotted in Fig. 4 with the test temperature being normalized by the reference nil-ductility transition temperature, RT_{NDT}. The ASME K_{Ic} curve (from Figure A-4200-1 of ref. [3]) is plotted in Fig. 4a as a solid line; the dashed line in Fig. 4a is an extension of the ASME K_{Ic} curve using the equation given in ref. [3]. In Fig. 4b, the highest frequency (i.e., the largest number of replicate tests) occurs at $(T - RT_{NDT}) = -170°F$. Note in Fig. 4c, that approximately 70 percent of the EPRI database occurs at normalized temperatures of $(T\text{-}RT_{NDT}) < -100°F$. In Figure A-4200-1 [3], the plotted ASME K_{Ic} curve extends from $-100°F = (T - RT_{NDT}) = +100°F$; therefore, only 30 percent of the 171 point EPRI database falls within the range of normalized temperatures covered by the lower bound curve in the ASME Code.

At ORNL, a survey was conducted to identify available K_{Ic} data generated more recently from pressure vessel steels that could augment the amended EPRI database published by Nanstad et al. [2]. Fracture toughness data subsequently included in the extended database

had to satisfy the specific validity requirements of ASTM E 399 [4]. That survey produced 83 K_{Ic} fracture toughness values (obtained from refs. [13-17]) that are plotted in Fig. 5 as a function of normalized temperature $(T - RT_{NDT})$; Table 1 provides additional details concerning the extended dataset, and the chemistry and heat treatment of the principal materials in the dataset are given in Table 2.

The extended K_{Ic} database, compiled from the amended EPRI data and from the ORNL survey, provided a total of 254 fracture toughness data points for input to the statistical model development described in Section 3 and applied in Section 4. A plot of the extended K_{Ic} database versus $T - RT_{NDT}$ is given in Fig. 6; the complete tabulation of the database is included in Appendix A.

2.2 K_{Ia} Database

The ORNL survey of available K_{Ia} data produced an additional 62 fracture toughness values [18-20] that were used to augment the 50 K_{Ia} data points [21, 22] obtained from EPRI NP-719-SR [1]. Sources and summary details of the additional data are identified in Table 3. A plot of the original EPRI dataset is given in Fig. 7; the additional K_{Ia} data are plotted in Fig. 8; and the combined dataset is presented in Fig. 9. The extended database consisting of 112 fracture toughness values provided the input to the statistical model development for K_{Ia} described in Section 4. A complete tabulation of the K_{Ia} database is included in Appendix A.

3. DEVELOPMENT OF THE STATISTICAL MODEL

3.1 Background

The Weibull distribution, introduced just over a half-century ago [23-24], has a long history in the fields of fatigue and fracture mechanics. The original applications involved the breaking strength of materials (e.g., cotton fibers) and the yield strength of steels [25-26]. Considering its pedigree in fracture mechanics, it is perhaps logical that the Weibull distribution should be the primary choice as the basis for the statistical model in the present study. Among candidate models that could also be considered are the 3-parameter gamma distribution, the lognormal distribution, and others.

3.2 The Weibull Density

In the case of the Weibull distribution, there are three parameters to estimate, and these refer to the location, a, of the random variate, the scale, b, of the random variate, and most importantly, the shape parameter, c. The density (see Fig. 10) is given by

$$w(x|a,b,c) = \frac{c}{b} \; y^{c-1} \; \exp\left(-y^{c}\right), \; (y = (x-a)/b, \;\; x > a, \;\; b,c > 0) \tag{1}$$

The Weibull density is derived from its distribution function

$$\Pr(X < x) = 1 - \exp(-y^{c}) \tag{2}$$

When the shape parameter, c, is small, the density is reverse J-shaped with a high probability for c in the vicinity of $c = 0^{+}$. When $c = 1$, the density becomes the exponential with moderate J-shape (skewness = 2 and kurtosis = 9), and as c increases the conventional bell-shape is reached.

3.3 Moments and Moment Ratios

The moments and moment ratio provide further insight into the Weibull model. The mean and variance are

$$\text{Mean:} \quad \mu_1'(x \mid a, b, c) = a + b \;\; \Gamma(1+1/c)$$
$$\text{Variance:} \quad \mu_2(x \mid a, b, c) = b^2\{\Gamma(1+2/c) - \Gamma^2(1+1/c)\}$$

where Γ is Euler's gamma function. Skewness, $\sqrt{\beta_1}$, as a moment ratio,

$$\alpha_1 = \sqrt{\beta_1} = \mu_3(x \mid a, b, c)/[\mu_2(x \mid a, b, c)]^{3/2} \quad ,$$

represents a measure of asymmetry. The kurtosis, β_2, as a moment ratio is

$$\beta_2 = \mu_4(x \mid a, b, c)/[\mu_2(x \mid a, b, c)]^2 \quad .$$

In general, the moments of a Weibull distribution can be expressed by

$$\mu_s(x \mid a, b, c) = b^s \int_0^\infty [t^{1/c} - \Gamma(1+1/c)]^s \exp(-t) \;\; dt \qquad (s = 1, 2, \cdots)$$

For example, the third moment is

$$\mu_3(x \mid a, b, c) = b^3\left[\Gamma(1+3/c) - 3\Gamma(1+2/c)\Gamma(1+1/c) + 2\Gamma^3(1+1/c)\right] \quad .$$

It is interesting to note that for the standard case ($a = 0$, $b = 1$):

- The mean , μ_1', lies between 0 and 1 and is asymptotic to 1.0 as $c \to 8$.
- The standard deviation, σ, decreases from unity, and $\sigma^2(x \mid a, b, c) \approx \pi^2/(6c^2)$ as $c \to 8$.

- The skewness, $\sqrt{\beta_1}$, decreases as c increases, is zero for $c = 3.602$ and asymptotic to -1.13 as $c \rightarrow 8$.

- The kurtosis, β_2, decreases from 9 at $c = 1$ to 2.71 approximately at $c = 3.2$ and then increases to an asymptotic 5.4 as $c \rightarrow 8$.

Table 4 and Fig. 11 present the mean, standard deviation, skewness, and kurtosis of Weibull densities for the standard case (a =0, b = 1).

3.4 Point Estimation Procedures

3.4.1 Maximum Likelihood Method

The 3-parameter Weibull case has been studied by Bowman and Shenton [27]. In ref. [27], it was found that the moments of the maximum likelihood estimators $\hat{a}$, $\hat{b}$, $\hat{c}$ for location, scale, and shape, respectively, only exist for specific values of c. For example, the existence of the mean requires that $c > 1$; the existence of the variance requires $c > 2$; the existence of the skewness requires $c > 3$; and the existence of the kurtosis requires $c > 4$. These requirements apply to all three maximum likelihood estimators. Thus if $2 < c < 3$, as is the case for some of the data in the extended K_{Ic} database, then only the means and variances exist. In addition, there is the problem of sample ($x_1, x_2, \ldots, x_N$) size N. If inferences are to be made concerning percentage points for a, b, c in the populations concerned, then N should be 250 or even 500 to achieve sharp enough intervals for each parameter. This aspect of the maximum likelihood method directed attention to other methods of point estimation.

3.4.2 The Method of Moments

Denoting the moment estimators for the 3-parameter case by a_3*, b_3*, and c_3*, we have

$$c_3^* = \frac{4.104683 - 1.148513\sqrt{b_1} + 0.441326 \quad b_1 - 0.053025(\sqrt{b_1})^3}{\sqrt{b_1} + \lambda} \tag{3}$$

where $\sqrt{b_1}$ is the sample skewness and, in terms of the Riemann zeta function,

$$\lambda = 2\zeta(3)/[\zeta(2)]^{3/2} = 1.139547.$$

The expression in Eq. (3) was found by regression analysis using the fact that for the Weibull variable

$$\sqrt{\beta_1(x)} \approx -\lambda \quad (c \to \infty).$$

The error involved in Eq. (3) is less than approximately 4% for $c > 1.1$. For the scale parameter

$$b_3^* = \sqrt{m_2/[\Gamma(1+2/c_3^*) - \Gamma^2(1+1/c_3^*)]}$$

where $m_2 = \sum\left(x_j - \bar{x}\right)^2 / N$ is the second central moment of the sample about $\bar{x}$, where $\bar{x} = \sum_{j=1}^{N} x_j / N$ is the mean of the sample. Finally, for the location parameter,

$$a_3^* = m_1' - b_3^* \ \Gamma(1+1/c_3^*) \ .$$

The subscripts on the estimators are used to indicate that the 3-parameter case is indicated.

Approximate distributions of these estimators may be derived from simulations studies. Examples are given in Table 5. For the simulation study in Table 5, the simulation cycle was 50,000, in batches of 10,000. Power series in terms of N^{-1} may be set up for the moments of a_3^* and b_3^*; however, the main point to note is that for the 3-parameter case samples as small as 20 will be linked to excessive values of the skewness and kurtosis as discussed in [28].

3.5 The Problem of the Location Parameter, *a*

If the shape parameter, c, is given, then one may consider the 2-parameter case, namely

$$w(x \mid a, b) = \frac{c}{b} y^{c-1} \exp(-y^c),$$

where $y = (x-a)/b$. From Sect. 3.4.2, we have the moment estimator for the scale parameter as

$$b_2^* = \sqrt{m_2 / [\Gamma(1+2/c) - \Gamma^2(1+1/c)]} \quad ,$$

and for the location parameter

$$a_2^* = m_1' - b_2^* \ \Gamma(1+1/c) \quad .$$

The moment estimators for the 2-parameter case are much simpler than for the 3-parameter model. For the latter, c_3^* is linked to both the scale and shape estimators. These linkages account for the increased complexity in the 3-parameter case.

Moments of b_2^* and a_2^* may be simulated by generating Weibull random variables (see Table 6). The skewness is quite small ($N \geq 15$), and acceptable percentage points may be derived by the procedures given in Bowman and Shenton [29-30]. For the simulations in Table 6, a cycle of 50,000 was used. For example, in the case of sample size $N = 50$, a resulting 250,000 random numbers from a Weibull distribution were used. Moments of these were also computed to ensure that the samples were taken from the given Weibull distribution. The *NAG* library [31] subroutine for random numbers from a Weibull distribution was used in the simulation.

A check on the above procedure is needed. Moments of sample moments or sample moment functions can be developed using Padé approximants based on infinite series. Thus a moment function $t(\underline{m})$, such as $\sqrt{m_2}$, $\sqrt{b_1}$, b_2, etc., may be expanded as

$$t(\underline{m}) = t_0 + t_1 / N + t_2 / N^2 \cdots \ (N \to \infty),$$

where $(t_s), s = 0,1,\cdots,$ are not functions of N. Padé sequences $\{ \ \pi_s^* / \pi_s \ \}$, where $\pi_s{}^*$ and π_s are polynomials in N of degrees s-1 and s , respectively, can be derived [32-34]. An example of a moment series is given in Table 7; the series possibly diverges and loss of accuracy may occur for terms n^{-s}, $s > 12$. A comparison of assessments by simulation and Padé for a_2* and b_2* are given in Table 8; some percentage points are also included. The agreement between the Padé and simulations assessment is most satisfactory, exceeding $N =$ 50.

Note that a_2* is positively biased and b_2* is negatively biased. Note also that moments have been set up under the assumption that $a = 0$, $b = 1$, i.e., the standard case. These moments may be converted to $a = a_0$, $b = b_0$ as follows:

for the mean

$$\mu_1'(a^* \mid a_0, b_0) = a_0 + b_0 \mu_1'(a^* \mid 0,1)$$
$$\mu_1'(b^* \mid a_0, b_0) = b_0 \mu_1'(b^* \mid 0,1)$$

and for the variance

$$\mu_2(a^* \mid a_0, b_0) = b_0{}^2 \mu_2(a^* \mid 0,1)$$
$$\mu_2(b^* \mid a_0, b_0) = b_0{}^2 \mu_2(b^* \mid 0,1)$$

4. APPLICATION OF THE STATISTICAL MODEL

4.1 The K_{Ic} Model

In the current study, the problem was to apply a Weibull model to the extended K_{Ic} database in which the test temperature has been normalized by the reference-nil-ductility-transition temperature, RT_{NDT}. A previous study [35] investigated the EPRI K_{Ic} database in the context of the *Master Curve* [36-38] where the test temperature is normalized by the reference temperature, T_0, and size corrections are applied to the toughness data to allow the comparison of data from a range of specimen sizes. A Weibull distribution is assumed in ref. [38] in which the shape parameter is fixed at 4 and the location parameter is fixed at the experimentally-determined value of 18.2 ksi-√in. (20 MPa-√m). The shape parameter of 4 is derived [36] from a theoretical treatment of cleavage initiation in which "weakest-link" mechanisms are assumed to dominate the scatter in the data at a given test temperature. This assumption allows a relationship to be developed between the probability of failure by cleavage and the stress and strain fields ahead of the crack front as characterized by the applied stress-intensity factor K_I. When two parameters are fixed, the Weibull model becomes a 1-parameter Weibull distribution in which the density is described by

$$w(x \mid b) = \frac{4}{b} y^3 \exp(-y^4) \quad (y = (x - 18.2)/b, x > 18.2; b > 0)$$

where in [38] $b = (K_0 - K_{\min})$ and $K_{\min}$ = 18.2 ksi-√in. (20 MPa-√m). With the 1-parameter Weibull distribution, the scale parameter, b or specifically K_0, is estimated in [38] with a maximum likelihood point estimator.

Due to the heterogeneity of the K_{Ic} database with its range of materials and specimen sizes (in some cases within the same grouping of replicate tests when normalized by RT_{NDT}), it was not clear that the theoretical treatment developed in previous studies necessarily accounted for all of the dominant modes that produced the observed scatter in the data. The decision was therefore taken to develop a strictly statistical model to characterize the trends and scatter in the extended K_{Ic} database.

The recent study by Bowman and Shenton [27] showed that for the asymptotic moment profile of maximum likelihood estimators to exist, the shape parameter c must be greater than 4. Furthermore, sample sizes at a single normalized temperature must be greater than approximately 250. It is, therefore, not feasible to attempt to develop a full 3-parameter Weibull model with the small sample sizes in either the K_{Ic} or K_{Ia} databases. In the following, maximum likelihood estimators are designated $\hat{a}, \hat{b}$, and $\hat{c}$ for the parameters a, b, and c, respectively.

In a preliminary study of the original 171 point EPRI dataset, the data were divided into six sets as follows: set 1 with 31 data points, set 2 with 41 points, set 3 with 47 points, set 4 with 17 points, set 5 with 16 points, and set 6 with 19 points. Different partitions were investigated, but these 6 divisions gave more uniform results than others. Between a value of 20 and the minimum value of each set, three trial values of a were selected. Maximum likelihood estimators $\hat{b}$ and $\hat{c}$ were computed given a trial value of a. Distributional properties of $\hat{b}$ and $\hat{c}$ are much better than those of the 3-parameter case. The asymptotic variance of $\hat{c}$ is

$$Var(\hat{c}) \approx c^2(0.6079/N + 3.8398/N^2) \quad (c \to \infty)$$

and that for $\hat{b}$ is

$$Var(\hat{b}) \approx \frac{b^2}{c^2}\left(\frac{1.1087}{N} + \frac{0.3624 - 1.9881/c + 1.8429/c^2}{N^2}\right) \quad (c \to \infty)$$

where N is the sample size. The values of $\hat{b}$ were different for each set, but the $\hat{c}$ values were between 2 to 3.

The focus of the analysis then turned to estimating the location parameter, a , as a function of the normalized temperature. The maximum likelihood estimators are not valid since the value of c must be greater than 4 for the asymptotic moment profile of maximum likelihood estimators to exist. There are no such restrictions on the moment estimators for $c > 0$.

Define $\lambda_1 = \Gamma(1+1/c)$ and $\lambda_2 = \Gamma(1+2/c)$, with a_2* and b_2* the estimators, then

$$b_2^* = \sqrt{m_2/(\lambda_2 - \lambda_1^2)} \ , \ a_2^* = m_1' - b_2^* \lambda_1 \quad .$$

To determine which set of parameters a, b, and c gives the best fit, a "χ^2 goodness of fit" test was applied. Sturges [39] proposed the formula $1 + \log n$ to estimate the number of groups within each dataset, where n is the sample size.

The extended K_{Ic} dataset of 254 data points was divided into 16 sets (see Table 9) and the following procedure was applied:

- For the 16 sets, a_2* and b_2* were calculated for 25 values of c in the interval 1.3(0.1)3.7*. The resulting moment estimators were tested to insure that $18.2 < a_2^* < \text{Data}_{\min}$, where $\text{Data}_{\min}$ is the smallest data value in the set. Eight to twenty values of a_2* (given c) were accepted according to the results of the test for each of the 16 sets.

- For each set, the data were partitioned into 4 groups to test the hypothesis that the data came from a Weibull density with estimates a_2*, b_2*, and given c. Turning to the question of goodness of fit of the 2-parameter Weibull distribution (c known), the χ^2 values for one degree of freedom are 3.8415 at the 95% level, 6.6349 at 99%, 7.8794 at 99.5%, and 10.8276 at 99.9%.

- In Table 10, the resulting χ^2 values are given for the 16 sets at selected values of $c(\overline{T})$ where $\overline{T}$ is the average $\overline{(T - RT_{NDT})}$ for the set. All of the sets produced acceptable χ^2 values, except for set 13 which was excluded from the final analysis.

- For the many combinations of the triplet (a_2*, b_2*, c) from which to choose, the selected c value was chosen to obtain an a_2* nearest to the preliminary study of the lower boundary.

---

* The notation $c_{\min}(\Delta c)c_{\max}$ designates a sequence of c-values from $c_{\min}$ to $c_{\max}$ in increments of Δc.

- As noted in the preceding section, a_2* is positively biased and b_2* is negatively biased for small samples. An almost unbiased estimator b_2**(T) can be derived from b_2*(T)/E(b_2*/b). An almost unbiased estimator a_2**(T) follows by using b_2**(T). Table 10 includes values of E(b_2*/b), derived from Padé sequences relating to the series development of E(b_2*). For example, where $c = 2.1$, $N = 12$, from Table 8b, the E(b_2*/b) is 0.935.

The data given in Table 10 (excluding set 13) formed the basis for the construction of the final model. Curve fitting the approximate unbiased estimators a_2**(T) and b_2**(T) and c(T) produced the following model definition for K_{Ic}:

$$\begin{aligned} a_2^{**}(\Delta T) &= 10.8957 + 23.4192 \ \exp(0.0023 \ (\Delta T)) \ [\text{ksi} - \sqrt{\text{in.}}] \\ b_2^{**}(\Delta T) &= 14.7582 + 42.6312 \ \exp(0.0124(\Delta T)) \ [\text{ksi} - \sqrt{\text{in.}}] \\ c(\Delta T) &= 2.03025 + 0.4983 \ \exp(0.0135(\Delta T)) \end{aligned} \tag{4}$$

where $\Delta T = (T\text{-}RT_{NDT})$ is in °F. The new statistical model for the extended K_{Ic} is, therefore,

$$w(x \mid a_2^{**}(\Delta T) \ , b_2^{**}(\Delta T) \ ) = \frac{c(\Delta T)}{b_2^{**}(\Delta T)} y^{c(\Delta T)-1} \exp(-y^{c(\Delta T)}), \ (y = (x - a_2^{**}(\Delta T) \ ) / b_2^{**}(\Delta T) \ ).$$

where $x = K_{Ic}$ in ksi-√in.

To calculate the percentiles (e.g., $x_{0.5}$, $x_{0.95}$, etc.), from Eq. (2) one obtains

$$\begin{aligned} x_{0.5}(\Delta T) &= \{-\ln(0.5)\}^{1/c(\Delta T)} b_2^{**}(\Delta T) \ + a_2^{**}(\Delta T), \\ x_{0.95}(\Delta T) &= \{-\ln(0.05)\}^{1/c(\Delta T)} b_2^{**}(\Delta T) \ + a_2^{**}(\Delta T), \\ x_p(\Delta T) &= \{-\ln(1-p)\}^{1/c(\Delta T)} b_2^{**}(\Delta T) \ + a_2^{**}(\Delta T). \quad (0 < p < 1) \end{aligned} \tag{5}$$

Figure 12 shows a plot of the lower boundary curve, a_2**, and the 1%, 50%, 95%, 99%, and 99.5% curves. Above the 99.5 percentile, there are 3 points where the expected number is 2. Above the 99% curve, there are 5 points where the expected number is 3. Above the 95%

curve, there are 14 points where the expected number is 13. For the 50% curve, there are 119 points against the expected value of 127. Considering the small sample for the sets involved, the fit of 254 data points to the Weibull model is considered satisfactory.

4.2 The K_{Ia} Model

The procedures summarized in Section 4.1 were then applied to K_{Ia}. The extended K_{Ia} dataset of 112 data points was initially divided into 13 sets for a preliminary analysis. To obtain an acceptable degree of smoothness in the resulting point estimates for a_2* and b_2*, the data were subsequently repartitioned into 4 sets (see Table 11), and the procedure applied to K_{Ic} was then repeated:

- For the 4 sets, a_2* and b_2* were calculated for 25 values of c in the interval 1.3(0.1)3.7. The resulting moment estimators were tested to insure that $18.2 < a_2^* < \text{Data}_{\min}$, where $\text{Data}_{\min}$ is the smallest data value in the set. Approximately twenty values of a_2* (given c) were accepted according to the results of the test for each of the 4 sets.

- For each set, the data were partitioned into 4 groups to test the hypothesis that the data came from a Weibull density with estimates a_2*, b_2*, and given c. The required χ^2 values for one degree of freedom are 3.8415 at the 95% confidence level, 6.6349 at 99%, 7.8794 at 99.5%, and 10.8276 at 99.9%.

- In Table 12, the resulting χ^2 values are given for the 4 sets at a fixed value of c. All of the sets produced acceptable χ^2 values.

- For the many combinations of the triplet (a_2*, b_2*, c) from which to choose, the selected c value was chosen to obtain an a_2* nearest to the minimum value of each set. It was determined that a fixed value of $c = 2.5$ provided the best result for positioning a_2* correctly.

- As noted in the preceding section, a_2* is positively biased and b_2* is negatively biased for small samples. The generalized equation given in Appendix C was applied to estimate values for $E(b_2^*/b)$ which in turn were used to calculate the almost unbiased estimator $b_2^{**}(T)$. The almost unbiased estimator $a_2^{**}(T)$ follows by using $b_2^{**}(T)$.

The data given in Table 12 formed the basis for the construction of the final model. Curve fitting (see Fig. 13) the approximate unbiased estimators $a_2^{**}(T)$ and $b_2^{**}(T)$ produced the following model definition for K_{Ia}:

$$\begin{aligned} a_2^{**}(\Delta T) &= 24.584 + 15.352 \ \exp(0.012639(\Delta T)) \ [\text{ksi} - \sqrt{\text{in.}}] \\ b_2^{**}(\Delta T) &= 36.201 + 0.060307 \ (\Delta T) \ [\text{ksi} - \sqrt{\text{in.}}] \\ c &= 2.5 \end{aligned} \tag{6}$$

where $\Delta T = (T\text{-}RT_{NDT})$ is in °F. The new statistical model for the extended K_{Ia} is, therefore,

$$w(x \mid a_2^{**}(\Delta T) \ , b_2^{**}(\Delta T) \ ) = \frac{2.5}{b_2^{**}(\Delta T)} y^{1.5} \exp(-y^{2.5}), \ (y = (x - a_2^{**}(\Delta T) \ ) / b_2^{**}(\Delta T) \ ).$$

where $x = K_{Ia}$ in ksi-√in.

To calculate the percentiles for $x_{0.5}$, $x_{0.95}$, etc., Eqs. (5) can again be used

$$\begin{aligned} x_{0.5}(\Delta T) &= \{-\ln(0.5)\}^{1/2.5} b_2^{**}(\Delta T) \ + a_2^{**}(\Delta T), \\ x_{0.95}(\Delta T) &= \{-\ln(0.05)\}^{1/2.5} b_2^{**}(\Delta T) \ + a_2^{**}(\Delta T), \\ x_p(\Delta T) &= \{-\ln(1-p)\}^{1/2.5} b_2^{**}(\Delta T) \ + a_2^{**}(\Delta T). \quad (0 < p < 1) \end{aligned}$$

Figure 14 shows a plot of the lower boundary curve, a_2^{**}, and the 1%, 50%, 95%, 99%, and 99.5% curves. Above the 99.5% curve, there is 1 point where the expected number for $N =$ 112 is 1. Above the 99% curve, there is 1 point where the expected number is 2. Above the 95% curve, there are 7 points where the expected number is 6. For the 50% curve, there are 57 points above and 55 below. Considering the small sample for the sets involved, the fit of 112 data points to the Weibull model is considered satisfactory.

5. CONCLUSIONS

This report has presented the technical basis for new statistical representations of the extended K_{Ic} and K_{Ia} databases. This effort was performed in the context of a probabilistic methodology appropriate for use in an overall effort by the Nuclear Regulatory Commission (NRC) to update its regulatory guidance for pressurized-thermal-shock (PTS) transients. These new representations for K_{Ic} and K_{Ia} were developed through the application of rigorous statistical procedures applied to extended fracture toughness databases for RPV steels.

In summary, the new statistical models have the following analytical forms:

K_{Ic} Density, $w(x|\, a_2^{**}(\Delta T), b_2^{**}(\Delta T))$

$$w(x\,|\,a_2^{**}(\Delta T)\ ,b_2^{**}(\Delta T)\ ) = \frac{c(\Delta T)}{b_2^{**}(\Delta T)} y^{c(\Delta T)-1} \exp(-y^{c(\Delta T)}),\ \ (y = (x - a_2^{**}(\Delta T)\ )/b_2^{**}(\Delta T)\ )$$

where the parameters of the distribution are calculated from Eq. (4)

$$\boxed{\begin{aligned} a_2^{**}(\Delta T)\ &= 10.8957 + 23.4192\ \ \exp(0.0023\ \ (\Delta T))\ \ [\text{ksi} - \sqrt{\text{in.}}] \\ b_2^{**}(\Delta T)\ &= 14.7582 + 42.6312\ \ \exp(0.0124(\Delta T))\ \ [\text{ksi} - \sqrt{\text{in.}}] \\ c(\Delta T)\ &= 2.03025 + 0.4983\ \ \exp(0.0135(\Delta T)) \end{aligned}}$$

with $x = K_{Ic}$ in ksi-√in., $\Delta T = (T\text{-}RT_{NDT})$ is in °F.

K_{Ia} Density, $w(x|\, a_2^{**}(\Delta T), b_2^{**}(\Delta T))$

$$w(x\,|\,a_2^{**}(\Delta T)\ ,b_2^{**}(\Delta T)\ ) = \frac{2.5}{b_2^{**}(\Delta T)} y^{1.5} \exp(-y^{2.5}),\ \ (y = (x - a_2^{**}(\Delta T)\ )/b_2^{**}(\Delta T)\ )$$

where the parameters of the distribution are calculated from Eq. (6)

$$\boxed{\begin{aligned} a_2^{**}(\Delta T)\ &= 24.584 + 15.352\ \ \exp(0.012639(\Delta T))\ \ [\text{ksi} - \sqrt{\text{in.}}] \\ b_2^{**}(\Delta T)\ &= 36.201 + 0.060307\ \ (\Delta T)\ \ [\text{ksi} - \sqrt{\text{in.}}] \\ c\ &= 2.5 \end{aligned}}$$

with $x = K_{Ia}$ in ksi-√in., $\Delta T = (T\text{-}RT_{NDT})$ is in °F.

Example Problem Applying the New Statistical Model for K_{Ic}

As an example of how to apply the new statistical model for K_{Ic}, let the test temperature be T = -5 °F for a material with RT_{NDT} = 5 °F; therefore, $\Delta T = T - RT_{NDT}$ = -10 °F. We then calculate the parameters of the model by Eq. (4)

$$a_2^{**}(\Delta T) = 10.8957 + 23.4192 \ \exp(0.0023 \ (\Delta T)) \ [\text{ksi} - \sqrt{\text{in.}}]$$
$$b_2^{**}(\Delta T) = 14.7582 + 42.6312 \ \exp(0.0124(\Delta T)) \ [\text{ksi} - \sqrt{\text{in.}}]$$
$$c(\Delta T) = 2.03025 + 0.4983 \ \exp(0.0135(\Delta T))$$

$$\boxed{\begin{aligned} a_2^{**}(-10) &= 10.8957 + 23.4192 \ \exp(0.0023 \ (-10)) = 33.78241 \ [\text{ksi} - \sqrt{\text{in.}}] \\ b_2^{**}(-10) &= 14.7582 + 42.6312 \ \exp(0.0124(-10)) = 52.41774 \ [\text{ksi} - \sqrt{\text{in.}}] \\ c(-10) &= 2.03025 + 0.4983 \ \exp(0.0135(-10)) \quad = 2.46562 \end{aligned}}$$

The median value of K_{Ic} representing a 50% cumulative probability of failure is then $x_{0.5}$. From Eq. (5) with $p = 0.5$

$$x_p(\Delta T) = \{-\ln(1-p)\}^{1/c(\Delta T)} b_2^{**}(\Delta T) \ + a_2^{**}(\Delta T). \quad (0 < p < 1)$$

$$\boxed{x_{0.5}(-10) = \{-\ln(1-0.5)\}^{1/2.46562} 52.41774 + 33.78241 = 78.96 \ \ [\text{ksi} - \sqrt{\text{in.}}]}$$

For a 1% cumulative probability of failure, the corresponding value of K_{Ic} is $x_{0.01}$ calculated from Eq. (5) with $p = 0.01$

$$\boxed{x_{0.01}(-10) = \{-\ln(1-0.01)\}^{1/2.46562} 52.41774 + 33.78241 = 41.90 \ \ [\text{ksi} - \sqrt{\text{in.}}]}$$

Additional properties of the distribution may also be calculated, for example the mean and standard deviation at this normalized temperature are

Mean:

$$K_{Ic(mean)}(-10) = a_2^{**}(-10) \ + b_2^{**}(-10) \ \ \Gamma(1 + 1/c(-10)) = \boxed{80.28 \ \ [\text{ksi} - \sqrt{\text{in.}}]}$$

Standard Deviation:

$$\sigma(-10) = b_2^{**}(-10)\sqrt{\{\Gamma(1 + 2/c(-10)) - \Gamma^2(1 + 1/c(-10))\}} = \boxed{20.14 \ \ [\text{ksi} - \sqrt{\text{in.}}]}$$

Note that for an asymmetric distribution, the median and the mean are not the same.

ACKNOWLEDGEMENTS

The surveys of the K_{Ic} and K_{Ia} literature and unpublished databases were carried out by Drs. M. A. Sokolov and S. K. Iskander, respectively, of the Metals and Ceramics Division. The support of Dr. R. K. Nanstad of the Metals and Ceramics Division in this project is also acknowledged. P. W. McGrady of the Computational Physics and Engineering Division performed the initial regression analyses of the EPRI K_{Ic} database. Consultations with Dr. D. A. Wolf of the Computer Science and Mathematics Division on various statistical aspects of the analysis are also gratefully acknowledged.

References

[1] EPRI Special Report, 1978, "Flaw Evaluation Procedures: ASME Section XI," EPRI NP-719-SR, Electric Power Research Institute, Palo Alto, CA.

[2] R. K. Nanstad, J. A. Keeney, and D. E. McCabe, "Preliminary Review of the Bases for the K_{Ic} Curve in the ASME Code," ORNL/NRC/LTR-93/15, Oak Ridge National Laboratory, Oak Ridge, TN, 1993.

[3] ASME Boiler and Pressure Vessel Code, Section XI, Article A-4000: Material Properties, American Society of Mechanical Engineers, New York, NY, (1998) 413-417.

[4] *Standard Test Method for Plane-Strain Fracture Toughness of Metallic Materials,* E 399-90, Annual Book of ASTM Standards - Section 3: Metals Test Methods and Analytical Procedures, Vol. 03.01 Metals – Mechanical Testing; Elevated and Low-Temperature Tests; Metallography, American Society for Testing and Materials, West Conshohocken, PA, 1998.

[5] ASME Boiler and Pressure Vessel Code, Section III, Article NB-2331, American Society of Mechanical Engineers, New York, NY, (1998).

[6] *Standard Test Method for Determining Plane-Strain Crack-Arrest Fracture Toughness, K_{Ia} , of Ferritic Steels,* E 1221-88, Annual Book of ASTM Standards Section 3: Metals Test Methods and Analytical Procedures, Vol. 03.01 Metals – Mechanical Testing; Elevated and Low-Temperature Tests; Metallography, American Society for Testing and Materials, West Conshohocken, PA, 1998.

[7] B. R. Bass, P. T. Williams, T. L. Dickson, and W. J. McAfee, "Revised K_{Ic}/K_{Ia} Fracture Toughness Curves for Application to PTS Assessments of Reactor Pressure Vessels," ORNL/LTR-99/??, Oak Ridge National Laboratory, Oak Ridge, TN, November 1999.

[8] T. L. Dickson, "An Overview of FAVOR: A Fracture Analysis Code for Nuclear Reactor Pressure Vessels," in *Transactions of the 13th International Conference on Structural Mechanics in Reactor Technology (SMiRT 13)*, Volume IV, Porto Alegre, Brazil, (1995) 701-706.

[9] W. O. Shabbits, W. H. Pryle, and E. T. Wessel, *Heavy Section Fracture Toughness Properties of A533, Grade B, Class-1 Steel Plate and Submerged Arc Weldments*, HSST Technical Report 6, WCAP-7414, December 1969.

[10] T. R. Mager, F. O. Thomas, and W. S. Hazelton, *Evaluation by Linear Elastic Fracture Mechanics of Radiation Damage to Pressure Vessel Steels,* HSST Technical Report 5, WCAP-7328, Revised, October 1969.

[11] T. R. Mager, *Fracture Toughness Characterization Study of A533, Grade B, Class-1 Steel,* HSST Technical Report 10, WCAP-7578, October 1970.

[12] N. E. Dowling, *Mechanical Behavior of Materials: Engineering Methods for Deformation, Fracture, and Fatigue,* 2nd ed., Prentice Hall, Upper Saddle River, N.J., (1999) 319.

[13] R. K. Nanstad, F. M. Haggag, and D. E. McCabe, *Irradiation Effects on Fracture Toughness of Two High-Copper Submerged-Arc Welds, HSSI Series 5,* USNRC Report NUREG/CR-5913 (ORNL/TM-12156/V1 and V2) Vol. 1 and 2, Oak Ridge National Laboratory, Oak Ridge, TN, October 1992.

[14] D. E. McCabe., *A Comparison of Weibull and β_{Ic} Analysis of Transition Range Fracture Toughness Data,* USNRC Report NUREG/CR-5788 (ORNL/TM-11959), Oak Ridge National Laboratory, Oak Ridge, TN, January 1992.

[15] T. Iawadate, Y. Tanaka, S. Ono, and J. Watanabe, "An Analysis of Elastic-Plastic Fracture Toughness Behavior for J_{Ic} Measurements in the Transition Region," *Elastic-Plastic Fracture: Second Symposium, Vol. II-Fracture Resistance Curves and Engineering Applications*, (edited by C. F. Shih and J. P. Gudas) ASTM STP 803, (1983) II531-II561.

[16] D. E. McCabe, R. K. Nanstad, S. K. Iskander, R. L. Swain, *Unirradiated Material Properties of Midland Weld WF-70,* USNRC Report NUREG/CR-6249 (ORNL/TM-12777), Oak Ridge National Laboratory, Oak Ridge, TN, October 1994.

[17] J. J. McGowan, R. K. Nanstad, and K. R. Thoms, *Characterization of Irradiated Current-Practice Welds and A533 Grade B Class 1 Plate for Nuclear Pressure Vessel Service*, USNRC Report NUREG/CR-4880 (ORNL-6484/V1 and V2), Oak Ridge National Laboratory, Oak Ridge, TN, July 1988.

[18] S. K. Iskander, W. R. Corwin, R. K. Nanstad, *Results of Crack-Arrest Tests on Two Irradiated High-Copper Welds,* USNRC Report NUREG/CR-5584 (ORNL/TM-11575), Oak Ridge National Laboratory, Oak Ridge, TN, December 1990.

[19] S. K. Iskander, C. A. Baldwin, D. W. Heatherly, D. E. McCabe, I. Remec, and R. L. Swain, *Detailed Results of Testing Unirradiated and Irradiated Crack-Arrest Toughness Specimens from the Low Upper-Shelf Energy, High Copper Weld, WF-70,* NUREG/CR-6621 (ORNL/TM-13764) under preparation.

[20] S. K. Iskander, R. K. Nanstad, D. E. McCabe, and R. L. Swain, "Effects of Irradiation on Crack-Arrest Toughness of a Low Upper-Shelf Energy, High-Copper Weld," *Effects of Radiation on Materials: 19th International Symposium, ASTM STP 1366,* M. L. Hamilton, A. S. Kumar, S. T. Rosinski, and M. L. Grossbeck, eds., American Society for Testing and Materials, to be published in 1999.

[21] E. J. Ripling and P. B. Crosley, "Strain Rate and Crack Arrest Studies," *HSST 5th Annual Information Meeting*, Paper No. 9, 1971.

[22] E. J. Ripling and P. B. Crosley, "Crack Arrest Studies," *HSST 6th Annual Information Meeting*, Paper No. 10, 1972.

[23] W. Weibull, "A Statistical Theory of the Strength of Materials," *Proceedings of the Royal Swedish Institute for Engineering Research*, No. 151, 1939.

[24] W. Weibull, "A Statistical Distribution Function of Wide Applicability," *Journal of Applied Mechanics* **18**, (1951) 293-297.

[25] S. Kotz, N. L. Johnson, and C. B. Read, *Encyclopedia of Statistical Science*, Vol. 9, (edited by C. E. Antle and L. J. Bain), John Wiley & Sons, New York, 1988.

[26] N. L. Johnson, S. Kotz, and N. Balakrishanan, *Discontinuous Univariate Distributions Volume 1, Second Edition,* John Wiley & Sons, New York, 1994.

[27] K. O. Bowman and L. R. Shenton, "Asymptotic Profile for Moments of Maximum Likelihood Estimators and the Weibull Densities," submitted for publication in *Commun. Statist. Theory and Method*, 1999.

[28] K. O. Bowman and L. R. Shenton, *Properties of Estimators for the Gamma Distribution*, Marcel Dekker, Inc., 1988.

[29] K. O. Bowman and L. R. Shenton, "Approximate Percentage Points for Pearson Distributions," *Biometrika* **66**, (1979) 147-151.

[30] K. O. Bowman and L. R. Shenton, "Further Approximate Pearson Percentage Points and Cornish-Fisher," *Comm. Stat. Computa.* **B**(8), (1979) 231-244.

[31] *NAG Fortran Library*,The Numerical Algorithms Group Ltd, Oxford UK. 1999

[32] G. A. Baker, Jr., *Essentials of Padé Approximants*, Academic Press, New York, 1975.

[33] L. R. Shenton and K. O. Bowman, "The Development of Techniques for the Evaluation of Sampling Moments," *Int. Statist. Rev.* **43**(3), (1975) 317-334.

[34] K. O. Bowman and L. R. Shenton, *Continued Fractions in Statistical Applications*, Marcel Dekker, Inc., 1989.

[35] M. A. Sokolov, "Statistical Analysis of the ASME K_{Ic} Database," *Transactions of the ASME* **120**, (1998) 24-28.

[36] K. Wallin, "The Scatter in K_{Ic}-Results, *Eng. Fracture Mech.* **19**(6), (1984) 1085-1093.

[37] J. G. Merkle, K. Wallin, and D. E. McCabe, "Technical Basis for an ASTM Standard on Determining the Reference Temperature, T_0, for Ferritic Steels in the Transition Range," NUREG/CR-5504 (ORNL/TM-13631) Oak Ridge National Laboratory, November 1998.

[38] *Standard Test Method for Determination of Reference Temperature, T_0, for Ferritic Steels in the Transition Range* E 1921-97, Annual Book of ASTM Standards Section 3: Metals Test Methods and Analytical Procedures, Vol. 03.01 Metals – Mechanical Testing; Elevated and Low-Temperature Tests; Metallography, American Society for Testing and Materials, West Conshohocken, PA, 1998.

[39] H. Sturges, "Sturges' Rule," *J. Amer. Statist. Assoc.* **21**, (1926) 65-66.

Table 1. Summary of K_{Ic} Extended Database

	Material	Source	Specimen Type	Size Range	Temp. Range (°F)	$(T\text{-}RT_{NDT})$ Range (°F)	No. of Data Points
EPRI	Database	EPRI NP-719-SR					
1	HSST 01 subarc weldment	Shabbits (1969)	C(T)	1T - 6T	-200 to -50	-200 to -50	8
2	A533B Cl. 1 subarc weld	Shabbits (1969)	C(T)	1T - 8T	-200 to 0	-200 to 0	8
3	HSST 01	Mager (1970)	C(T)	1T	-150	-170	17
4	HSST 03	Mager (1970)	C(T)	1T	-150	-170	9
5	A533B Cl. 1	Mager (1969)	WOL	1T - 2T	-320 to -150	-385 to -215	13
6	HSST 02	Mager (1969)	WOL & C(T)	1T - 2T	-200 to 0	-200 to 0	41
6	HSST 02	Shabbits (1969)	C(T)	1T - 11T	-250 to 50	-250 to 50	28
7	A533B Cl. 1 weldment	Mager (1969)	WOL	1T - 2T	-320 to -200	-275 to -155	10
8	A533 B Cl. 1 weldment/HAZ	Mager (1969)	WOL	1T - 2T	-320 to -200	-320 to -200	6
9	A508 Cl.2 European Forging	Mager (1969)	WOL	1T - 2T	-320 to -100	-370 to -150	12
10	A508 Class 2	unpublished	C(T)	2T - 6T	-150 to 0	-201 to -51	9
11	A508 Class 2	unpublihsed	C(T)	2T - 8T	-125 to -75	-190 to -30	10
						Total	171
Additional Data	Additional Data						
12	HSSI Weld 72W	NUREG/CR-5913.	C(T)	1T-4T	-238 to 5	-229 to 14	12
13	HSSI Weld 73W	NUREG/CR-5913	C(T)	1T-4T	-238 to -58	-209 to -29	10
14	HSST Plate 13A	NUREG/CR-5788	C(T)	1T-4T	-238 to -103	-229 to -94	43
15	A508 Cl. 3	ASTM STP 803	Bx2B C(T)	1T-4T	-238 to -4	-225 to 9	6
16	Midland Nozzle Course Weld	NUREG/CR-6249	C(T)	1T	-148 to -58	-200 to -110	6
17	Midland Beltline	NUREG/CR-6249	C(T)	1T	-148	-171	2
18	Plate 02 4th Irr. Series (68-71W)	NUREG/CR-4880	C(T)	1T	-148 to -139	-148 to -139	4
						Total	83
						Grand Total	254

REFERENCES FOR TABLES 1 AND 2

EPRI Special Report, 1978, *Flaw Evaluation Procedures: ASME Section XI*, EPRI NP-719-SR, Electric Power Research Institute, Palo Alto, CA.

W. O. Shabbits, W. H. Pryle, and E. T. Wessel, *Heavy Section Fracture Toughness Properties of A533, Grade B, Class-1 Steel Plate and Submerged Arc Weldments*, HSST Technical Report 6, WCAP-7414, December 1969.

T. R. Mager, F. O. Thomas, and W. S. Hazelton, *Evaluation by Linear Elastic Fracture Mechanics of Radiation Damage to Pressure Vessel Steels*, HSST Technical Report 5, WCAP-7328, Revised, October 1969.

T. R. Mager, *Fracture Toughness Characterization Study of A533, Grade B, Class-1 Steel*, HSST Technical Report 10, WCAP-7578, October 1970.

R. K. Nanstad, F. M. Haggag, and D. E. McCabe, *Irradiation Effects on Fracture Toughness of Two High-Copper Submerged-Arc Welds, HSSI Series 5*, USNRC Report NUREG/CR-5913 (ORNL/TM-12156/V1 and V2) Vol. 1 and 2, Oak Ridge National Laboratory, Oak Ridge, TN, October 1992.

D. E. McCabe., *A Comparison of Weibull and β_{Ic} Analysis of Transition Range Fracture Toughness Data*, USNRC Report NUREG/CR-5788 (ORNL/TM-11959), Oak Ridge National Laboratory, Oak Ridge, TN, January 1992.

T. Iawadate, Y. Tanaka, S. Ono, and J. Watanabe, "An Analysis of Elastic-Plastic Fracture Toughness Behavior for J_{Ic} Measurements in the Transition Region," *Elastic-Plastic Fracture: Second Symposium, Vol. II-Fracture Resistance Curves and Engineering Applications*, ASTM STP 803, (1983) II531-II561.

D. E. McCabe, R. K. Nanstad, S. K. Iskander, R. L. Swain, *Unirradiated Material Properties of Midland Weld WF-70,* USNRC Report NUREG/CR-6249 (ORNL/TM-12777), Oak Ridge National Laboratory, Oak Ridge, TN, October 1994.

J. J. McGowan, R. K. Nanstad, and K. R. Thoms, *Characterization of Irradiated Current-Practice Welds and A533 Grade B Class 1 Plate for Nuclear Pressure Vessel Service*, USNRC Report NUREG/CR-4880 (ORNL-6484/V1 and V2), Oak Ridge National Laboratory, Oak Ridge, TN, July 1988.

Table 2. Chemistry and Heat Treatment of Principal Materials

Material ID	Specification	Source	Chemistry – wt (%)										Heat Treatment
			C	P	Mn	Ni	Mo	Si	Cr	Cu	S	Al	
HSST 01	A533B Cl. 1	Mager (1970)	.22	.012	1.48	.68	.52	.25	-	-	.018	-	Note 1
HSST 02	A533B Cl. 1	Mager (1969)	.22	.012	1.48	.68	.52	.25	-	-	.018	-	Note 2
HSST 03	A533B Cl. 1	Mager (1970)	.20	.011	1.26	.56	.45	.25	.10	.13	.018	.034	Note 3
HSST 02	A533B Cl. 1	Shabbits (1969)	.22	.012	1.48	.68	.52	.25	-	-	.018	-	Note 4
HSST 01 subarc weld	A533B Cl. 1	Shabbits (1969)	.12	.014	1.35	.65	.52	.23	-	-	.012	-	Note 5
B&W subarc weldment	A533B Cl. 1	Shabbits (1969)	.10	.009	1.77	.64	.42	.36	-	-	.015	-	Note 6
PW/PH weldment	A533B Cl. 1	Mager (1969)	.09	.019	1.25	1.08	.52	.23	.05	.22	.13	.037	Note 7
MD07 European	A508 Cl. 2 Ring forging	Mager (1969)	.18	.009	1.16	.72	.51	.24	.28	-	.10	-	Note 8
-	A533B Cl. 1	Mager (1969)	.19	.012	1.37	.52	.45	.25	.13	.15	.016	.048	Note 9
72W	A533B weld	5788	.09	.006	1.66	.60	.58	.04	.27	.23	.006	-	
73W	A533B weld	5788	.10	.005	1.56	.60	.58	.04	.25	.21	.005	-	

Notes:

1.	Normalizing:	1675 °F	4 hr, air cooled
	Austentizing:	1600 °F	4 hr
	Quenching:	Water quench	
	Tempering:	1225 °F	4 hr, furnace cooled
	Stress Relief:	1150 °F	40 hr, furnace cooled
2.	Normalizing:	1675 °F	4 hr, air cooled
	Austentizing:	1600 °F	4 hr
	Quenching:	Water quench	
	Tempering:	1225 °F	4 hr, furnace cooled
	Stress Relief:	1150 °F	40 hr, furnace cooled
3.	Normalizing:	1675 °F	12 hr, air cooled
	Austentizing:	1575 °F	12 hr
	Quenching:	Water quench	
	Tempering:	1175 °F	12 hr, furnace cooled
	Stress Relief:	1125 °F	40 hr, furnace cooled
4.	Normalizing:	1675 ± 25 °F	4 hr
	Austentizing:	1520 °F – 1620 °F	4 hr
	Quenching:	Water quench.	
	Tempering:	1200 °F – 1245 °F	4 hr, air cooled
	Stress Relief:	1150 ± 25 °F	40 hr, furnace cooled to 600 °F
5.	Post Weld:	1150 ± 25 °F	12 hr
	Intermediate	1100 ± 25 °F	15 min

6.	Post Weld	1100 °F – 1150 °F	12 hr
	Intermediate	1100 °F – 1150 °F	15 min
7.		620 °C	27 hr, air cooled
8.		925 °C	5 hr
	Quenching:	Water quench	
		650 °C	3 hr, furnace cooled
		620 °C	24 hr, air cooled
9.		910 °C	8 hr
	Quenching:	Water quench	
		680 °C	10 hr, furnace cooled
		850 °C	8 hr
	Quenching:	Water quench	
		690 °C	8 hr, air cooled
		620 °C	24 hr, air cooled

Table 3. Summary of K_{Ia} Extended Database

	Material	Source	Specimen Type	Size Range	Test Temp. Range (°F)	(T-RTNDT) Range (°F)	No. of Data Points
EPRI	Database	EPRI NP-719-SR					
1	HSST 02	Ripling (1971)	C(T)	1T-3T	-150 to 121	-150 to 121	50
Additional Data	Additional Data						
2	HSSI Weld 72W	NUREG/CR-5584	C(T) crack arrest		-78 to 41	-68 to 51	32
3	HSSI Weld 73W	NUREG/CR-5584	C(T) crack arrest		-78 to 59	-48 to 89	26
4	MW15J	NUREG/CR-6621	C(T) crack arrest		-4 to 50	-36 to 18	4
						Total =	112

REFERENCES FOR TABLE 3

EPRI Special Report, 1978, *Flaw Evaluation Procedures: ASME Section XI*, EPRI NP-719-SR, Electric Power Research Institute, Palo Alto, CA.

E. J. Ripling and P. B. Crosley, "Strain Rate and Crack Arrest Studies," *HSST 5th Annual Information Meeting*, Paper No. 9, 1971.

S. K. Iskander, W. R. Corwin, R. K. Nanstad, *Results of Crack-Arrest Tests on Two Irradiated High-Copper Welds*, USNRC Report NUREG/CR-5584 (ORNL/TM-11575), Oak Ridge National Laboratory, Oak Ridge, TN, December 1990.

S. K. Iskander, C. A. Baldwin, D. W. Heatherly, D. E. McCabe, I. Remec, and R. L. Swain, *Detailed Results of Testing Unirradiated and Irradiated Crack-Arrest Toughness Specimens from the Low Upper-Shelf Energy, High Copper Weld, WF-70,* NUREG/CR-6621 (ORNL/TM-13764) under preparation.

S. K. Iskander, R. K. Nanstad, D. E. McCabe, and R. L. Swain, "Effects of Irradiation on Crack-Arrest Toughness of a Low Upper-Shelf Energy, High-Copper Weld," *Effects of Radiation on Materials: 19th International Symposium, ASTM STP 1366*, M. L. Hamilton, A. S. Kumar, S. T. Rosinski, and M. L. Grossbeck, eds., American Society for Testing and Materials, to be published in 1999.

Table 4. Mean, Standard Deviation, Skewness, and Kurtosis of Weibull Density

Shape Parameter c	Mean μ_1'	Std. Deviation σ	Skewness $\sqrt{\beta_1}$	Kurtosis β_2
1.2	0.9407	0.7872	1.52	6.24
1.4	0.9114	0.6596	1.20	4.84
1.6	0.8966	0.5737	0.96	4.04
1.8	0.8893	0.5112	0.78	3.56
2.0	0.8862	0.4633	0.63	3.25
2.2	0.8856	0.4249	0.51	3.04
2.4	0.8865	0.3935	0.40	2.91
2.6	0.8882	0.3670	0.32	2.82
2.8	0.8905	0.3443	0.24	2.76
3.0	0.8930	0.3246	0.17	2.73
3.2	0.8957	0.3072	0.11	2.71
3.4	0.8984	0.2918	0.05	2.71
3.6	0.9011	0.2780	0.00	2.72
3.8	0.9038	0.2656	-0.05	2.73
4.0	0.9064	0.2543	-0.09	2.75
4.2	0.9089	0.2440	-0.13	2.77
4.4	0.9114	0.2345	-0.16	2.79
4.6	0.9137	0.2258	-0.19	2.82
4.8	0.9160	0.2178	-0.23	2.85
5.0	0.9182	0.2103	-0.25	2.88
5.2	0.9202	0.2034	-0.28	2.91
5.4	0.9222	0.1969	-0.31	2.94
5.6	0.9241	0.1908	-0.33	2.97
5.8	0.9260	0.1851	-0.35	3.00
6.0	0.9277	0.1798	-0.37	3.04
6.2	0.9294	0.1747	-0.39	3.07
6.4	0.9310	0.1700	-0.41	3.10
6.6	0.9325	0.1655	-0.43	3.13
6.8	0.9340	0.1612	-0.45	3.16
7.0	0.9354	0.1572	-0.46	3.19
∞	1.0000	0	-1.13	5.4

Table 5. Simulation Study of 3-Parameter Weibull Density ($a = 0$, $b = 1$)

c	N		Mean	σ	$\sqrt{\beta_1}$	β_2
1.5	20	a_3*	-0.1778	0.2933	-3.0524	56.9235
		b_3*	1.2008	0.3801	1.8130	23.2091
		c_3*	2.0087	0.8358	7.3181	288.2254
	50	a_3*	-0.0808	0.1674	-0.4247	3.6671
		b_3*	1.0928	0.2311	0.3559	3.3975
		c_3*	1.7139	0.4113	0.8262	4.5043
2.0	50	a_3*	-0.0628	0.1884	-0.7211	4.6178
		b_3*	1.0653	0.2265	0.6018	4.1276
		c_3*	2.2294	0.5753	1.1289	6.1499
3.0	50	a_3*	-0.0600	0.2774	-2.7998	50.5081
		b_3*	1.0583	0.2954	2.4757	40.3715
		c_3*	3.3110	1.1351	3.8903	88.6025
4.0	50	a_3*	-0.0996	1.1047	-94.6727	13422
		b_3*	1.0971	1.1088	93.6296	13234
		c_3*	4.5401	5.8649	60.7017	12151

Table 6. Moments of Moment Estimators a_2*, b_2* Given c by Simulation ($a = 0$, $b = 1$)

		a_2*				b_2*			
c	N	μ_1'	σ	$\sqrt{\beta_1}$	β_2	μ_1'	σ	$\sqrt{\beta_1}$	β_2
1.1	15	0.0748	0.1941	-0.5312	4.5585	0.9220	0.2885	0.8453	4.3463
	30	0.0403	0.1456	-0.5520	4.3182	0.9578	0.2142	0.6473	3.8629
	50	0.0247	0.1175	-0.5439	4.0882	0.9745	0.1706	0.5449	3.6760
1.5	15	0.0544	0.1683	-0.1981	3.5019	0.9394	0.2248	0.5264	3.4893
	30	0.0285	0.1214	-0.1964	3.3790	0.9682	0.1628	0.3800	3.2782
	50	0.0172	0.0956	-0.1954	3.2947	0.9812	0.1279	0.3137	3.2221
2.0	15	0.0468	0.1608	-0.3695	3.1557	0.9470	0.1896	0.3147	3.1570
	30	0.0242	0.1140	-0.4315	3.1263	0.9726	0.1353	0.2156	3.0787
	50	0.0145	0.0889	-0.4358	3.0928	0.9839	0.1054	0.1755	3.0710
2.5	15	0.0445	0.1615	0.0087	3.0314	0.9496	0.1755	0.1949	3.0408
	30	0.0229	0.1139	0.0025	3.0458	0.9742	0.1242	0.1267	3.0184
	50	0.0137	0.0884	0.0047	3.0355	0.9848	0.0964	0.0991	3.0223
3	15	0.0441	0.1648	0.0077	2.9666	0.9504	0.1707	0.1323	2.9891
	30	0.0226	0.1161	0.0091	3.0047	0.9747	0.1204	0.0801	2.9939
	50	0.0135	0.0900	0.0153	3.0092	0.9850	0.0933	0.0573	3.0022
3.5	15	0.0444	0.1688	-0.0131	2.9294	0.9505	0.1702	0.1080	2.9604
	30	0.0228	0.1190	-0.0008	2.9797	0.9747	0.1200	0.0609	2.9796
	50	0.0136	0.0922	0.0099	2.9940	0.9850	0.0929	0.0387	2.9919
4.0	15	0.0450	0.1730	-0.0423	2.9103	0.9502	0.1718	0.1075	2.9447
	30	0.0231	0.1220	-0.0181	2.9644	0.9746	0.1212	0.0589	2.9700
	50	0.0138	0.0945	-0.0027	2.9852	0.9849	0.0939	0.0350	2.9861
4.5	15	0.0458	0.1770	-0.0746	2.9046	0.9497	0.1743	0.1206	2.9394
	30	0.0235	0.1250	-0.0385	2.9563	0.9743	0.1231	0.0671	2.9644
	50	0.0140	0.0969	-0.0185	2.9808	0.9848	0.0954	0.0404	2.9835
5.0	15	0.0465	0.1807	-0.1072	2.9091	0.9492	0.1772	0.1411	2.9430
	30	0.0239	0.1278	-0.0601	2.9538	0.9740	0.1253	0.0810	2.9631
	50	0.0143	0.0991	-0.0355	2.9797	0.9846	0.0972	0.0510	2.9835

Table 7a. Asymptotic Series for Moments of a_2* when $c = 2.1$, $a = 0$, $b = 1$

N^s	μ_1'	μ_2	μ_3	μ_4
1	0.67891756E+00	0.39190262E+00	0.00000000E+00	0.00000000E+00
2	0.12065197E+00	-0.12936388E+00	-0.62858268E-01	0.46076300E+00
3	0.22596801E+00	0.39926399E+00	0.65259996E+00	0.87633222E-01
4	-0.94143717E-01	-0.57533240E+00	-0.12345449E+01	-0.45578535E+00
5	0.96779137E+00	0.23255354E+01	0.39983611E+01	0.34831723E+01
6	-0.10428443E+02	-0.24242021E+02	-0.38215069E+02	-0.40062234E+02
7	0.66616458E+02	0.16238149E+03	0.26774912E+03	0.28350636E+03
8	-0.82602889E+03	-0.18977491E+04	-0.30275244E+04	-0.34750509E+04
9	0.10768022E+05	0.24561289E+05	0.39176514E+05	0.46256651E+05
10	-0.15348588E+06	-0.34850034E+06	-0.55694455E+06	-0.67302490E+06
11	0.26402856E+07	0.59300523E+07	0.94425785E+07	0.11655858E+08
12	-0.49216457E+08	-0.11011743E+09	-0.17548365E+09	-0.21976221E+09
13	0.10176100E+10	0.22674047E+10	0.36138770E+10	0.45838897E+10
14	-0.23129054E+11	-0.51357576E+11	-0.81872046E+11	-0.10495521E+12
15	0.56876611E+12	0.12598299E+13	0.20096260E+13	0.25992204E+13
16	-0.15107494E+14	-0.33404345E+14	-0.53326454E+14	-0.69525005E+14
17	0.42259638E+15	0.93595653E+15	0.14998528E+16	0.19721783E+16
18	-0.14408778E+17	-0.31119021E+17	-0.48868476E+17	-0.63863669E+17
19	0.32275602E+18	0.77677964E+18	0.13275018E+19	0.18288223E+19
20	-0.25705929E+20	-0.49572875E+20	-0.72137529E+20	-0.89681505E+20

Table 7b. Asymptotic Series for Moments of b_2* when $c = 2.1$, $a = 0$, $b = 1$

N^s	μ_1'	μ_2	μ_3	μ_4
1	-0.76653772E+00	0.53307543E+00	0.00000000E+00	0.00000000E+00
2	-0.13622315E+00	-0.31513378E+00	0.42414305E+00	0.85250825E+00
3	-0.25513113E+00	0.30142190E+00	-0.54175408E+00	-0.54631884E+00
4	0.10629377E+00	-0.62227956E+00	0.10815229E+01	0.42079527E-01
5	-0.10926932E+01	0.22788332E+01	-0.34612660E+01	0.14272741E+01
6	0.11774324E+02	-0.25259961E+02	0.35523787E+02	-0.28133440E+02
7	-0.75213885E+02	0.16823523E+03	-0.25469337E+03	0.21130414E+03
8	0.93263503E+03	-0.19779396E+04	0.28792702E+04	-0.27350607E+04
9	-0.12157728E+05	0.25731005E+05	-0.37781724E+05	0.38011792E+05
10	0.17329456E+06	-0.36501582E+06	0.53803912E+06	-0.56144208E+06
11	-0.29810372E+07	0.62249534E+07	-0.91590334E+07	0.98972354E+07
12	0.55568265E+08	-0.11566618E+09	0.17061368E+09	-0.18861713E+09
13	-0.11489413E+10	0.23823551E+10	-0.35170950E+10	0.39629734E+10
14	0.26114053E+11	-0.53976022E+11	0.79750846E+11	-0.91286141E+11
15	-0.64216946E+12	0.13241005E+13	-0.19583356E+13	0.22703091E+13
16	0.17057576E+14	-0.35090021E+14	0.51940681E+14	-0.60867305E+14
17	-0.47713457E+15	0.98075810E+15	-0.14523905E+16	0.17166386E+16
18	0.16266128E+17	-0.33212689E+17	0.49214936E+17	-0.58878863E+17
19	-0.36411951E+18	0.75367963E+18	-0.11234241E+19	0.13282242E+19
20	0.29018090E+20	-0.59146123E+20	0.86434712E+20	-0.10733751E+21

Table 8a. Padé Approximation of Moments and Percentage Points of a_2* when $c = 2.1$, $b = 1.0$, $a = 0$

N		μ_1'	σ	$\sqrt{\beta_1}$	β_2	5%	25%	50%	75%	95%
10	Padé	0.069	0.196	-0.011	3.185	-0.25	-0.06	0.07	0.20	0.39
	MC	0.070	0.196	-0.000	3.205					
11	Padé	0.063	0.187	-0.016	3.174	-0.24	-0.06	0.06	0.19	0.37
	MC	0.063	0.186	-0.030	3.139					
12	Padé	0.058	0.179	-0.019	3.164	-0.24	-0.06	0.06	0.18	0.35
	MC	0.058	0.179	-0.017	3.144					
13	Padé	0.053	0.172	-0.022	3.155	-0.23	-0.06	0.05	0.17	0.33
	MC	0.054	0.172	-0.019	3.138					
14	Padé	0.049	0.166	-0.024	3.146	-0.22	-0.06	0.05	0.16	0.32
	MC	0.050	0.166	-0.023	3.106					
15	Padé	0.046	0.160	-0.026	3.139	-0.22	-0.06	0.05	0.15	0.31
	MC	0.046	0.161	-0.022	3.122					
20	Padé	0.034	0.139	-0.031	3.110	-0.20	-0.06	0.03	0.13	0.26
	MC	0.035	0.139	-0.028	3.099					
30	Padé	0.023	0.114	-0.032	3.077	-0.17	-0.05	0.02	0.10	0.21
	MC	0.024	0.114	-0.029	3.104					
40	Padé	0.017	0.099	-0.031	3.059	-0.15	-0.05	0.02	0.08	0.18
	MC	0.018	0.099	-0.041	3.057					
50	Padé	0.014	0.088	-0.029	3.048	-0.13	-0.05	0.01	0.07	0.16
	MC	0.014	0.089	-0.029	3.076					

Table 8b. Padé Approximation of Moments and Percentage Points of b_2* when $c = 2.1$, $b = 1.0$, $a = 0$

N		μ_1'	σ	$\sqrt{\beta_1}$	β_2	5%	25%	50%	75%	95%
10	Padé	0.922	0.225	0.335	3.141	0.58	0.76	0.91	1.07	1.31
	MC	0.921	0.224	0.327	3.122					
11	Padé	0.929	0.215	0.320	3.130	0.60	0.78	0.92	1.07	1.30
	MC	0.929	0.215	0.330	3.113					
12	Padé	0.935	0.206	0.307	3.121	0.62	0.79	0.92	1.07	1.29
	MC	0.934	0.206	0.302	3.085					
13	Padé	0.940	0.198	0.295	3.112	0.63	0.80	0.93	1.07	1.28
	MC	0.939	0.199	0.296	3.118					
14	Padé	0.944	0.191	0.285	3.105	0.65	0.81	0.94	1.07	1.27
	MC	0.944	0.192	0.285	3.091					
15	Padé	0.948	0.185	0.275	3.099	0.66	0.82	0.94	1.07	1.27
	MC	0.948	0.186	0.285	3.124					
20	Padé	0.961	0.161	0.240	3.076	0.71	0.85	0.95	1.07	1.24
	MC	0.960	0.161	0.236	3.068					
30	Padé	0.974	0.132	0.197	3.052	0.76	0.88	0.97	1.06	1.20
	MC	0.973	0.132	0.193	3.061					
40	Padé	0.981	0.115	0.171	3.039	0.80	0.90	0.98	1.06	1.17
	MC	0.980	0.115	0.194	3.070					
50	Padé	0.985	0.103	0.153	3.032	0.82	0.91	0.98	1.05	1.16
	MC	0.984	0.103	0.157	3.057					

Table 9. The Extended K_{Ic} Database Binned into 16 Groups

Bin	(T-RT_{NDT}) (°F)	Static Initiation Toughness Data, K_{Ic} (ksi-√in.)
1	-385	31.6,32.5
	-370	39.6,27.5,47.5
	-320	25.9,23.7,30.3
2	-315	40.9,37.1,44.0,40.8,31.2
	-300	43.2,47.9,41.6,51.3
3	-275	29.7,27.2
	-265	30.6,29.0,35.6,42.8
	-250	37.3,35.2,40.4,30.5,44.2,55.0,43.3,37.3
4	-228.6	35.09,35.45,37.82,25.36,26.18,29.27,29.45,30.18,31.00,32.82
		33.82,36.00,36.36,32.09,33.73,34.27,34.91,35.09,36.00,37.45
		37.45,39.55,39.73,40.36,42.36,43.73,46.45,49.55,49.64,30.09
		33.00,36.55,37.00,39.36,39.91,40.91,41.45,42.18,46.45,48.64
		53.18
	-225	37.29,39.89,44.22
5	-215	46.9,66.9
	-208.8	34.64,37.82,38.18,39.45
	-205	37.6,37.8,43.6,55.6
	-201	52.2,45.5
6	-200	46.6,35.1,45.2,30.5,37.5,41.0,31.2,30.8,44.0,34.6,
		39.9,38.5,44.4,34.6,39.9,34.8,71.2,57.2,45.63,44.63,
		42.81,33.45,32.36
7	-190	47.2,40.9,42.5,42.5
	-180	40.1,52.8,66.2
	-176	46.0,64.3,50.0,45.6,68.0
	-175	55.8,43.5,56.2
8	-171	36.45,34.91
	-170	43.9,39.4,31.3,47.3,50.4,41.2,54.0,50.9,35.5,33.2,37.2,37.1,37.1
		34.7,35.0,32.6,29.4,44.0,31.4,39.3,31.3,33.0,38.1,31.1,44.9,39.4
9	-155	70.7
	-153	43.36
	-150	56.1,29.7,31.5,41.2,30.5,42.1,37.7,40.7,44.1,37.4,41.8,56.0
	-148	38.09
10	-140.4	42.55
	-140	52.0,64.6,56.6
	-139	33.45,39.27,40.09
	-125	61.1,39.1,48.3,43.4,38.1
11	-110	49.81
	-102.6	45.09,58.73,67.64
	-100	96.0,55.2,51.4,59.0,56.2,50.2,42.2,48.5,48.5,54.8,54.4,48.3
		48.3,41.9,49.7

Bin	(T-RT_{NDT}) (°F)	Static Initiation Toughness Data, K_{Ic} (ksi-√in.)
12	-93.6	32.64,55.82,53.73,62.09,70.82
	-90	64.7,62.4
	-82.8	58.18,60.64,65.55
	-76	45.0
	-75	90.3,93.1,50.3,46.6
	-63.0	63.30
13	-51	107.0
	-50	72.6,71.6,65.1,65.0,67.5,65.0,56.7,64.6,64.7
	-48.6	63.27,73.82,90.91
14	-30	81.0
	-28.8	66.09,75.55,76.45
	-25	105.9,61.0,58.7,45.9
	-12.6	93.45
15	0	113.1,66.4,93.7,83.4,73.9,66.9,87.2,87.5
16	9.0	69.37
	14.4	74.64
	25	98.9,74.5,90.5,110.3
	50	148.6,137.3,139.0

Table 10. Sixteen K_{Ic} Datasets Fitted to Weibull Density

Bin	N	$\overline{T}$(°F)	m_1'	$\sqrt{m_2}$	$a_2^*(T)$	$a_2^{**}(T)$	$b_2^*(T)$	$b_2^{**}(T)$	$c(T)$	χ^2	$E(b^*_2/b)$
1	8	-355.00	32.33	7.81	22.91	21.60	10.20	11.61	1.3	2.37	0.878
2	9	-308.33	42.00	5.81	23.80	20.17	12.37	13.49	3.7	2.30	0.917
3	14	-257.86	37.00	7.66	24.82	24.04	13.66	14.53	1.7	2.42	0.940
4	44	-228.35	37.76	6.30	25.31	25.09	14.06	14.30	2.1	0.63	0.983
5	12	-207.27	44.68	9.49	26.52	22.83	20.51	24.65	2.1	1.34	0.935
6	23	-200.00	40.69	9.29	26.50	25.93	15.83	16.46	1.6	3.14	0.962
7	15	-180.33	50.77	9.41	27.25	26.04	26.42	27.78	2.8	1.01	0.951
8	28	-170.07	38.56	6.57	27.70	27.37	11.94	12.31	1.7	0.47	0.970
9	15	-150.40	42.73	10.91	28.16	27.97	15.99	16.20	1.4	5.54	0.937
10	12	-133.53	46.55	9.96	29.96	28.75	18.65	20.01	1.8	2.13	0.932
11	19	-100.94	53.99	11.91	31.82	30.87	25.02	26.09	2.0	2.45	0.959
12	16	-83.46	60.95	15.27	31.39	29.87	33.37	35.09	2.1	1.46	0.951
13	13	-49.75	71.37	13.43	34.80	32.59	40.89	43.36	3.1	11.78	0.943
14	9	-25.44	73.78	18.40	36.16	42.47	47.84	51.61	2.6	0.24	0.915
15	8	0.00	84.01	15.44	38.38	33.65	50.71	55.97	3.5	0.61	0.906
16	9	30.38	104.79	30.61	42.20	36.38	70.66	77.22	2.3	1.48	0.915

Table 11. The Extended K_{Ia} Database Binned into Four Groups

Bin	(T-RT_{NDT}) (°F)	Crack Arrest Toughness, K_{Ia} (ksi-vin.)
1	-150	28.0
	-70	43.0, 48.0, 43.0
	-67.8	60.1
	-66	48.2, 69.2
	-64.2	51.9
	-47.8	62.8
	-46	52.8
	-44.2	65.5
	-42.6	61.0, 64.6
	-39	66.4, 67.3 69.2, 83.7
	-36.2	63.7
2	-19	47.3, 66.4, 68.3, 77.4
	-18.2	79.0
	-17.2	64.6
	-15.6	83.7
	-12	54.6, 55.5, 77.4, 82.8, 89.2, 94.6, 97.4
	-0.2	97.1
	0.0	68.0, 58.0, 48.0, 57.0, 62.0, 58.0, 60.0, 65.0, 60.0, 58.0, 53.0, 58.0, 70.0, 57.0, 57.0, 61.0
3	4.4	77.4
	6.2	68.3
	8	61.0, 72.8, 91.0
	9.8	70.1, 81.0
	13.2	88.3
	15	85.5, 85.5, 86.5, 93.7
	16.8	82.8
	17.8	119.7
	22	68.0
	33.2	100.1
	35	59.0, 84.0, 62.0, 106.5, 111.9, 112.8
	38.4	93.7
	40.2	113.8
	40.4	101.0
	42	84.6, 97.4, 103.7
	43.8	98.3
4	49.2	113.8
	50	92.0, 73.0, 75.0
	51	104.7
	53	91.9
	71	97.4, 101.9, 102.8, 108.3

Bin	(T-RT_{NDT}) (°F)	Crack Arrest Toughness, K_{Ia} (ksi-vin.)
	75	94.0, 107.0, 77.0, 81.0, 91.0, 101.0
	80	109.0
	83	87.0, 94.0, 107.0, 111.0
	89	120.1
	96	111.0
	102	117.0
	105	118.0, 103.0, 107.0, 130.0
	107	87.0
	110	88.0, 88.0
	112	112.0
	115	111.0
	121	116.0

Table 12. Four K_{Ia} Datasets Fitted to Weibull Density

Bin	N	$\overline{T}$(°F)	m_1'	$\sqrt{m_2}$	$a_2^*(T)$	$a_2^{**}(T)$	$b_2^*(T)$	$b_2^{**}(T)$	$c(T)$	χ^2	$E(b^*_2/b)$
1	18	-52.32	60.02	10.51	35.46	34.33	27.68	28.95	2.5	2.63	0.956
2	31	-6.81	67.27	13.92	34.74	33.94	36.67	37.56	2.5	4.87	0.976
3	29	24.69	88.29	16.45	49.86	48.85	43.32	44.45	2.5	0.96	0.974
4	34	83.27	100.82	13.66	68.89	68.18	35.99	36.78	2.5	1.69	0.978

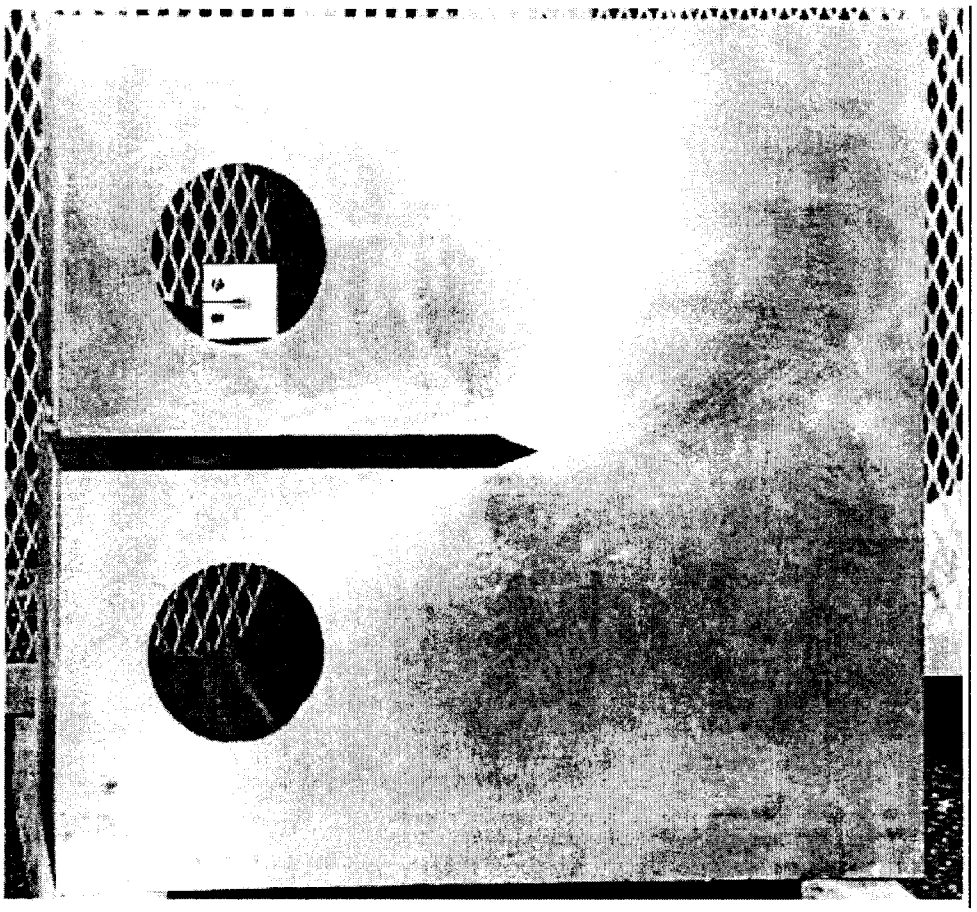

Fig. 1. Two compact fracture toughness specimens, C(T), with $W = 5.1$ cm for the smaller specimen and $W = 61$ cm for the larger (adapted from Fig. 8.28 in Ref. [11]).

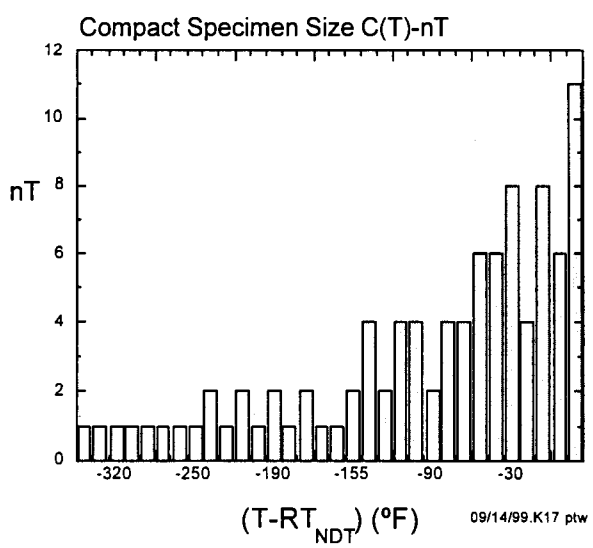

Fig. 2. Size distribution of C(T) specimens in the EPRI K_{Ic} database [1].

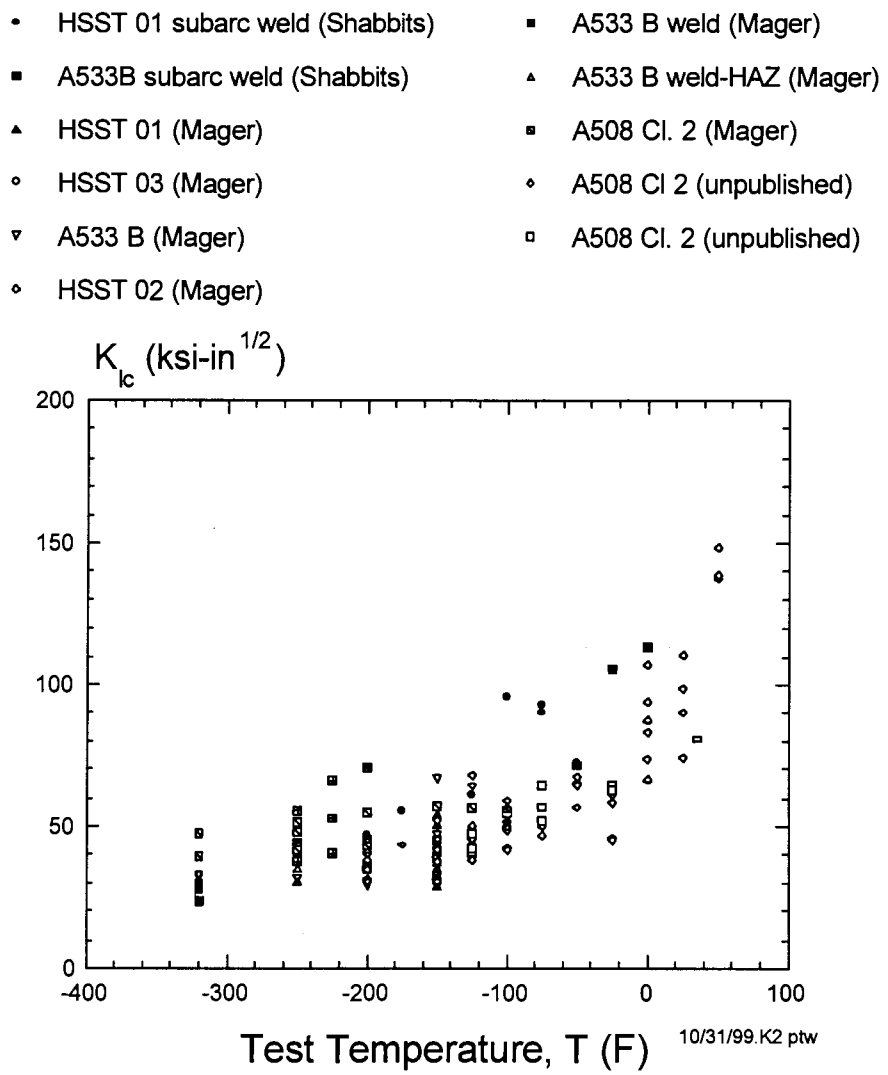

(a)

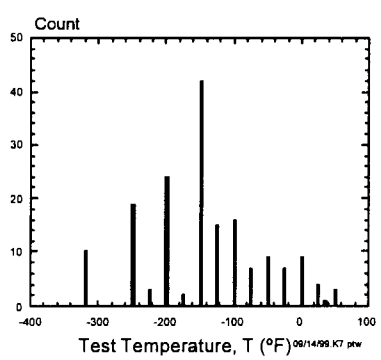

(b)

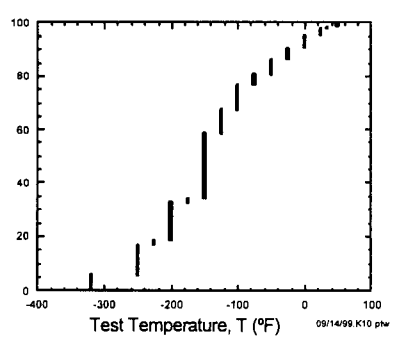

(c)

Fig. 3. Distribution of EPRI data base with test temperature: (a) K_{Ic} data, (b) frequency histogram and (c) cumulative frequency distribution.

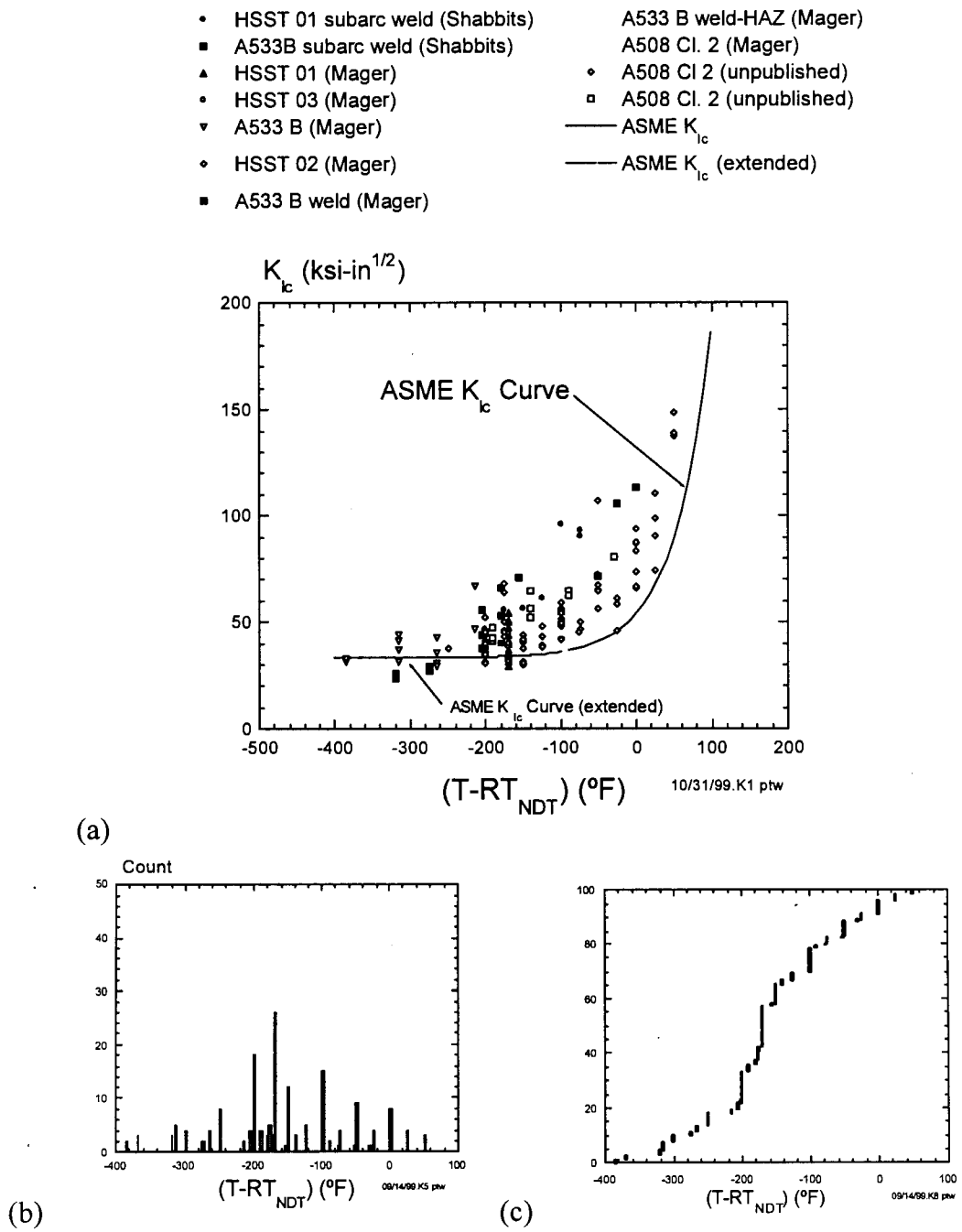

Fig. 4 Distribution of EPRI K_{Ic} database with normalized temperature ($T - RT_{NDT}$): (a) K_{Ic} data, (b) frequency histogram, and (c) cumulative frequency distribution.

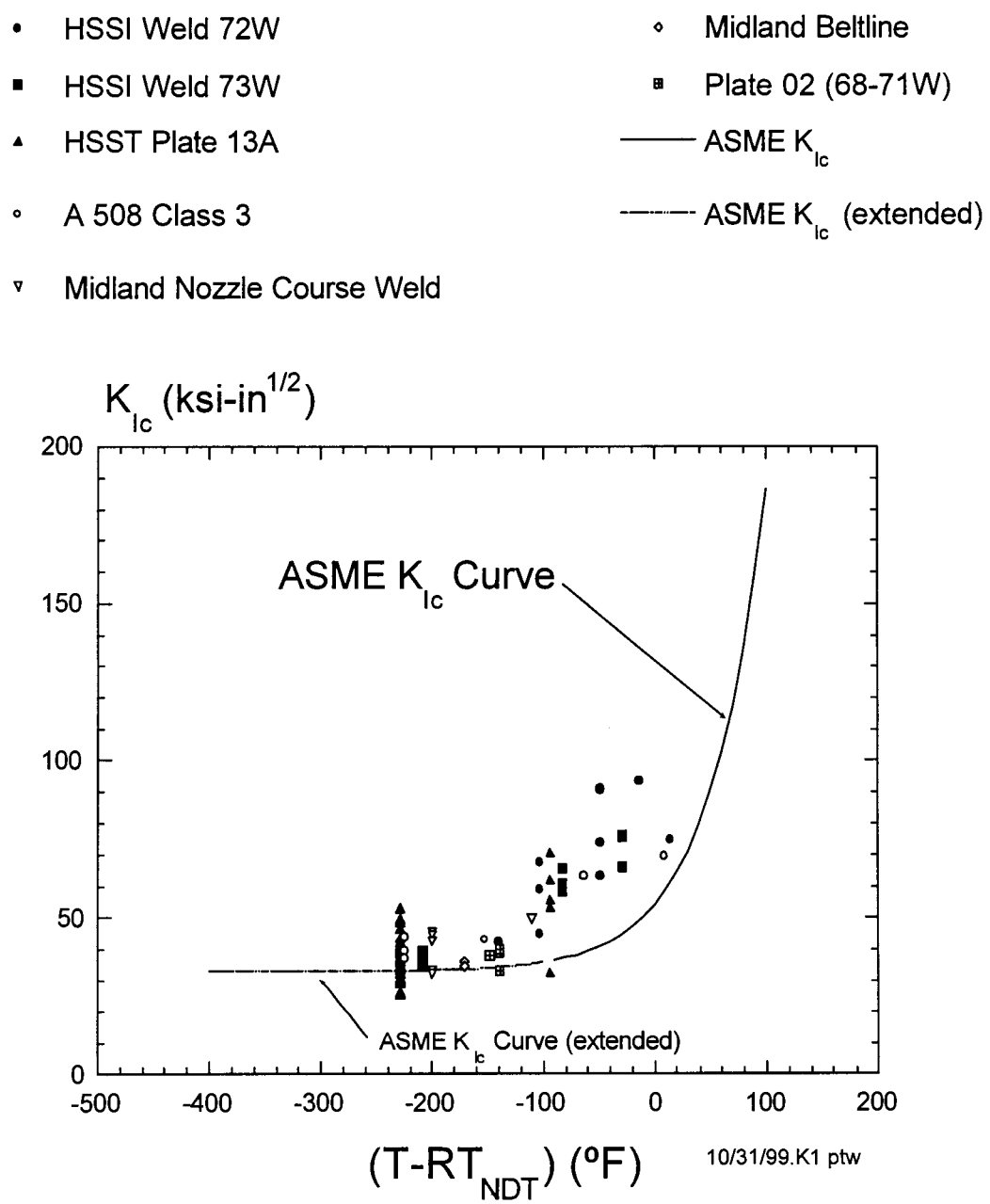

Fig. 5. Additional K_{Ic} data.

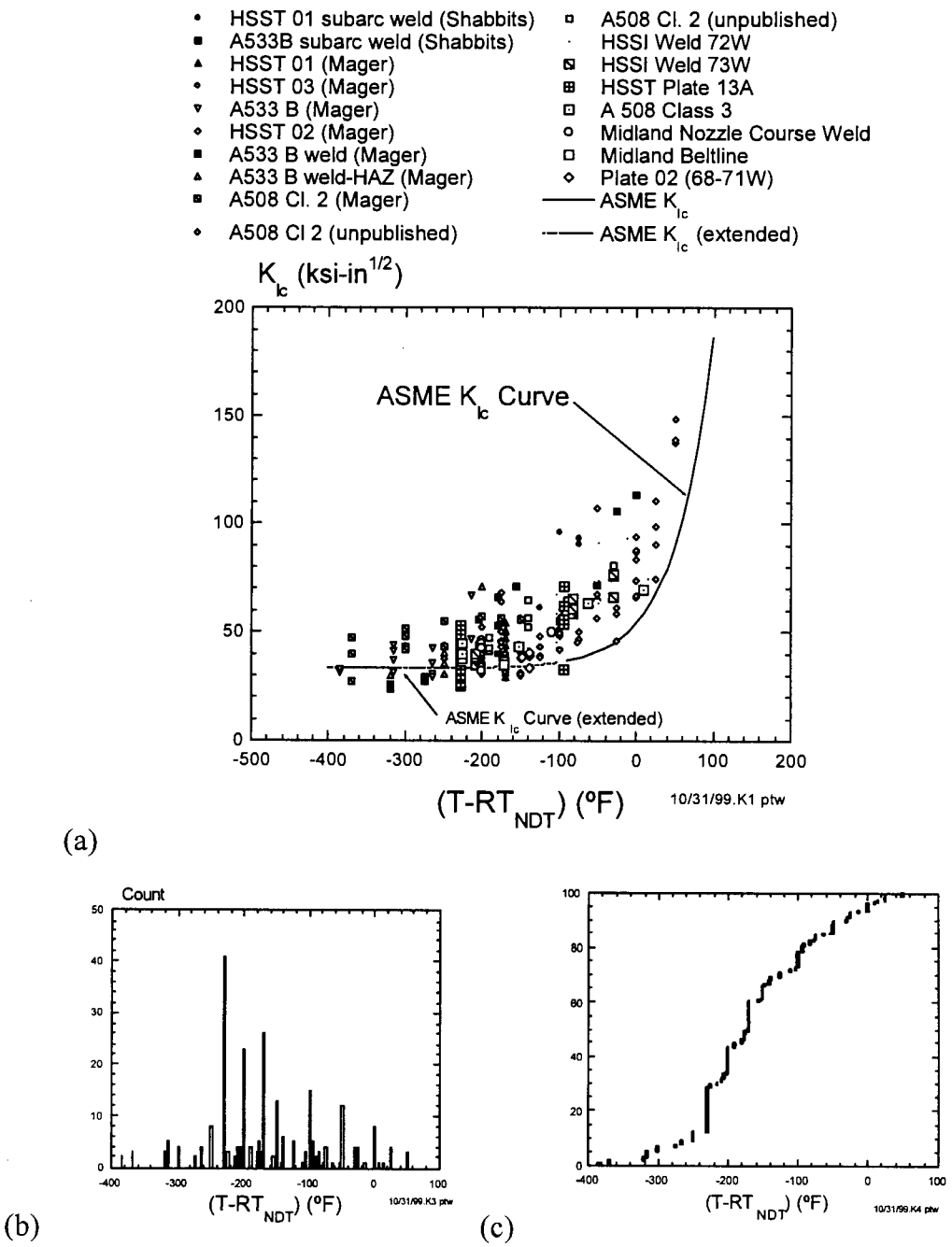

Fig. 6 Distribution of extended K_{Ic} database with normalized temperature $(T - RT_{NDT})$: (a) K_{Ic} data, (b) frequency histogram, and (c) cumulative frequency distribution.

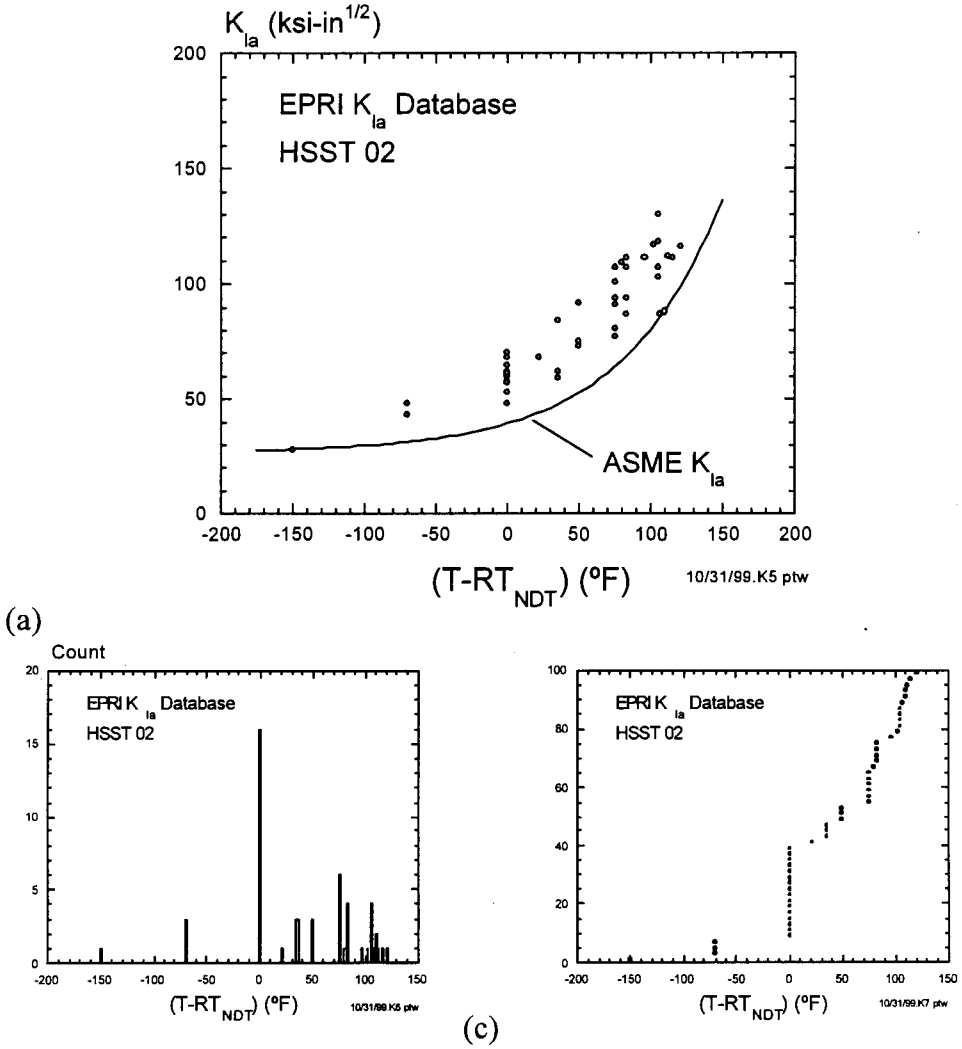

Fig. 7. Distribution of EPRI K_{Ia} database with normalized temperature $(T - RT_{NDT})$: (a) K_{Ia} data, (b) frequency histogram, and (c) cumulative frequency distribution.

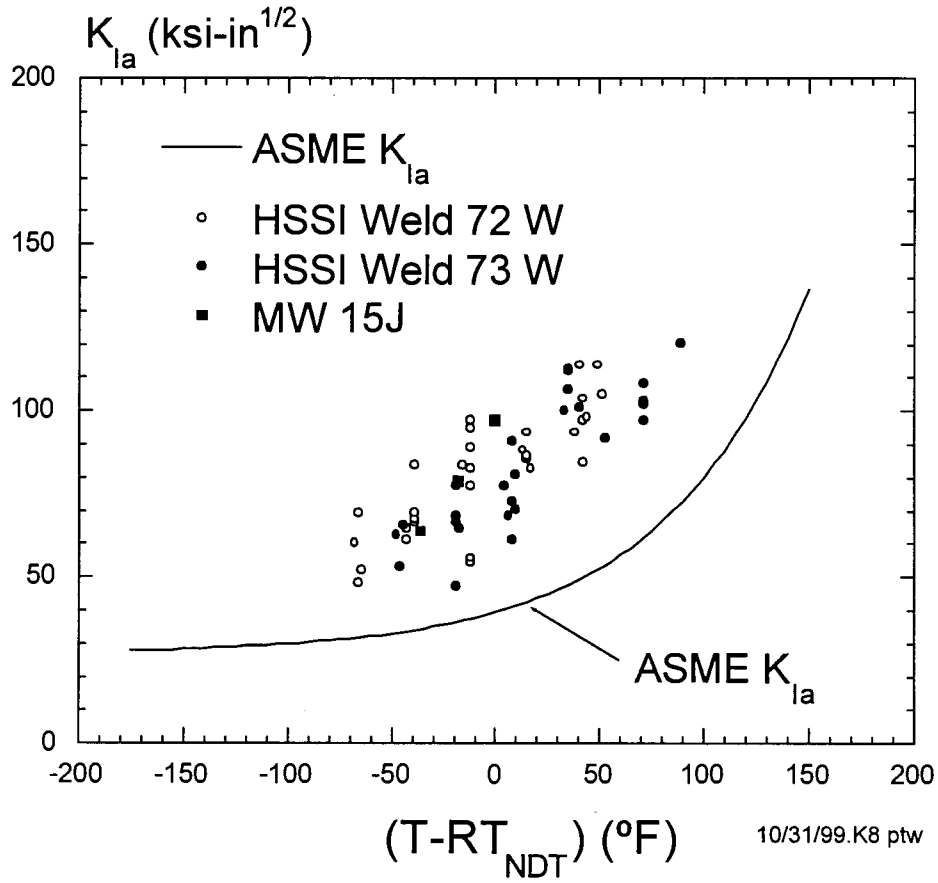

Fig. 8. Additional K_{Ia} data.

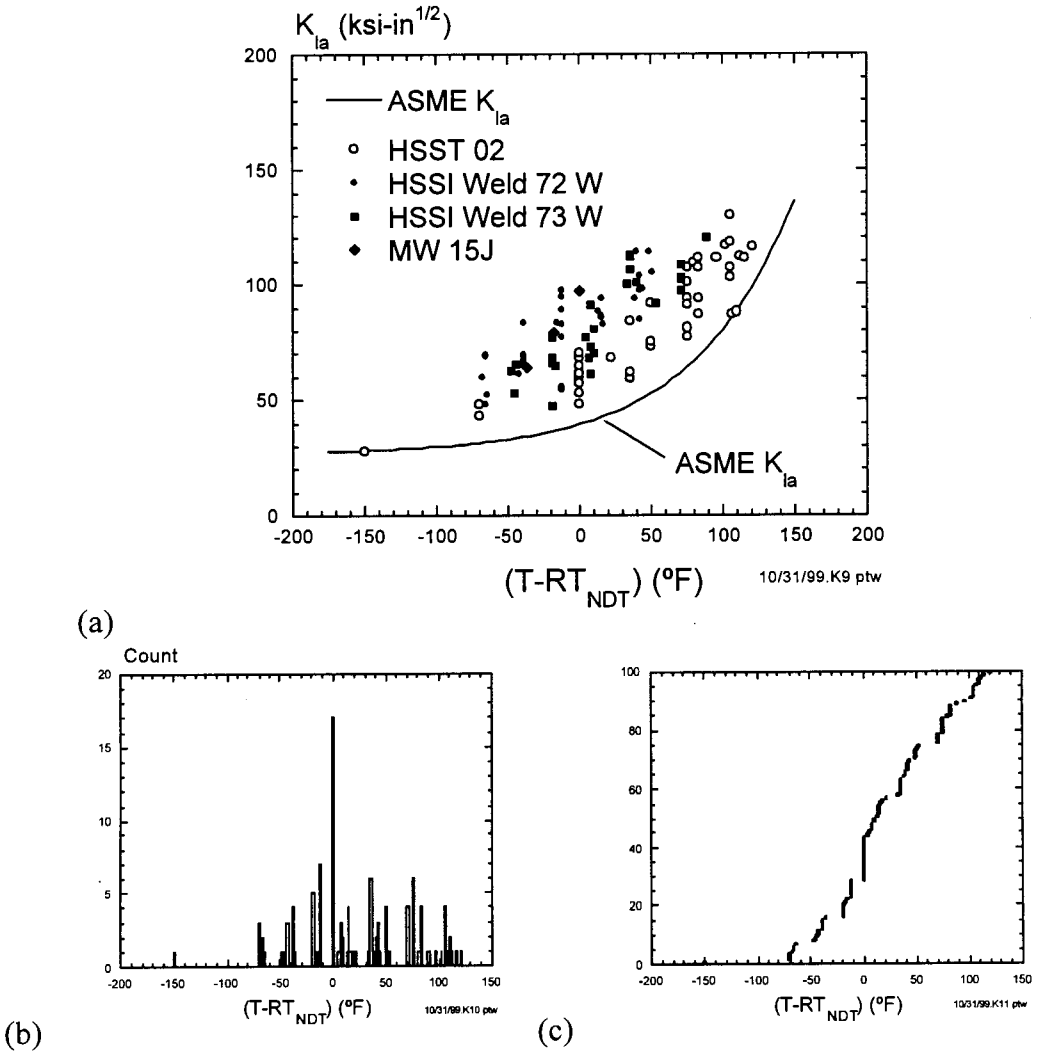

Fig. 9 Distribution of extended K_{Ia} database with normalized temperature ($T - RT_{NDT}$): (a) K_{Ia} data, (b) frequency histogram, and (c) cumulative frequency distribution.

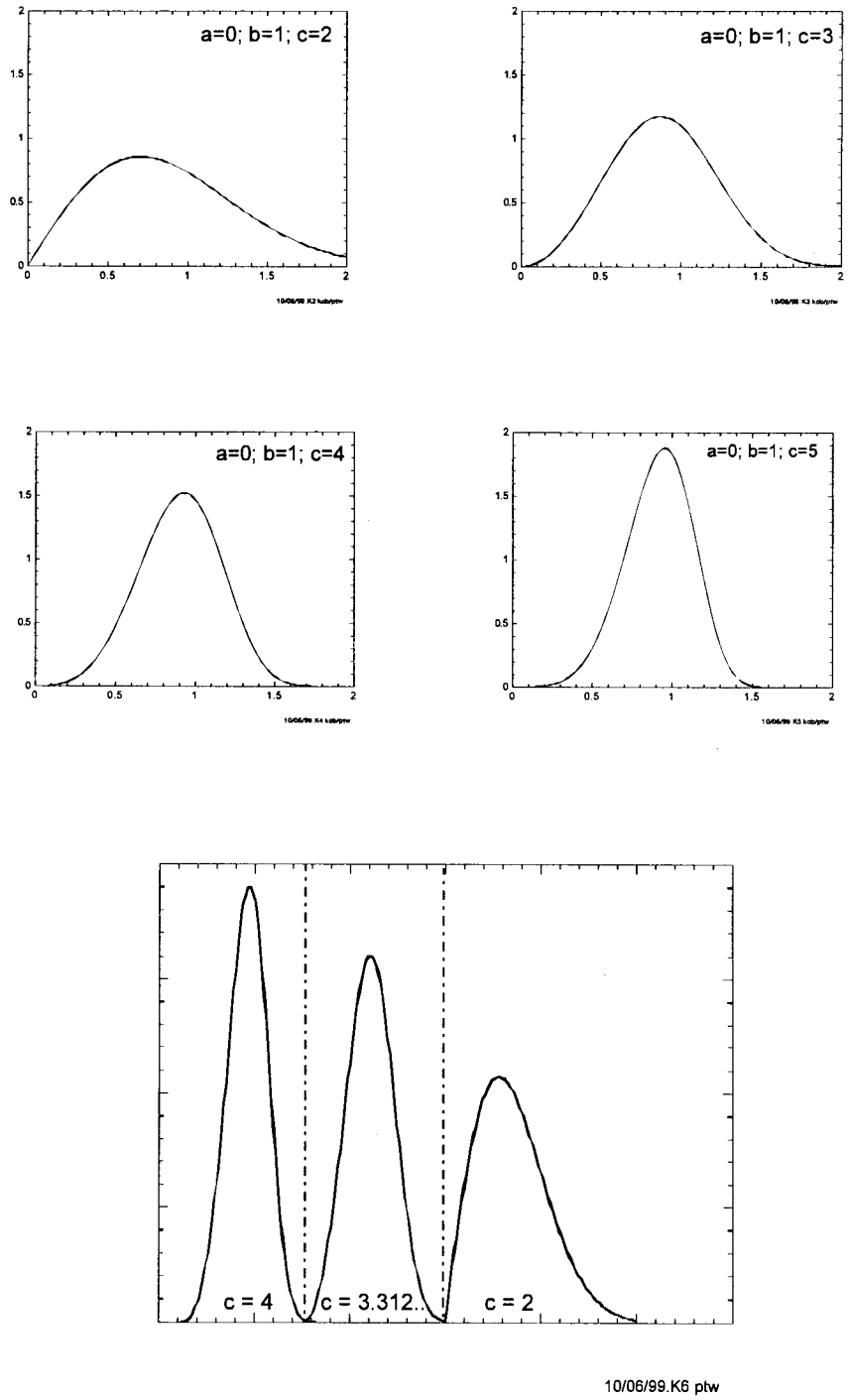

Fig. 10. Weibull densities for the standard case ($a = 0$, $b = 1$).

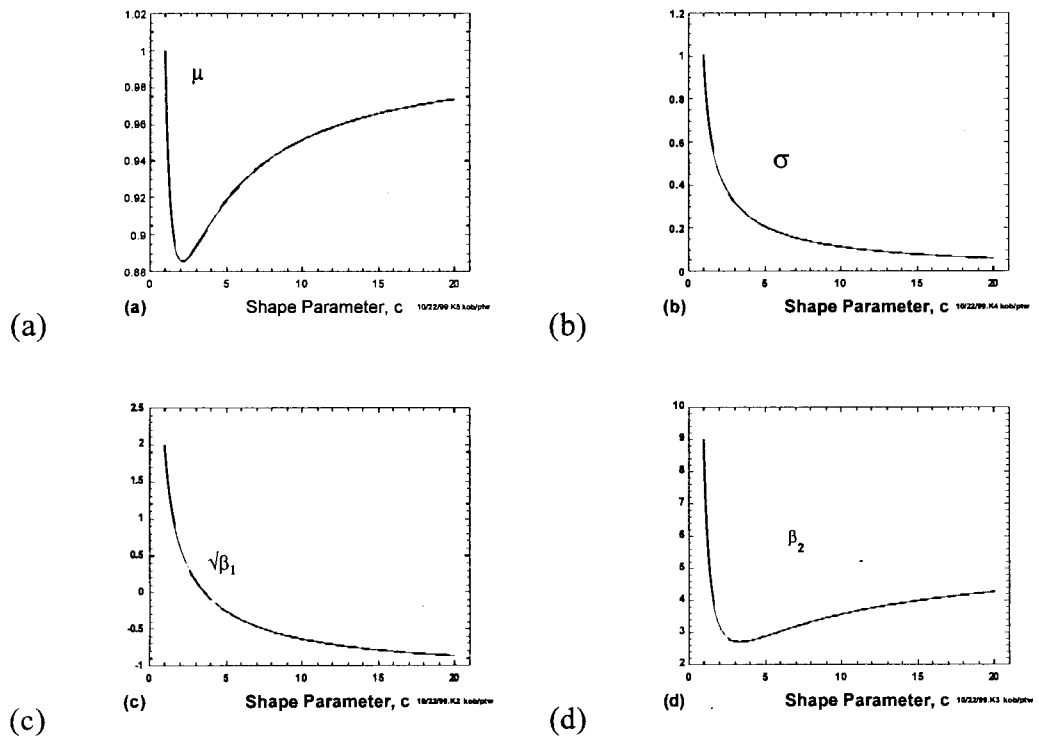

Fig. 11. (a) Mean, (b) standard deviation, (c) skewness, and (d) kurtosis of Weibull random variates.

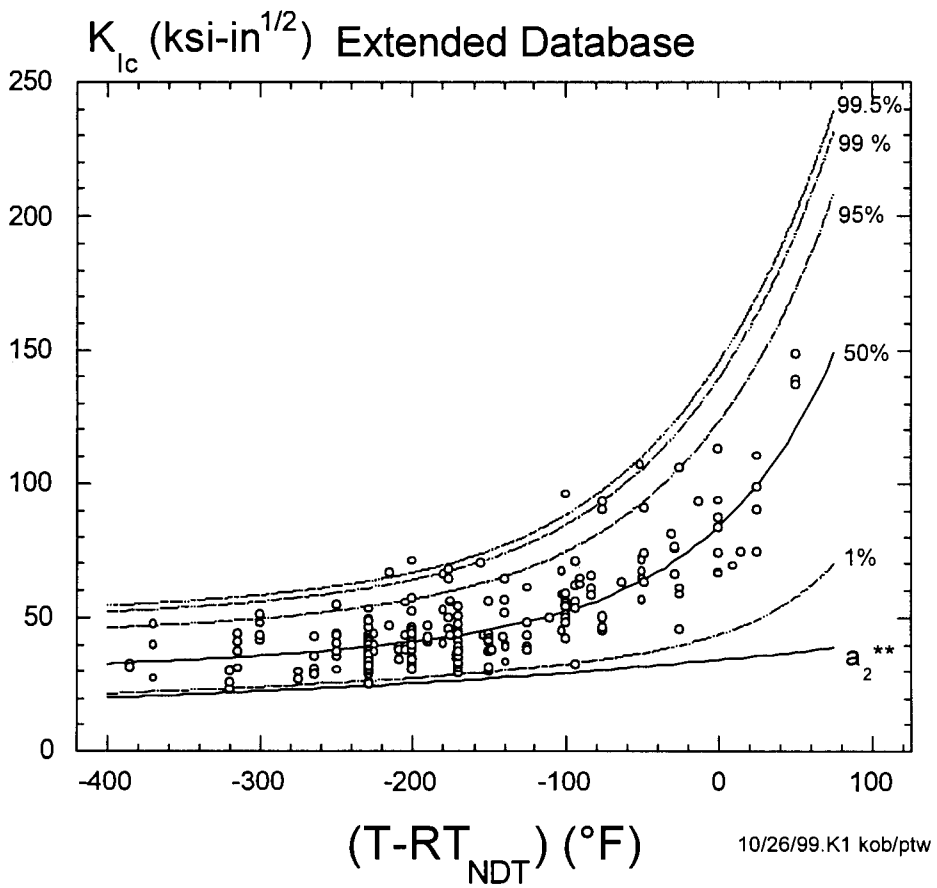

Fig. 12. Weibull model of K_{Ic} fracture toughness vs. normalized temperature (T - RT_{NDT}).

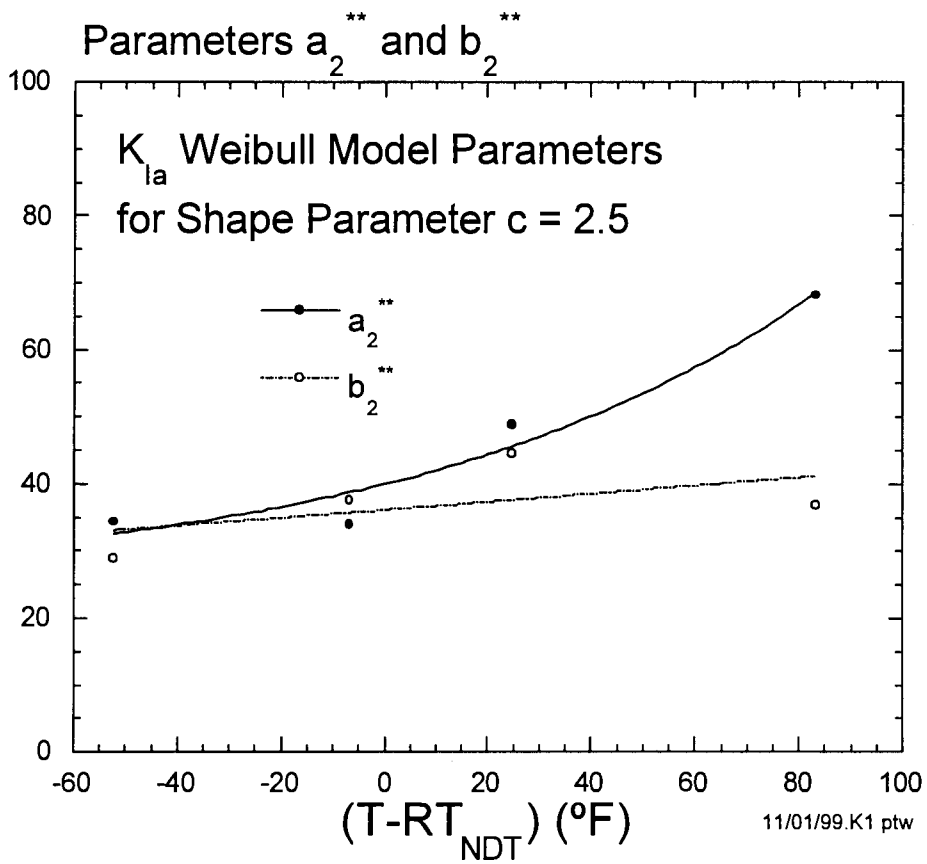

Fig. 13. Point estimates of Weibull location and scale parameters for a given shape parameter, c = 2.5. Point estimation by method of moments.

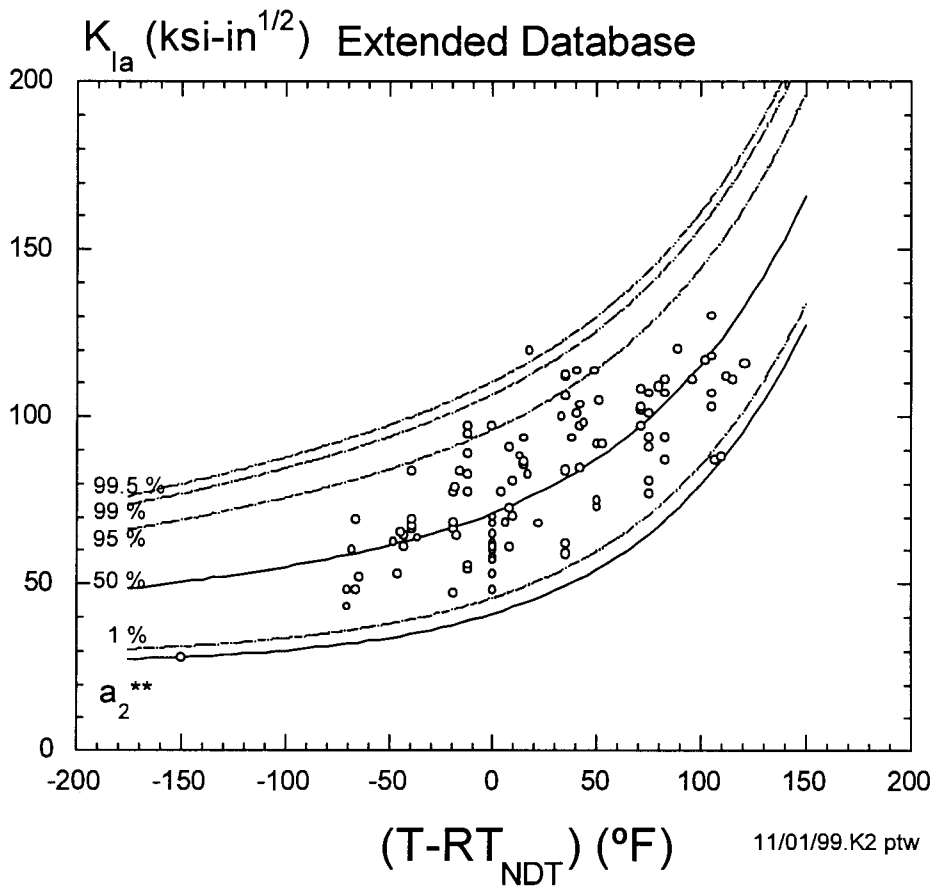

Fig. 14. Weibull model of K_{Ia} fracture toughness vs. normalized temperature (T - RT_{NDT}).

Appendix A – Listings of K_{Ic} and K_{Ia} Extended Databases

Table A1 – Static Initiation Toughness K_{Ic} Extended Database

Table A2 - Crack Arrest Toughness K_{Ia} Extended Database

Table A1. Static Initiation Toughness K_{Ic} Extended Database

Material	Reference Source	Specimen ID	Type No.	Orientation	Temp (°F)	RT_{NDT} (°F)	T - RT_{NDT} (°F)	K_{Ic} (ksivin)
HSST 01	Shabbits	1T-CT	1		-200	0	-200	46.6
subarc	(1969)	1T-CT	1		-175	0	-175	55.8
weldment		4T-CT	4		-150	0	-150	56.1
		4T-CT	4		-125	0	-125	61.1
		4T-CT	4		-100	0	-100	96.0
		4T-CT	4		-75	0	-75	90.3
		4T-CT	4		-75	0	-75	93.1
		6T-CT	6		-50	0	-50	72.6
A533B Class 1	Shabbits	1T-CT	1		-200	0	-200	35.1
subarc	(1969)	1T-CT	1		-200	0	-200	45.2
weldment		1T-CT	1		-320	0	-320	25.9
		1T-CT	1		-320	0	-320	23.7
		4T-CT	4		-100	0	-100	55.2
		4T-CT	4		-50	0	-50	71.6
		4T-CT	4		-25	0	-25	105.9
		8T-CT	8		0	0	0	113.1
HSST 01	Mager (1969)	1T-CT	1	RW	-150	20	-170	43.9
		1T-CT	1	RW	-150	20	-170	39.4
		1T-CT	1	RW	-150	20	-170	31.3
		1T-CT	1	RW	-150	20	-170	47.3
		1T-CT	1	RW	-150	20	-170	50.4
		1T-CT	1	RW	-150	20	-170	41.2
		1T-CT	1	RW	-150	20	-170	54.0
		1T-CT	1	RW	-150	20	-170	50.9
		1T-CT	1	RW	-150	20	-170	35.5
		1T-CT	1	RW	-150	20	-170	33.2
		1T-CT	1	RW	-150	20	-170	37.2
		1T-CT	1	RW	-150	20	-170	37.1
		1T-CT	1	RW	-150	20	-170	37.1
		1T-CT	1	RW	-150	20	-170	34.7
		1T-CT	1	RW	-150	20	-170	35.0
		1T-CT	1	RW	-150	20	-170	32.6
		1T-CT	1	RW	-150	20	-170	29.4
HSST 03	Mager (1969)	1T-CT	1	RW	-150	20	-170	44.0
		1T-CT	1	RW	-150	20	-170	31.4
		1T-CT	1	RW	-150	20	-170	39.3
		1T-CT	1	RW	-150	20	-170	31.3
		1T-CT	1	RW	-150	20	-170	33.0
		1T-CT	1	RW	-150	20	-170	38.1
		1T-CT	1	RW	-150	20	-170	31.1
		1T-CT	1	RW	-150	20	-170	44.9
		1T-CT	1	RW	-150	20	-170	39.4
A533B Class 1	Mager (1969)	1X-WOL	1	RW	-320	65	-385	31.6
		1T-WOL	1	RW	-320	65	-385	32.5
		1X-WOL	1	RW	-250	65	-315	40.9
		1X-WOL	1	RW	-250	65	-315	37.1
		1X-WOL	1	RW	-250	65	-315	44.0
		1T-WOL	1	RW	-250	65	-315	40.8
		1T-WOL	1	RW	-250	65	-315	31.2

Material	Reference Source	Specimen ID	Type No.	Orientation	Temp (°F)	RT_{NDT} (°F)	T - RT_{NDT} (°F)	K_{Ic} (ksivin)
		1X-WOL	1	RW	-200	65	-265	30.6
		1X-WOL	1	RW	-200	65	-265	29.0
		1T-WOL	1	RW	-200	65	-265	35.6
		1T-WOL	1	RW	-200	65	-265	42.8
		2T-WOL	2	RW	-150	65	-215	46.9
		2T-WOL	2	RW	-150	65	-215	66.9
HSST 02	Mager (1969)	1X-WOL	1	RW	-200	0	-200	30.5
		1X-WOL	1	RW	-200	0	-200	37.5
		1X-WOL	1	RW	-200	0	-200	41.0
		1T-WOL	1	RW	-200	0	-200	31.2
		1T-WOL	1	RW	-200	0	-200	30.8
		1T-WOL	1	RW	-175	0	-175	43.5
		1X-WOL	1	RW	-150	0	-150	29.7
		1X-WOL	1	RW	-150	0	-150	31.5
		1X-WOL	1	RW	-150	0	-150	41.2
		1X-WOL	1	RW	-150	0	-150	30.5
		1X-WOL	1	RW	-125	0	-125	39.1
		1T-WOL	1	RW	-125	0	-125	48.3
		1T-WOL	1	RW	-125	0	-125	43.4
		1T-WOL	1	RW	-125	0	-125	38.1
		2T-WOL	2	RW	-100	0	-100	51.4
		2T-WOL	2	RW	-100	0	-100	59.0
		2T-WOL	2	RW	-100	0	-100	56.2
		2T-WOL	2	RW	-100	0	-100	50.2
		2T-WOL	2	RW	-50	0	-50	65.1
		2T-WOL	2	RW	-50	0	-50	65.0
		2T-WOL	2	RW	-50	0	-50	67.5
		2T-WOL	2	RW	-50	0	-50	65.0
		1X-WOL	1	RW	-250	0	-250	37.3
		1X-WOL	1	RW	-200	0	-200	44.0
		1X-WOL	1	RW	-200	0	-200	34.6
		1X-WOL	1	RW	-200	0	-200	39.9
		1X-WOL	1	RW	-200	0	-200	38.5
		1T-CT	1	RW	-150	0	-150	42.1
		1T-CT	1	RW	-150	0	-150	37.7
		1T-CT	1	RW	-150	0	-150	40.7
		1T-CT	1	RW	-100	0	-100	42.2
		1T-CT	1	RW	-100	0	-100	48.5
		1T-CT	1	RW	-100	0	-100	48.5
		1T-CT	1	RW	-75	0	-75	50.3
		1T-CT	1	RW	-75	0	-75	46.6
		1T-CT	1	RW	-100	0	-100	54.8
		1T-CT	1	RW	-100	0	-100	54.4
		2T-WOL	2	RW	-50	0	-50	56.7
		2T-WOL	2	RW	0	0	0	66.4
		2T-WOL	2	RW	0	0	0	93.7
		2T-WOL	2	RW	0	0	0	83.4
A533B Class 1 weld	Mager (1969)	1X-WOL	1		-320	-45	-275	29.7
		1X-WOL	1		-320	-45	-275	27.2
		1X-WOL	1		-250	-45	-205	37.6
		1X-WOL	1		-250	-45	-205	37.8
		1T-WOL	1		-250	-45	-205	43.6
		2T-WOL	2		-250	-45	-205	55.6
		1T-WOL	1		-225	-45	-180	40.1

Material	Reference Source	Specimen ID	Type No.	Orientation	Temp (°F)	RT_{NDT} (°F)	T - RT_{NDT} (°F)	K_{Ic} (ksivin)
		1T-WOL	1		-225	-45	-180	52.8
		2T-WOL	2		-225	-45	-180	66.2
		2T-WOL	2		-200	-45	-155	70.7
A533B Class 1 weld-HAZ	Mager (1969)	1X-WOL	1		-320	0	-320	30.3
		1X-WOL	1		-250	0	-250	35.2
		1X-WOL	1		-250	0	-250	40.4
		1T-WOL	1		-250	0	-250	30.5
		1T-WOL	1		-250	0	-250	44.2
		2T-WOL	2		-200	0	-200	71.2
A508 Class 2 European Forging "ring forging"	Mager (1969)	1X-WOL	1		-320	50	-370	39.6
		1X-WOL	1		-320	50	-370	27.5
		1T-WOL	1		-320	50	-370	47.5
		1X-WOL	1		-250	50	-300	43.2
		1X-WOL	1		-250	50	-300	47.9
		1X-WOL	1		-250	50	-300	41.6
		1T-WOL	1		-250	50	-300	51.3
		1T-WOL	1		-200	50	-250	55.0
		2T-WOL	2		-200	50	-250	43.3
		2T-WOL	2		-150	50	-200	57.2
		2T-WOL	2		-125	50	-175	56.2
		2T-WOL	2		-100	50	-150	56.0
HSST 02	Shabbits (1969)	6T-CT	6	RW	25	0	25	98.9
		6T-CT	6	RW	25	0	25	74.5
		6T-CT	6	RW	25	0	25	90.5
		6T-CT	6	RW	0	0	0	73.9
		6T-CT	6	RW	0	0	0	66.9
		11T-CT	11	RW	50	0	50	148.6
		10T-CT	10	RW	50	0	50	137.3
		10T-CT	10	RW	50	0	50	139.0
		4T-CT	4	RW	0	0	0	87.2
		4T-CT	4	RW	-25	0	-25	61.0
		4T-CT	4	RW	-25	0	-25	58.7
		4T-CT	4	RW	-25	0	-25	45.9
		10T-CT	10	RW	0	0	0	87.5
		10T-CT	10	RW	25	0	25	110.3
		1T-CT	1	RW	-250	0	-250	37.3
		1T-CT	1	RW	-200	0	-200	44.4
		1T-CT	1	RW	-200	0	-200	34.6
		1T-CT	1	RW	-200	0	-200	39.9
		1T-CT	1	RW	-200	0	-200	34.8
		1T-CT	1	RW	-150	0	-150	44.1
		1T-CT	1	RW	-150	0	-150	37.4
		1T-CT	1	RW	-150	0	-150	41.8
		1T-CT	1	RW	-100	0	-100	48.3
		1T-CT	1	RW	-100	0	-100	48.3
		1T-CT	1	RW	-100	0	-100	41.9
		2T-CT	2	RW	-100	0	-100	49.7
		2T-CT	2	RW	-50	0	-50	64.6
		2T-CT	2	RW	-50	0	-50	64.7
A508 Class 2	unpublished outside of EPRI NP-719-SR	2T-CT	2		-150	51	-201	52.2
		2T-CT	2		-150	51	-201	45.5
		2T-CT	2		-125	51	-176	46.0
		2T-CT	2		-125	51	-176	64.3
		2T-CT	2		-125	51	-176	50.0

Material	Reference Source	Specimen ID	Type No.	Orientation	Temp (°F)	RT_{NDT} (°F)	T - RT_{NDT} (°F)	K_{Ic} (ksivin)
		4T-CT	4		-25	51	-76	45.0
		6T-CT	6		0	51	-51	107.0
		2T-CT	2		-125	51	-176	45.6
		2T-CT	2		-125	51	-176	68.0
A508 Class 2	unpublished	2T-CT	2		-75	65	-140	52.0
	outside of	2T-CT	2		-75	65	-140	64.6
	EPRI NP-719-SR	2T-CT	2		-75	65	-140	56.6
		2T-CT	2		-25	65	-90	64.7
		2T-CT	2		-25	65	-90	62.4
		8T-CT	8		35	65	-30	81.0
		2T-CT	2		-125	65	-190	47.2
		2T-CT	2		-125	65	-190	40.9
		2T-CT	2		-125	65	-190	42.5
		2T-CT	2		-125	65	-190	42.5
HSSI Weld	NUREG/CR-	1T-CT	1	T-L	-238	-9.4	-228.6	35.09
72W	5913	1T-CT	1	T-L	-238	-9.4	-228.6	35.45
		1T-CT	1	T-L	-238	-9.4	-228.6	37.82
		1T-CT	1	T-L	-149.8	-9.4	-140.4	42.55
		1T-CT	1	T-L	-112	-9.4	-102.6	45.09
		2T-CT	2	T-L	-112	-9.4	-102.6	58.73
		2T-CT	2	T-L	-112	-9.4	-102.6	67.64
		2T-CT	2	T-L	-58	-9.4	-48.6	63.27
		4T-CT	4	T-L	-58	-9.4	-48.6	73.82
		4T-CT	4	T-L	-58	-9.4	-48.6	90.91
		4T-CT	4	T-L	-22	-9.4	-12.6	93.45
		4T-CT	4	T-L	5	-9.4	14.4	74.64
HSSI	NUREG/CR-	1T-CT	1	T-L	-238	-29.2	-208.8	34.64
73W	5913	1T-CT	1	T-L	-238	-29.2	-208.8	37.82
		1T-CT	1	T-L	-238	-29.2	-208.8	38.18
		1T-CT	1	T-L	-238	-29.2	-208.8	39.45
		2T-CT	2	T-L	-112	-29.2	-82.8	58.18
		2T-CT	2	T-L	-112	-29.2	-82.8	60.64
		2T-CT	2	T-L	-112	-29.2	-82.8	65.55
		2T-CT	2	T-L	-58	-29.2	-28.8	66.09
		4T-CT	4	T-L	-58	-29.2	-28.8	75.55
		4T-CT	4	T-L	-58	-29.2	-28.8	76.45
HSST Plate 13	NUREG/CR-	1T-CT	1	L-T	-103	-9.4	-93.6	32.64
	5788 (A533B	2T-CT	2	L-T	-103	-9.4	-93.6	55.82
	Plate 13A)	4T-CT	4	L-T	-103	-9.4	-93.6	53.73
		4T-CT	4	L-T	-103	-9.4	-93.6	62.09
		4T-CT	4	L-T	-103	-9.4	-93.6	70.82
		½T-CT	0.5	L-T	-238	-9.4	-228.6	25.36
		½T-CT	0.5	L-T	-238	-9.4	-228.6	26.18
		½T-CT	0.5	L-T	-238	-9.4	-228.6	29.27
		½T-CT	0.5	L-T	-238	-9.4	-228.6	29.45
		½T-CT	0.5	L-T	-238	-9.4	-228.6	30.18
		½T-CT	0.5	L-T	-238	-9.4	-228.6	31.00
		½T-CT	0.5	L-T	-238	-9.4	-228.6	32.82
		½T-CT	0.5	L-T	-238	-9.4	-228.6	33.82
		½T-CT	0.5	L-T	-238	-9.4	-228.6	36.00
		½T-CT	0.5	L-T	-238	-9.4	-228.6	36.36
		1T-CT	1	L-T	-238	-9.4	-228.6	32.09
		1T-CT	1	L-T	-238	-9.4	-228.6	33.73
		1T-CT	1	L-T	-238	-9.4	-228.6	34.27

Material	Reference Source	Specimen ID	Type No.	Orientation	Temp (°F)	RT_{NDT} (°F)	T - RT_{NDT} (°F)	K_{Ic} (ksivin)
		1T-CT	1	L-T	-238	-9.4	-228.6	34.91
		1T-CT	1	L-T	-238	-9.4	-228.6	35.09
		1T-CT	1	L-T	-238	-9.4	-228.6	36.00
		1T-CT	1	L-T	-238	-9.4	-228.6	37.45
		1T-CT	1	L-T	-238	-9.4	-228.6	37.45
		1T-CT	1	L-T	-238	-9.4	-228.6	39.55
		1T-CT	1	L-T	-238	-9.4	-228.6	39.73
		1T-CT	1	L-T	-238	-9.4	-228.6	40.36
		1T-CT	1	L-T	-238	-9.4	-228.6	42.36
		1T-CT	1	L-T	-238	-9.4	-228.6	43.73
		1T-CT	1	L-T	-238	-9.4	-228.6	46.45
		1T-CT	1	L-T	-238	-9.4	-228.6	49.55
		1T-CT	1	L-T	-238	-9.4	-228.6	49.64
		2T-CT	2	L-T	-238	-9.4	-228.6	30.09
		2T-CT	2	L-T	-238	-9.4	-228.6	33.00
		2T-CT	2	L-T	-238	-9.4	-228.6	36.55
		2T-CT	2	L-T	-238	-9.4	-228.6	37.00
		2T-CT	2	L-T	-238	-9.4	-228.6	39.36
		2T-CT	2	L-T	-238	-9.4	-228.6	39.91
		2T-CT	2	L-T	-238	-9.4	-228.6	40.91
		2T-CT	2	L-T	-238	-9.4	-228.6	41.45
		2T-CT	2	L-T	-238	-9.4	-228.6	42.18
		2T-CT	2	L-T	-238	-9.4	-228.6	46.45
		2T-CT	2	L-T	-238	-9.4	-228.6	48.64
		2T-CT	2	L-T	-238	-9.4	-228.6	53.18
A508 Class 3	Iwadate, et al.	Bx2B	1	NA	-238	-13	-225	37.29
	ASTM STP	Bx2B	1	NA	-238	-13	-225	39.89
	803	Bx2B	1	NA	-238	-13	-225	44.22
		Bx2B	4	NA	-166	-13	-153	43.36
		Bx2B	4	NA	-76	-13	-63	63.30
		Bx2B	3	NA	-4	-13	9	69.37
Midland Nozzle	NUREG/CR-	C(T)	1		-58	52	-110	49.81
Course Weld	6249	C(T)	1		-148	52	-200	45.63
		C(T)	1		-148	52	-200	44.63
		C(T)	1		-148	52	-200	42.81
		C(T)	1		-148	52	-200	33.45
		C(T)	1		-148	52	-200	32.36
Midland Beltline	NUREG/CR-	C(T)	1		-148	23	-171	36.45
	6249	C(T)	1		-148	23	-171	34.91
Plate 02 4th Irr.	NUREG/CR-	C(T)	1	T-L	-148	0	-148	38.09
Series	4880, 1988	C(T)	1	T-L	-139	0	-139	33.45
	Plate 02	C(T)	1	T-L	-139	0	-139	39.27
	(68-71W)	C(T)	1	T-L	-139	0	-139	40.09

REFERENCES FOR TABLE A1

EPRI Special Report, 1978, *Flaw Evaluation Procedures: ASME Section XI*, EPRI NP-719-SR, Electric Power Research Institute, Palo Alto, CA.

W. O. Shabbits, W. H. Pryle, and E. T. Wessel, *Heavy Section Fracture Toughness Properties of A533, Grade B, Class-1 Steel Plate and Submerged Arc Weldments*, HSST Technical Report 6, WCAP-7414, December 1969.

T. R. Mager, F. O. Thomas, and W. S. Hazelton, *Evaluation by Linear Elastic Fracture Mechanics of Radiation Damage to Pressure Vessel Steels,* HSST Technical Report 5, WCAP-7328, Revised, October 1969.

T. R. Mager, *Fracture Toughness Characterization Study of A533, Grade B, Class-1 Steel*, HSST Technical Report 10, WCAP-7578, October 1970.

R. K. Nanstad, F. M. Haggag, and D. E. McCabe, *Irradiation Effects on Fracture Toughness of Two High-Copper Submerged-Arc Welds, HSSI Series 5,* USNRC Report NUREG/CR-5913 (ORNL/TM-12156/V1 and V2) Vol. 1 and 2, Oak Ridge National Laboratory, Oak Ridge, TN, October 1992.

D. E. McCabe., *A Comparison of Weibull and β_{Ic} Analysis of Transition Range Fracture Toughness Data,* USNRC Report NUREG/CR-5788 (ORNL/TM-11959), Oak Ridge National Laboratory, Oak Ridge, TN, January 1992.

T. Iawadate, Y. Tanaka, S. Ono, and J. Watanabe, "An Analysis of Elastic-Plastic Fracture Toughness Behavior for J_{Ic} Measurements in the Transition Region," *Elastic-Plastic Fracture: Second Symposium, Vol. II-Fracture Resistance Curves and Engineering Applications*, ASTM STP 803, (1983) II531-II561.

D. E. McCabe, R. K. Nanstad, S. K. Iskander, R. L. Swain, *Unirradiated Material Properties of Midland Weld WF-70,* USNRC Report NUREG/CR-6249 (ORNL/TM-12777), Oak Ridge National Laboratory, Oak Ridge, TN, October 1994.

J. J. McGowan, R. K. Nanstad, and K. R. Thoms, *Characterization of Irradiated Current-Practice Welds and A533 Grade B Class 1 Plate for Nuclear Pressure Vessel Service*, USNRC Report NUREG/CR-4880 (ORNL-6484/V1 and V2), Oak Ridge National Laboratory, Oak Ridge, TN, July 1988.

Table A2. Crack Arrest Toughness K_{Ia} Extended Database

Material	Reference Source	Specimen ID	Size No.	Orientation	Temp (°F)	RT_{NDT} (°F)	$T\text{-}RT_{NDT}$ (°F)	K_{Ia} (ksivin)
HSST-02	EPRI NP	C(T)	1.4	L-T	-150	0	-150	28.0
HSST-02	719-SR	C(T)	1	L-T	-70	0	-70	43.0
HSST-02	Ripling (1971)	C(T)	2	L-T	-70	0	-70	48.0
HSST-02		C(T)	2	L-T	-70	0	-70	43.0
HSST-02		C(T)	1	L-T	0	0	0	68.0
HSST-02		C(T)	1	L-T	0	0	0	58.0
HSST-02		C(T)	1	L-T	0	0	0	48.0
HSST-02		C(T)	1	L-T	0	0	0	57.0
HSST-02		C(T)	1	L-T	0	0	0	62.0
HSST-02		C(T)	1.3	L-T	0	0	0	58.0
HSST-02		C(T)	1.3	L-T	0	0	0	60.0
HSST-02		C(T)	1.3	L-T	0	0	0	65.0
HSST-02		C(T)	1.6	L-T	0	0	0	60.0
HSST-02		C(T)	1.6	L-T	0	0	0	58.0
HSST-02		C(T)	2	L-T	0	0	0	53.0
HSST-02		C(T)	2	L-T	0	0	0	58.0
HSST-02		C(T)	2	L-T	0	0	0	70.0
HSST-02		C(T)	2	L-T	0	0	0	57.0
HSST-02		C(T)	3	L-T	0	0	0	57.0
HSST-02		C(T)	3	L-T	0	0	0	61.0
HSST-02		C(T)	2	L-T	22	0	22	68.0
HSST-02		C(T)	1.4	L-T	35	0	35	59.0
HSST-02		C(T)	1.6	L-T	35	0	35	84.0
HSST-02		C(T)	2	L-T	35	0	35	62.0
HSST-02		C(T)	1.4	L-T	50	0	50	92.0
HSST-02		C(T)	2	L-T	50	0	50	73.0
HSST-02		C(T)	3	L-T	50	0	50	75.0
HSST-02		C(T)	1	L-T	75	0	75	94.0
HSST-02		C(T)	1.6	L-T	75	0	75	107.0
HSST-02		C(T)	2	L-T	75	0	75	77.0
HSST-02		C(T)	2	L-T	75	0	75	81.0
HSST-02		C(T)	2	L-T	75	0	75	91.0
HSST-02		C(T)	2	L-T	75	0	75	101.0
HSST-02		C(T)	2	L-T	80	0	80	109.0
HSST-02		C(T)	2	L-T	83	0	83	87.0
HSST-02		C(T)	3	L-T	83	0	83	94.0
HSST-02		C(T)	3	L-T	83	0	83	107.0
HSST-02		C(T)	3	L-T	83	0	83	111.0
HSST-02		C(T)	2	L-T	96	0	96	111.0
HSST-02		C(T)	2	L-T	102	0	102	117.0
HSST-02		C(T)	1.8	L-T	105	0	105	118.0
HSST-02		C(T)	2	L-T	105	0	105	103.0
HSST-02		C(T)	2	L-T	105	0	105	107.0
HSST-02		C(T)	3	L-T	105	0	105	130.0
HSST-02		C(T)	2	L-T	107	0	107	87.0
HSST-02		C(T)	2	L-T	110	0	110	88.0
HSST-02		C(T)	2	L-T	110	0	110	88.0
HSST-02		C(T)	1.1	L-T	112	0	112	112.0
HSST-02		C(T)	2	L-T	115	0	115	111.0
HSST-02		C(T)	1.1	L-T	121	0	121	116.0
72W	NUREG/CR-5584	C(T)		Crack	-77.8	-10	-68	60.1

Material	Reference Source	Specimen ID	Size No.	Orientation	Temp (°F)	RT_{NDT} (°F)	$T-RT_{NDT}$ (°F)	K_{Ia} (ksivin)
72W		C(T)		runs	-76	-10	-66	48.2
72W		C(T)		in	-76	-10	-66	69.2
72W		C(T)		welding	-74.2	-10	-64.2	51.9
72W		C(T)		direction	-52.6	-10	-42.6	61.0
72W		C(T)			-52.6	-10	-42.6	64.6
72W		C(T)			-49	-10	-39	66.4
72W		C(T)			-49	-10	-39	67.3
72W		C(T)			-49	-10	-39	69.2
72W		C(T)			-49	-10	-39	83.7
72W		C(T)			-25.6	-10	-15.6	83.7
72W		C(T)			-22	-10	-12	54.6
72W		C(T)			-22	-10	-12	55.5
72W		C(T)			-22	-10	-12	77.4
72W		C(T)			-22	-10	-12	82.8
72W		C(T)			-22	-10	-12	89.2
72W		C(T)			-22	-10	-12	94.6
72W		C(T)			-22	-10	-12	97.4
72W		C(T)			3.2	-10	13.2	88.3
72W		C(T)			5	-10	15	85.5
72W		C(T)			5	-10	15	85.5
72W		C(T)			5	-10	15	86.5
72W		C(T)			5	-10	15	93.7
72W		C(T)			6.8	-10	16.8	82.8
72W		C(T)			28.4	-10	38.4	93.7
72W		C(T)			30.2	-10	40.2	113.8
72W		C(T)			32	-10	42	84.6
72W		C(T)			32	-10	42	97.4
72W		C(T)			32	-10	42	103.7
72W		C(T)			33.8	-10	43.8	98.3
72W		C(T)			39.2	-10	49.2	113.8
72W		C(T)			41	-10	51	104.7
73W	NUREG/CR-5584	C(T)		Crack	-77.8	-30	-47.8	62.8
73W		C(T)		runs	-76	-30	-46	52.8
73W		C(T)		in	-74.2	-30	-44.2	65.5
73W		C(T)		welding	-49	-30	-19	47.3
73W		C(T)		direction	-49	-30	-19	66.4
73W		C(T)			-49	-30	-19	68.3
73W		C(T)			-49	-30	-19	77.4
73W		C(T)			-47.2	-30	-17.2	64.6
73W		C(T)			-25.6	-30	4.4	77.4
73W		C(T)			-23.8	-30	6.2	68.3
73W		C(T)			-22	-30	8	61.0
73W		C(T)			-22	-30	8	72.8
73W		C(T)			-22	-30	8	91.0
73W		C(T)			-20.2	-30	9.8	70.1
73W		C(T)			-20.2	-30	9.8	81.0
73W		C(T)			3.2	-30	33.2	100.1
73W		C(T)			5	-30	35	106.5
73W		C(T)			5	-30	35	111.9
73W		C(T)			5	-30	35	112.8
73W		C(T)			10.4	-30	40.4	101.0
73W		C(T)			23	-30	53	91.9
73W		C(T)			41	-30	71	97.4
73W		C(T)			41	-30	71	101.9

Material	Reference Source	Specimen ID	Size No.	Orientation	Temp (°F)	RT_{NDT} (°F)	$T\text{-}RT_{NDT}$ (°F)	K_{Ia} (ksivin)
73W		C(T)			41	-30	71	102.8
73W		C(T)			41	-30	71	108.3
73W		C(T)			59	-30	89	120.1
MW15JC	NUREG/CR-6621	C(T)		Crack	-4	32.2	-36.2	63.7
MW15JB*r*		C(T)		runs	14	32.2	-18.2	79.0
MW15JE*r1*		C(T)		in welding	32	32.2	-0.2	97.1
MW15JF		C(T)		direction	50	32.2	17.8	119.7

REFERENCES FOR TABLE A2

EPRI Special Report, 1978, *Flaw Evaluation Procedures: ASME Section XI*, EPRI NP-719-SR, Electric Power Research Institute, Palo Alto, CA.

E. J. Ripling and P. B. Crosley, "Strain Rate and Crack Arrest Studies," *HSST 5th Annual Information Meeting*, Paper No. 9, 1971.

S. K. Iskander, W. R. Corwin, R. K. Nanstad, *Results of Crack-Arrest Tests on Two Irradiated High-Copper Welds,* USNRC Report NUREG/CR-5584 (ORNL/TM-11575), Oak Ridge National Laboratory, Oak Ridge, TN, December 1990.

S. K. Iskander, C. A. Baldwin, D. W. Heatherly, D. E. McCabe, I. Remec, and R. L. Swain, *Detailed Results of Testing Unirradiated and Irradiated Crack-Arrest Toughness Specimens from the Low Upper-Shelf Energy, High Copper Weld, WF-70,* NUREG/CR-6621 (ORNL/TM-13764) under preparation.

S. K. Iskander, R. K. Nanstad, D. E. McCabe, and R. L. Swain, "Effects of Irradiation on Crack-Arrest Toughness of a Low Upper-Shelf Energy, High-Copper Weld," *Effects of Radiation on Materials: 19th International Symposium, ASTM STP 1366*, M. L. Hamilton, A. S. Kumar, S. T. Rosinski, and M. L. Grossbeck, eds., American Society for Testing and Materials, to be published in 1999.

Appendix B – Results of Preliminary Regression Analysis

The first phase of this study involved a least-squares regression analysis to investigate potential parametric representations of the K_{Ic} and K_{Ia} databases. The software package *TableCurve2D* [B1] was employed to analyze the EPRI K_{Ic} database. *TableCurve2D* is a regression analysis tool with 3,491 built-in linear and 176 nonlinear functions that can be quickly solved and ranked for goodness of fit for a given dataset. These model forms include, among others, polynomial, exponential, rational, Chebyshev polynomials, and Fourier series. TableCurve2D also allows user-defined linear and nonlinear functions to be input as candidate model forms for curve fitting. Linearity here refers to the linearity of the coefficients (parameters) of the function being fitted. The resulting curve fits can be ranked by a selection of different statistics to determine an optimal fit. For this study, the F-statistic measure of merit was applied to rank the curve fits.

The data were initially grouped by material type and then curve fits were performed. Some of these groups had too few data points for a meaningful curve fit; however, three material groups did warrant further investigation. HSST 02 data reported by Shabbits [B2] and Mager et al. [B3] had the most data points and also the broadest normalized temperature distribution. Two other materials, A533 B Class 1 weldment [B3] and A 533 B Class 1 weldment/HAZ [B3], were also analyzed, although their normalized temperature ranges did not extend very far into the transition region. A 3-parameter nonlinear exponential function of the form

$$K_{Ic} = a + b\exp[c(T - RT_{NDT})] \tag{B.1}$$

was used. Equation (B.1) is linear in its parameters a and b and nonlinear in the parameter c. As presented in Fig. B1, the curve fit of the HSST 02 material group looked very similar to the overall curve fit of the data. This result suggested that the data can be represented by a family of curves. The curve fits of the last two groups also looked similar in the lower-shelf region but turned up abruptly at lower temperatures due to a lack of data in the transition region.

The entire data set was then analyzed, and the fits were ranked using the F-statistic. The top 88 out of a total of 242 curve fits discovered by TableCurve2D are listed in Table B1 where the first column is the ranking, the second column is the F-statistic, and the third column is the model form used in the curve fit. The F-statistic measure of merit is defined by

$$F = \frac{\left(\dfrac{\sum_{i=1}^{n}(y_i - \bar{y}_i)^2 - \sum_{i=1}^{n}(y_i - \hat{y}_i)^2}{k-1} \right)}{\dfrac{\sum_{i=1}^{n}(y_i - \hat{y}_i)^2}{n-k}} \tag{B.2}$$

where n is the number of data points, k is the number of coefficients fitted, y_i are the data values, $\bar{y}$ is the sample mean, and $\hat{y}$ is the predicted value.

The four top-ranked curve-fit candidates are shown in Figs. B2-B5 along with their 99 percent prediction curves and histogram residual plots. These four fits have the following model forms:

<u>Model 1:</u>

$$\ln(K_{Ic}) = a + b(T - RT_{NDT}) \tag{B.3}$$

<u>Model 2:</u>

$$(K_{Ic})^{1/2} = a + b(T - RT_{NDT}) \tag{B.4}$$

<u>Model 3:</u>

$$K_{Ic} = \frac{a + c(T - RT_{NDT})}{1 + b(T - RT_{NDT})} \tag{B.5}$$

<u>Model 4:</u>

$$K_{Ic} = a + b\exp[c(T - RT_{NDT})] \tag{B.6}$$

Models 3 and 4 are both nonlinear forms. Although all of these four functions fit the data with a high F-statistic, some exhibit undesirable behavior outside of the limits of the data. Models 1 and 2 do not have a lower asymptote with decreasing normalized temperature. Models 3 and 4 do have a lower asymptote; however, Model 3 does not follow a consistent trend as the normalized temperature increases beyond the upper bound of the data. Model 4 exhibits the best behavior at both ends of the range of the data set, but the lower 99 percent prediction curve falls below the estimated K_{min} of 18.2 ksivin (20 MPavm). The fit to Model 4 has the following parameters: $a = 36.68$ ksivin, $b =$ 51.49 ksivin, and $c =$ 0.01153°F. These coefficients are almost identical to the independently-derived curve fit (for the same model form) in Ref. [B4].

When derived as a maximum likelihood estimator, the least-squares technique assumes that the errors are independent and distributed normally about the predicted regression curve. The assumption of a constant standard deviation inherent in the standard least squares method can be relaxed through the use of a *weighted* regression analysis; however, these weights must be estimated and input by the user. A nonweighted regression analysis was used in this study. The degree of normality of the error modes in the data relative to the predicted curve fit can be inferred by inspection of the residuals, defined as the difference between the actual data and the predicted value. The histograms presented in Figs. B2b to B5b indicate some degree of skewness in the residuals that imply the possible presence of nonrandom error modes in the dataset. This result is consistent with the findings of other researchers [B5] and has motivated the investigation of a different model form that is not dependent upon an underlying symmetric normal distribution to describe the deviations from the predicted curves.

References for Appendix B

B1. TableCurve2D, User's Manual, Version 4 for Windows 95, NT & 3.1,SPSS Inc., Chicago, IL, 1997.

B2. W. O. Shabbits, W. H. Pryle, and E. T. Wessel, *Heavy Section Fracture Toughness Properties of A533, Grade B, Class-1 Steel Plate and Submerged Arc Weldments*, HSST Technical Report 6, WCAP-7414, December 1969.

B3. T. R. Mager, F. O. Thomas, and W. S. Hazelton, *Evaluation by Linear Elastic Fracture Mechanics of Radiation Damage to Pressure Vessel Steels,* HSST Technical Report 5, WCAP-7328, Revised, October 1969.

B4. R. K. Nanstad, J. A. Keeney, and D. E. McCabe, "Preliminary Review of the Bases for the K_{Ic} Curve in the ASME Code," ORNL/NRC/LTR-93/15, Oak Ridge National Laboratory, 1993.

B5. J. G. Merkle, K. Wallin, and D. E. McCabe, "Technical Basis for an ASTM Standard on Determining the Reference Temperature, T_0, for Ferritic Steels in the Transition Range," NUREG/CR-5504 (ORNL/TM-13631) Oak Ridge National Laboratory, November 1998.

Table B1. Top-Ranked Model Forms Calculated by TableCurve2D

Rank	*F*-Statistic	Model Form
1	**212.08316474**	**lny = a + bx**
2	**202.73543020**	**y^(0.5) = a + bx**
3	**202.10095146**	**y = (a + cx)/(1 + bx) [NL]**
4	**194.44231080**	**y = a + b *exp*(cx) [NL]**
5	176.25900038	y^(-1) = a + bx
6	171.28645651	y = a + bx
7	170.24942226	y^(0.5) = a + bx + cx^2
8	164.27947091	y = a + bx + cx^2
9	159.13106263	lny = a + bx + cx^2
10	149.87823234	lny = a + bx + c *exp*(x)
11	146.13142246	y = a + bx + c *exp*(x)
12	143.76110728	lny = a + bx + cx^3
13	141.07999819	y = a + bx + cx^3
14	137.29791795	y = a + bx + cx^2 + d *exp*(x)
15	137.22995434	Fourier Series Polynomial 1x2
16	134.99360842	y = (a + cx)/(1 + bx + dx^2) [NL]
17	130.98649922	y = a + bx + cx^3 + d *exp*(x)
18	124.92269692	Chebyshev = >Std Polynomial Order 3
19	124.92269692	Chebyshev Polynomial Order 3
20	124.92269692	y = a + bx + cx^2 + dx^3
21	123.06568751	y^(0.5) = a + bx + cx^2 + dx^3
22	115.33293665	y^2 = a + bx + cx^2
23	109.76890768	lny = a + bx + cx^2 + dx^3
24	104.70649060	y = a + bx + cx^2 + dx^3 + e *exp*(x)
25	101.55552931	y^2 = a + bx + cx^2 + dx^3
26	99.886096880	y = (a + cx + ex^2)/(1 + bx + dx^2) [NL]
27	98.539924648	y^(-1) = a + bx + c *exp*(x)
28	98.407676705	y = a + bx^2 + cx^3 + d *exp*(x)
29	95.436616294	High Precision Polynomial Order 4
30	95.436616294	Chebyshev Polynomial Order 4
31	95.436616294	Chebyshev = >Std Polynomial Order 4
32	95.436616294	y = a + bx + cx^2 + dx^3 + ex^4
33	95.256825667	y^(-1) = a + bx + cx^2
34	94.403752943	y^(-1) = a + bx + cx^3
35	93.064358636	y^(0.5) = a + bx + cx^2 + dx^3 + ex^4
36	90.888406094	Fourier Series Polynomial 2x2
37	84.126204190	y = a + bx^2 + c *exp*(x)
38	82.500766448	lny = a + bx + cx^2 + dx^3 + ex^4
39	81.574302114	y^2 = a + bx + cx^2 + dx^3 + ex^4

Table B1. Top-Ranked Model Forms Calculated by TableCurve2D

Rank	*F*-Statistic	Model Form
40	78.019197528	High Precision Polynomial Order 5
41	78.019197528	Chebyshev = >Std Polynomial Order 5
42	78.019197528	Chebyshev Polynomial Order 5
44	76.248415354	y = a + b *exp*(x)
45	76.220106695	y^(0.5) = a + bx + cx^2 + dx^3 + ex^4 + fx^5
47	73.648681893	lny = a + bx^2 + c *exp*(x)
49	67.900165448	Chebyshev Polynomial Order 6
50	67.900165448	High Precision Polynomial Order 6
51	67.900165448	Chebyshev = >Std Polynomial Order 6
52	67.749311766	y = a + bx^2 + cx^3
53	67.736722397	lny = a + bx + cx^2 + dx^3 + ex^4 + fx^5
54	66.589185788	Fourier Series Polynomial 3x2
55	63.418238130	y = a + bx^3 + c *exp*(x)
56	63.126196234	y^(-1) = a + bx + cx^2 + dx^3
57	60.358790633	y^(0.5) = a + b *exp*(x)
58	60.255288266	Chebyshev = >Std Polynomial Order 7
59	60.255288266	Chebyshev Polynomial Order 7
60	60.255288266	High Precision Polynomial Order 7
61	60.222001357	y = a + bx^2 + cx^4
64	57.747180396	y = a + bx^2
65	57.285235500	y^(0.5) = a + bx^2
66	55.585467658	lny = (a + cx)/(1 + bx)
67	54.862287108	y^(0.5) = (a + cx)/(1 + bx)
68	52.511231768	Fourier Series Polynomial 4x2
69	52.399927006	Chebyshev = >Std Polynomial Order 8
70	52.399927006	Chebyshev Polynomial Order 8
71	52.399927006	High Precision Polynomial Order 8
72	50.377723858	lny = a + bx^2 + cx^3
74	47.134766769	y^(-1) = a + bx + cx^2 + dx^3 + ex^4
75	46.357029818	Chebyshev Polynomial Order 9
76	46.357029818	High Precision Polynomial Order 9
77	46.357029818	Chebyshev = >Std Polynomial Order 9
78	44.972169153	y^2 = a + b*exp(x)*
79	42.493046529	lny = a + bx^3 + c*exp(x)*
81	41.595572118	y^(-1) = a + bx^2 + c*exp(x)*
82	41.553003885	Fourier Series Polynomial 5x2
83	41.522828495	Chebyshev Polynomial Order 10
84	41.522828495	High Precision Polynomial Order 10
85	41.522828495	Chebyshev = >Std Polynomial Order 10

Table B1. Top-Ranked Model Forms Calculated by TableCurve2D

Rank	*F*-Statistic	Model Form
87	40.422344924	Chebyshev Rational Order 4/4
88	40.422344924	Chebyshev = >Std Rational Order 4/4
89	39.521249612	y^(-1) = a + bx + cx^2 + dx^3 + ex^4 + fx^5
90	38.415760094	High Precision Polynomial Order 11
91	38.415760094	Chebyshev = >Std Polynomial Order 11
92	38.415760094	Chebyshev Polynomial Order 11
93	35.062442660	Chebyshev = >Std Polynomial Order 12
94	35.062442660	Chebyshev Polynomial Order 12
95	35.062442660	High Precision Polynomial Order 12
96	34.629893962	Fourier Series Polynomial 6x2
97	33.566708227	Chebyshev = >Std Polynomial Order 13
98	33.566708227	Chebyshev Polynomial Order 13
99	33.566708227	High Precision Polynomial Order 13

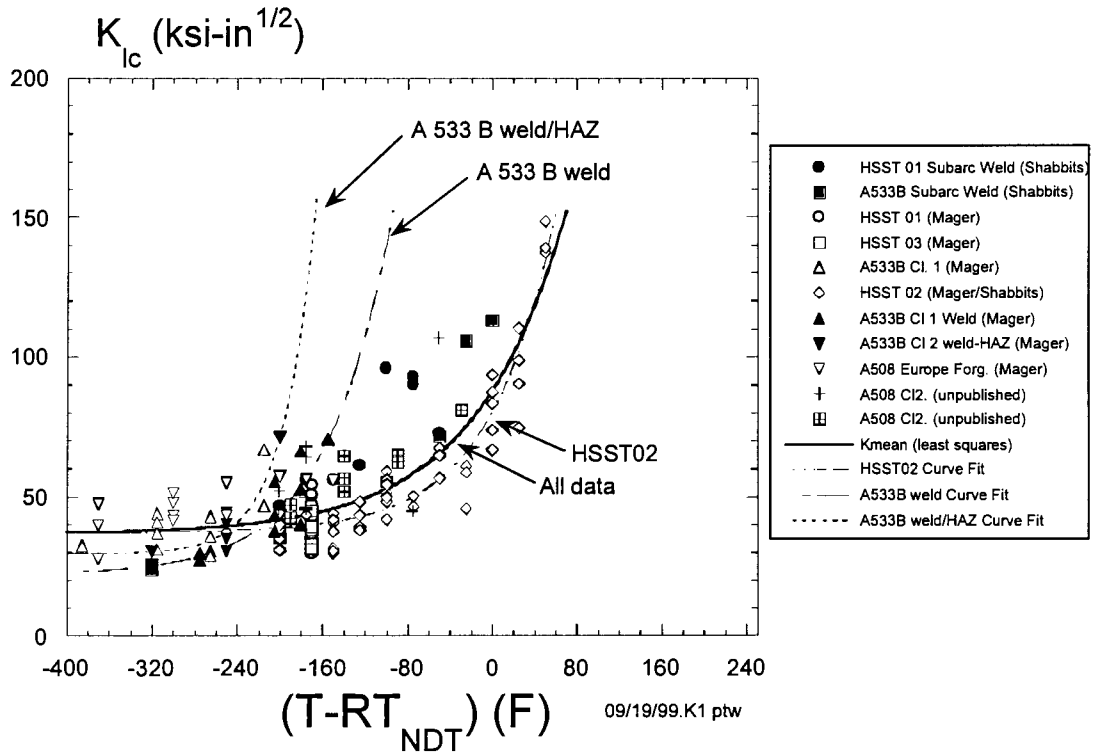

Fig. B1. TableCurve2D curve fits using a 3-parameter exponential function for 4 material groups compared to a general curve fit of all of the data.

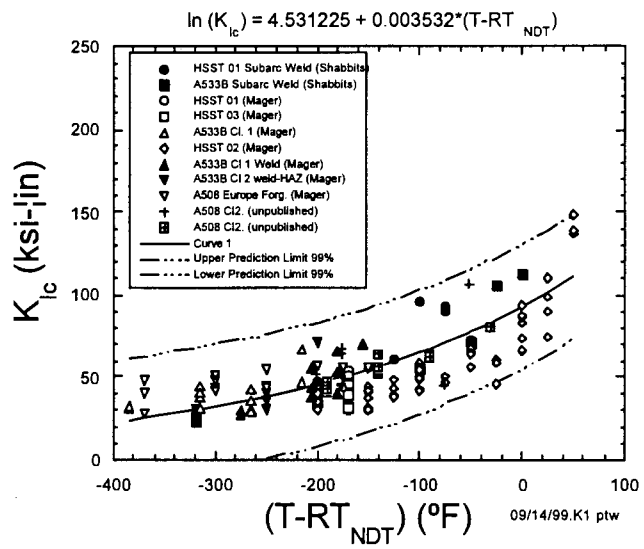

(a)

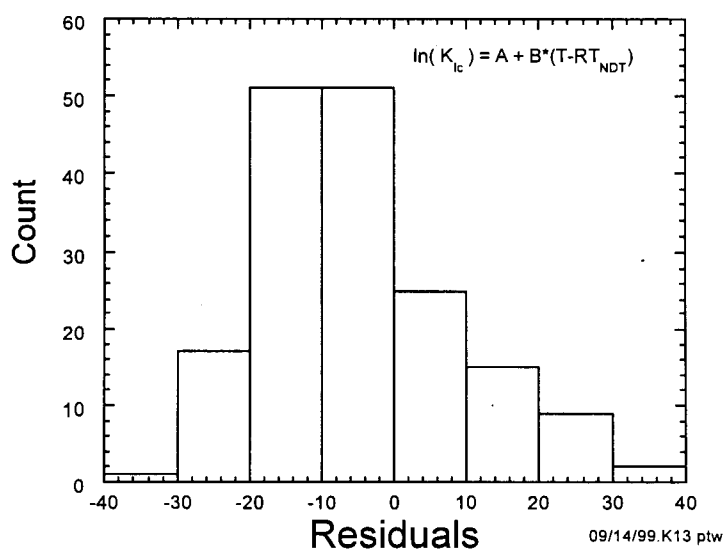

(b)

Fig. B2. Results of regression analysis for the Rank 1 functional form (a) curve with K_{Ic} data and (b) frequency histogram of residuals.

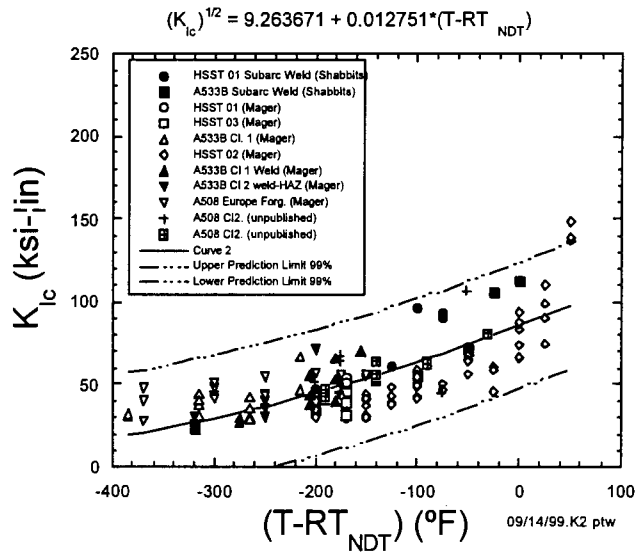

(a)

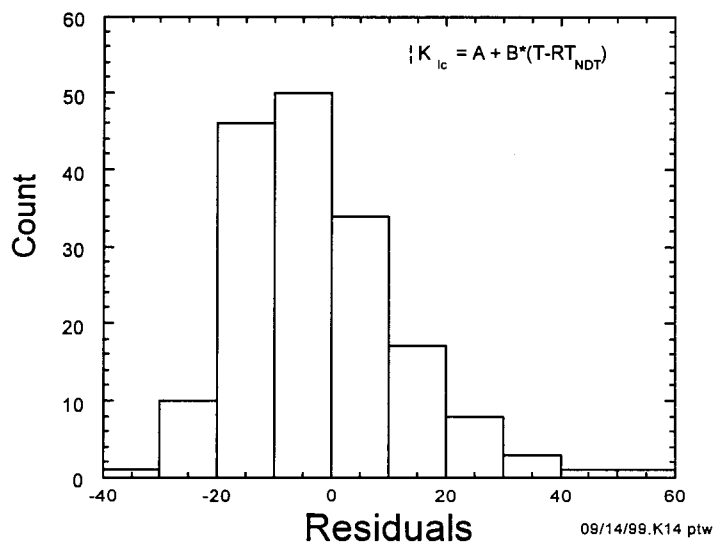

(b)

Fig. B3. Results of regression analysis for the Rank 2 functional form (a) curve with K_{Ic} data and (b) frequency histogram of residuals.

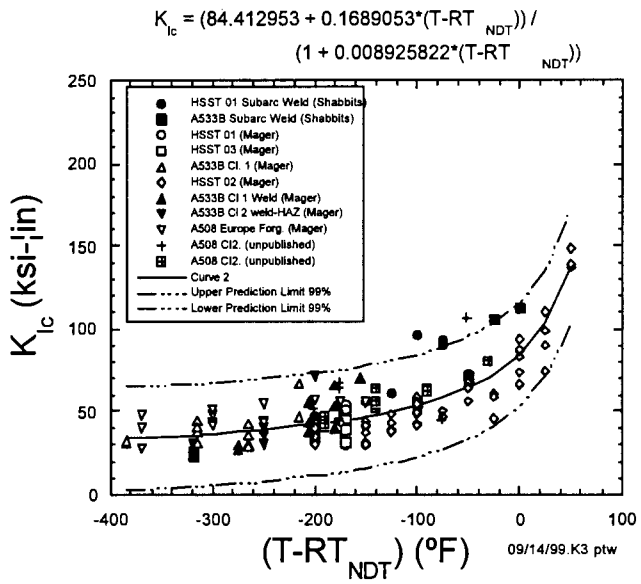

(a)

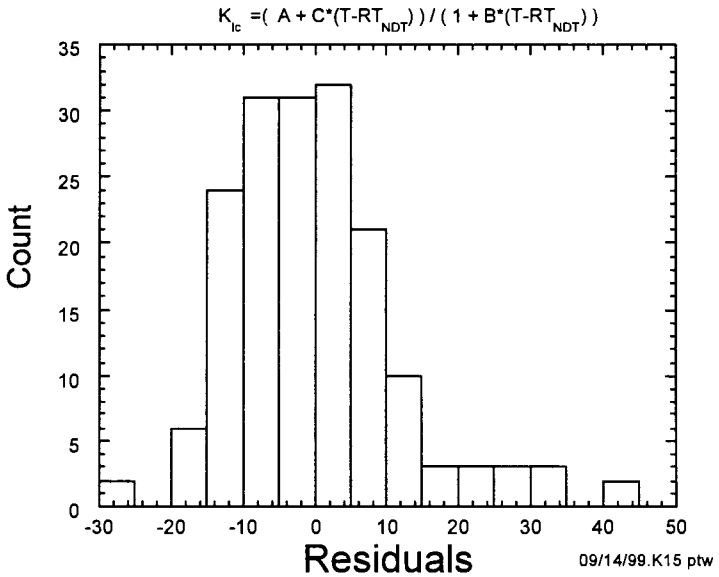

(b)

Fig. B4. Results of regression analysis for the Rank 3 functional form (a) curve with K_{Ic} data and (b) frequency histogram of residuals.

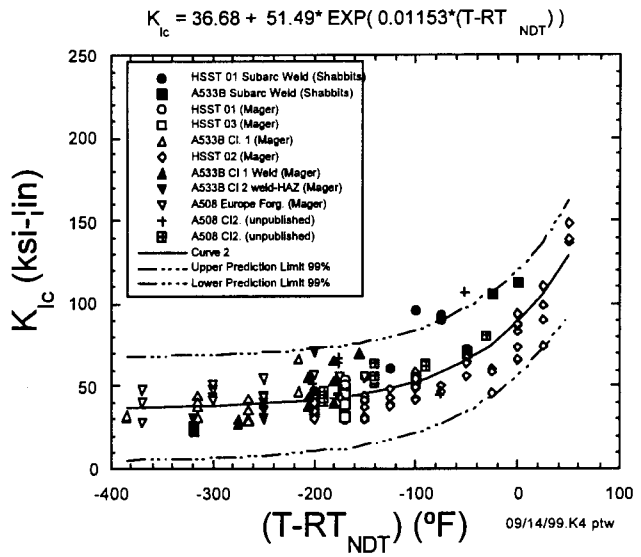

(a)

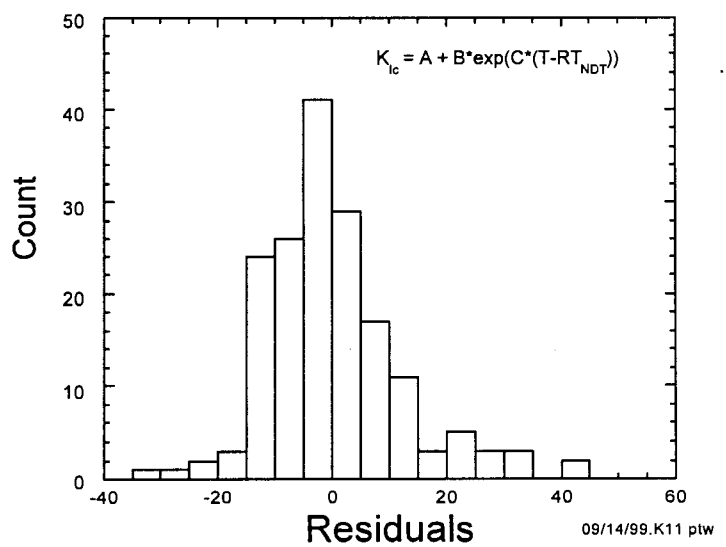

(b)

Fig. B5. Results of regression analysis for Rank 4 curve fit: 3-term exponential functional form (a) curve with K_{Ic} data and (b) frequency histogram of residuals.

Appendix C – Derivation of Almost Unbiased Estimator b_2^{**} and a_2^{**}

In general,

$$Var\left(\sqrt{m_2}\right)=\left(1-\frac{1}{n}\right)\mu_2-\left(E\sqrt{m_2}\right)^2$$

Hence, if the mean and variance of the population exist, then

$$E\sqrt{\frac{m_2}{\mu_2}}\leq\sqrt{1-\frac{1}{n}}<1 \quad (n=2,3,\cdots)$$

This is true for the Weibull density case. By moment,

$$b^*\sqrt{\Gamma\left(1+\frac{2}{c}\right)-\Gamma^2\left(1+\frac{1}{c}\right)}=\sqrt{m_2}$$

and, since $\sqrt{\mu_2}=b\sqrt{\Gamma(1+\frac{2}{c})-\Gamma^2(1+\frac{1}{c})}$, we have

$$\frac{b^*}{b}=\frac{\sqrt{m_2}}{\sqrt{\mu_2}}<1 \qquad (n=2,3,\cdots)$$

and

$$E(b^*)<b$$

Now for a^*, we have

$$\mu_1'(x)=a+b\Gamma\left(1+\frac{1}{c}\right) \qquad m_1'(x)=a^*+b^*\Gamma\left(1+\frac{1}{c}\right)$$

Hence

$$a^*=m_1'-b^*\Gamma\left(1+\frac{1}{c}\right)$$

and

$$\begin{aligned}a^*-a&=m_1'-b^*\Gamma\left(1+\frac{1}{c}\right)-\mu_1'+b\Gamma\left(1+\frac{1}{c}\right)\\&=\mu_1'-\mu_1'+(b-b^*)\ \Gamma\left(1+\frac{1}{c}\right)\end{aligned}$$

and in expectation

$$E(a^*-a) = E(b-b^*)\,\Gamma\left(1+\frac{1}{c}\right)$$

and

$$a = E\left[a^* - (b-b^*)\,\Gamma\left(1+\frac{1}{c}\right)\right] \rightarrow a < E(a^*)$$

since $b > E(b^*)$.

An almost unbiased estimator, b_2^{**}, can be calculated from

$$b_2^{**} = \frac{b_2^*}{(E(b_2^*)/b)} \tag{C.1}$$

An approximation for $E(b_2^*)/b$ is

$$\frac{E(b_2^*)}{b} \sim 1 + \frac{A_1}{N} + \frac{A_2}{N^2} \tag{C.2}$$

where

$$A_1 = -0.827043 + \frac{0.806668}{c} - \frac{1.423234}{c^2}$$

$$A_2 = 0.436183 - \frac{3.990936}{c} + \frac{5.658460}{c^2}$$

Eq. (C.2) is valid for $c \geq 1.1, N \geq 10$ and with errors less than 0.1%, except for $c = 1.1$, $N = 10$, which has an error of 0.175%. Eq. (C.2) was derived by using 35 values of c (1.1(0.1)4.5)* and 29 values of N (10(1)25(5)80(10)100). To calculate an almost unbiased estimator for a, b_2^{**} is used in the moment estimator for a, specifically,

$$a_2^{**} = m_1' - b_2^{**}\ \Gamma\left(1+\frac{1}{c}\right)$$

* The notation $c_{min}(\Delta c)c_{max}$ designates a sequence of c-values from c_{min} to c_{max} in increments of Δc.

APPENDIX D

Estimation Problems for the Weibull Distribution

K.O. Bowman
Computer Science and Mathematics Division
Oak Ridge National Laboratory
P.O.Box 2008
Oak Ridge, Tennessee 37831-6367
bowmanko@ornl.gov

December 14, 1999

Abstract

Asymptotic central moments and asymptotic moment ratios are given, the latter involving Riemann Zeta functions. Maximum likelihood estimators for the Weibull density have been discussed elsewhere (Bowman and Shenton, 1999b), and an important discovery was that these moments only exist if the shape parameter is restricted. For this reason, particular attention is paid to moment estimators and the part played by sample sizes, the 2 parameter and 3 parameter cases being considered. Extended series for the moment estimators of the parameters are studied, these having the appearance of divergency when arranged in descending powers of the sample size. For these series terms are taken as far as those of order 20, and coefficients of the higher order terms may exceed 10^{15}, so that convergence accelerating processes are required. The Padé rational fraction sequences are invoked. Validation of the approximants is derived by comparative simulation studies. A set of useful algorithms is given for the estimators of the parameters, these including means, variances, skewness and kurtosis. Also, a brief account of Padé processes goes back to Stieltjes, who, one hundred years ago, gave the semi-convergent series for $\ln \Gamma(z)$, identified the residue in terms of Bernoulli numbers, and finally set up the corresponding Stieltjes continued fraction, defining the first half-dozen partial numerators. It is interesting to note that G.H. Hardy (Cambridge mathematician in the early part of the century), who to a large extent introduced the rigors of the "New Maths", dallied with the old and showed how the semi-convergent series involved in $\ln \Gamma(1)$ could in fact be "useful". Finally, in the early part of the present century much dedicated effort and skill in algebraic analysis was spent on evaluating moments and cumulants of sample moments. A brief description of a powerful algorithm is included.

1 Introduction

1.1 The Weibull Model

This paper supplies more information on the statistical methodology used in "Technical Basis for Statistical Models of Extended K_{Ic} and K_{Ia} Fracture Toughness Databases for RPV Steels" (Bowman and williams, 1999). The main field of theoretical statistics includes statistical distributional models and the estimation of the parameters involved. Having decided on a suitable model, questions of plausible inferences arise.

For fracture toughness data the model preferred is the Weibull distribution. Its density is

$$w(x; a, b, c) = \frac{y^{c-1}}{b} e^{-y^c}, \qquad (y = \frac{x-a}{b}, x > a, b, c > 0).$$

Here a, b, c refer to location, scale, and shape parameters.

This case has recently been studied by Bowman and Shenton (1998, 1999a, 1999b). There are special cases, and in particular the 2 parameter case with c (shape parameter) known turns out to be useful. The density is

$$w(x, a, b|c) = \frac{(x-a)^{c-1}}{b^c} e^{-(\frac{x-a}{b})^c}, \qquad (x > a, b > 0, c > 0).$$

1.2 Methods of Estimation

Conventionally the method of maximum likelihood takes front place. But here, from Bowman and Shenton (1999b) moments of maximum likelihood estimators are tied to the value of the shape parameter c. In fact, for example, the variance of $\hat{c}$, the maximum likelihood estimator of c, only exists if $c > 2$. Similarly the skewness of the distribution of $\hat{c}$ only exists if $c > 3$, and kurtosis requires $c > 4$. The maximum likelihood approach is therefore discarded.

1.3 Moment Estimators

The moment estimators for the 3 parameter case can be solved using

$$c_3^* = \frac{4.104683 - 1.148513\sqrt{b_1} + 0.441326b_1 - 0.053025(\sqrt{b_1})^3}{\sqrt{b_1} + \lambda}$$

$$(\sqrt{b_1} \text{ is a sample skewness}),$$

where in terms of the Riemann zeta function

$$\lambda = 2\zeta(3)/[\zeta(2)]^{3/2} = 1.139547.$$

Here, c_3^* is derived from $\sqrt{\beta_1}$ of the Weibull density.

For the scale parameter

$$b_3^* = \sqrt{m_2/[\Gamma(1 + 2/c_3^*) - \Gamma^2(1 + 1/c_3^*)]},$$

where $m_2 = \sum(x_j - \bar{x})^2/N$, with $\bar{x} = \sum_{j=1}^{N} x_j/N$. Finally, for the location,

$$a_3^* = m_1' - b_3^*\Gamma(1 + 1/c_3^*).$$

The subscripts on the estimators are used to indicate that the 3 parameter case is intended.

It turns out; however, that the skewness and kurtosis of the distribution of c_3^* for example are large numerically, requiring sample sizes of 300-500 to reduce the departure from the normal distribution. A significant departure would be $\beta_1 > 4$, $\beta_2 > 6$. So, interest is focussed on the 2 parameter case.

Moment estimators a_2^* and b_2^* for the 2 parameter Weibull density are defined by

$$\frac{b_2^*}{b} = \frac{\sqrt{m_2}}{\sqrt{\mu_2}}, \quad (\mu_2 = b^2[\Gamma(1 + 2/c) - \Gamma^2(1 + 1/c)]$$
$$a_2^* = m_1' - b_2^*\Gamma(1 + 1/c),$$

where m_1' = sample mean, m_2 = sample second central moment. Note that $\sqrt{m_2/\mu_2}$ is location and scale free.

In the remaining sequel only the 2 parameter case is considered, the corresponding subscript 2 being omitted.

1.4 Moments of a^* and b^*

The moments of a^* and b^* can be expanded in terms of the incremental deviates $\varepsilon_1 = m_1' - \mu_1'$, $\varepsilon_2 = m_2' - \mu_2'$, and $\varepsilon_3 = m_3' - \mu_3'$, m_r' being a sample rth non-central moment. Then, there is an algorithm to derive

$$E(m_1' - \mu_1')^{r_1}(m_2' - \mu_2')^{r_2}(m_3' - \mu_3')^{r_3}$$

and its 4 dimensional analogue (Shenton and Bowman, 1975).

The expected value of the ensuing series in terms of $(\varepsilon_1, \varepsilon_2, \varepsilon_3)$ and the sample size N is arranged in descending powers of N and may be divergent (or semi-convergent). Nonetheless, Padé sequences may be set up and studied for convergency tendencies when N is not small.

For example,

$$\begin{aligned}\sqrt{m_2} &= (m_2' - m_1'^2)^{1/2} = [\mu_2' + \varepsilon_2 - (\mu_1' + \varepsilon_1)^2]^{1/2} \\ &= (\mu_2' - \mu_1'^2 - 2\mu_1'\varepsilon_1 + \varepsilon_2 - \varepsilon_1^2)^{1/2} = \sqrt{\mu_2}\left(1 + \frac{\varepsilon_2 - 2\mu_1'\varepsilon_1 - \varepsilon_1^2}{\mu_2}\right)^{1/2} \\ &= \sqrt{\mu_2}\left[1 + \frac{1}{2}\left(\frac{\varepsilon_2 - 2\mu_1'\varepsilon_1 - \varepsilon_1^2}{\mu_2}\right) + \cdots\right]\end{aligned}$$

formally.

2 Moments of $\sqrt{m_2/\mu_2}$, the Standardized $s.d.$

2.1 Mean and Variance

Assuming the existence of moments, we have

$$E\sqrt{\frac{m_2}{\mu_2}} = \sqrt{1 - \frac{1}{N}}E\left[1 + \frac{m_2 - E(m_2)}{\left(1 - \frac{1}{N}\right)\mu_2}\right]^{1/2} \qquad (N = 2, 3, \cdots). \tag{1}$$

Let

$$\sqrt{1 + \frac{x}{M}} = \sum \frac{a_s x^s}{M^s} \tag{2}$$

formally; then

$$a_s = \frac{(-1)^{s-1} 1 \cdot 3 \cdots (2s-3)}{2^s s!}, \qquad (s = 2, 3, \cdots;\ a_0 = 1,\ a_1 = 1/2)$$

$$a_s = -\left(1 - \frac{3}{2s}\right) a_{s-1}.$$

In particular, concerning expression (1)

$$E\sqrt{\frac{m_2}{\mu_2}} \sim \sqrt{1 - \frac{1}{N}} E\left(1 + \frac{X}{2\bar{\mu}_2} - \frac{X^2}{8\bar{\mu}_2{}^2} + \frac{X^3}{16\bar{\mu}_2{}^3} - \frac{5X^4}{128\bar{\mu}_2{}^4} + \frac{7X^5}{256\bar{\mu}_2{}^5} - \frac{21X^6}{1024\bar{\mu}_2{}^6} + \cdots\right) \tag{3}$$

where $\bar{\mu}_2 = \left(1 - \frac{1}{N}\right)\mu_2$ and $X = m_2 - E(m_2)$. Thus

$$E(X^s) = \mu_s(m_2), \qquad (s = 1, 2, \cdots)$$

and $\mu_1(m_2) = 0$, $\mu_1'(m_2) = \left(1 - \frac{1}{N}\right)\mu_2$.

2.2 Moments of m_2

Several decades ago the problem of deriving moments of sample moments was approached by the skillful application of symmetric functions (David, Kendall and Barton, 1966, MacMahon, 1960, Kotz, Johnson and Read, 1988). This approach involves sophisticated and laborious algebraic analysis; for example, $\mu_3(m_4)$, and $\mu_4(m_4)$ are not undertaken in a cavalier mathematical mood.

A recent study by Y.C. Patel (see Bowman and Shenton, 1988) using symmetric functions considers moments up to $Var(m_4 - 3m_2^2)$ which includes terms of order N^{-1} to N^{-7}. For our present purpose, here are the results we need in expression (3):

$$\mu_2(m_2) = Var(m_2) = \left(\frac{\beta_2 - 1}{N} - \frac{2\beta_2 - 4}{N^2} + \frac{\beta_2 - 3}{N^3}\right)\mu_2^2,$$

$$E_2\left(\frac{m_2^3}{\mu_2^3}\right) = \beta_4 - 12\beta_2 - 6\beta_1 + 20,$$

$$E_3\left(\frac{m_2^3}{\mu_2^3}\right) = -\beta_4 + 15\beta_2 + 10\beta_1 - 30;$$

$$E_3\left(\frac{m_2^4}{\mu_2^4}\right) = \beta_6 - 20\beta_4 - 24\beta_3 - 15\beta_2^2 + 180\beta_2 + 192\beta_1 - 218.$$

Here, $E_s(\cdot)$ refers to the coefficient of N^{-s}, and in Pearson's notation,

$$\beta_6 = \mu_8/\mu_2^4, \quad \beta_4 = \mu_6/\mu_2^3, \quad \beta_3 = \mu_3\mu_5/\mu_2^4, \quad \beta_2 = \mu_4/\mu_2^2, \quad \beta_1 = \mu_3^2/\mu_2^3.$$

Note that

$$\mu_2(m_2) \text{ involves coefficients of } N^{-1} \text{ to } N^{-3},$$

$$\mu_3(m_2) \text{ involves coefficients of } N^{-2} \text{ to } N^{-5},$$

$$\mu_4(m_2) \text{ involves coefficients of } N^{-2} \text{ to } N^{-7}.$$

Returning to (3), all the terms contribute to the N^{-3} term in $E\sqrt{m_2/\mu_2}$. The N^{-1} term, from (3) is found from

$$\sqrt{1-\frac{1}{N}}\left[-\frac{1}{8}Var\left(\sqrt{\frac{m_2}{\mu_2}}\right)\right] \qquad \text{i.e.}\sqrt{1-\frac{1}{N}}\left(\frac{1-\beta_2}{8}\right).$$

For the N^{-2} term, we use

$$\sqrt{1-\frac{1}{N}}\left[1-\frac{Var(m_2)}{8\mu_2^2\left(1-\frac{1}{N}\right)^2}\right]+\frac{\mu_3(m_2)}{16\mu_2^3}-\frac{5\mu_4(m_2)}{128\mu_2^4},$$

for which in the last two terms the factors $(1-1/N)^3$ and $(1-1/N)^4$ may be ignored since $\mu_3(m_2)$ and $\mu_4(m_2)$ are each of order N^{-2}.

2.3 Expression to Order N^{-2} for the Moments of $\sqrt{m_2/\mu_2}$ in General Sampling

The following formulas have been derived.

$$E\sqrt{\frac{m_2}{\mu_2}} \sim \sqrt{1-\frac{1}{N}}\left[1+\frac{1-\beta_2}{8N}+\frac{\frac{\beta_4}{16}-\frac{15\beta_2^2}{128}+\frac{3\beta_2}{64}-\frac{3\beta_1}{8}-\frac{31}{128}}{N^2}\right] \quad (N\to\infty) \tag{4}$$

$$\begin{aligned} Var\left(\sqrt{\frac{m_2}{\mu_2}}\right) &= 1-\frac{1}{N}-\left[E\left(\sqrt{\frac{m_2}{\mu_2}}\right)\right]^2 \\ &\sim \left(1-\frac{1}{N}\right)\left(\frac{\beta_2-1}{4N}-\frac{\frac{\beta_4}{8}-\frac{7\beta_2^2}{32}+\frac{\beta_2}{16}-\frac{3\beta_1}{4}-\frac{15}{32}}{N^2}\right) \end{aligned} \tag{5}$$

$$\mu_3\left(\sqrt{\frac{m_2}{\mu_2}}\right) \sim \frac{\frac{\beta_4}{8} - \frac{9\beta_2^2}{32} + \frac{3\beta_2}{16} - \frac{3\beta_1}{4} + \frac{3(\beta_2-1)^2}{32} - \frac{1}{32}}{N^2}. \tag{6}$$

The forth central moment is derived from

$$\mu_4\left(\sqrt{\frac{m_2}{\mu_2}}\right) = E\left(\frac{m_2}{\mu_2}\right)^2 - 4E\left(\sqrt{\frac{m_2}{\mu_2}}\right)\mu_3\left(\sqrt{\frac{m_2}{\mu_2}}\right)$$
$$-6\left[E\left(\sqrt{\frac{m_2}{\mu_2}}\right)\right]^2 \mu_2\left(\sqrt{\frac{m_2}{\mu_2}}\right) - \left[E\left(\sqrt{\frac{m_2}{\mu_2}}\right)\right]^4. \tag{7}$$

The expressions (4) and (5) for mean and variance involve the N^{-2} term contribution. However the third central moment (6) provides only the basic asymptotic; the N^{-3} and N^{-4} terms would be much more complicated. Note that the mean has a component $\sqrt{1-1/N}$, the variance, a component $1-1/N$. In (7), the component function appears to be $1-1/N$, this arising from $E(m_2/\mu_2)^2$. Further study of the formulas in (4)-(7) is given in the sequel.

2.4 Asymptotic Moments of the Weibull Random Variate

We have

$$\mu_s(x) = \int_0^\infty e^{-t}\left[t^{\frac{1}{c}} - \Gamma\left(1+\frac{1}{c}\right)\right]^s dt, \tag{8}$$

and

$$t^{\frac{1}{c}} - \Gamma\left(1+\frac{1}{c}\right) = \frac{1}{c}[\ln(t) - \Gamma^{(1)}(1)] + \frac{1}{2!c^2}[\ln^2(t) - \Gamma^{(2)}(1)] + \frac{1}{3!c^3}[\ln^3(t) - \Gamma^{(3)}(1)]$$
$$+\cdots + \frac{1}{s!c^s}[\ln^s(t) - \Gamma^{(s)}(1)],$$

where $\Gamma^{(s)}(x) = \frac{d^s}{ds}\Gamma(x)$, $s = 0, 1, \cdots$. $\Gamma^{(0)}(x) = \Gamma(x)$. Expression (8) shows that asymptotically

$$\mu_s(x) \sim \frac{1}{c^s}\int_0^\infty e^{-t}[\ln(t) - \Gamma^{(1)}(1)]^s dt, \quad (c \to \infty). \tag{9}$$

Now (9) can be evaluated recursively. For there is the generating function

$$\begin{aligned} G(\alpha) &= \int_0^\infty e^{-t} e^{\alpha[\ln(t) - \Gamma^{(1)}(1)]} dt \\ &= \int_0^\infty e^{-t} t^{\alpha - \alpha\Gamma^{(1)}(1)} dt \quad (\alpha > -1) \\ &= e^{-\alpha\psi(1)}\Gamma(\alpha+1) \qquad \left(\text{since } \Gamma^{(1)}(1) = \frac{\Gamma'(1)}{\Gamma(1)} = \psi(1)\right). \end{aligned}$$

Taking logarithms and differentiating we have

$$\frac{G'(\alpha)}{G(\alpha)} = -\alpha\psi(1) + \psi(\alpha+1).$$

Let

$$G(\alpha) = A_0 + \frac{A_1\alpha}{1!} + \frac{A_2\alpha^2}{2!} + \cdots, \quad (A_0 = 1).$$

Then

$$A_1 + \frac{A_2\alpha}{1!} + \frac{A_3\alpha^2}{2!} + \cdots + \frac{A_s\alpha^{s-1}}{(s-1)!}\cdots = \left(1 + \frac{A_1\alpha}{1!} + \frac{A_2\alpha^2}{2!} + \cdots\right)\left(\alpha\psi_1 + \frac{\alpha^2\psi_2}{2!} + \cdots\right)$$

where $\psi_r(\alpha) = \frac{d^r\psi(\alpha)}{d\alpha^r}$.

Equating coefficient of α^0, α^1, $\alpha^2, \cdots$, we have

$$\begin{aligned}
A_1 &= 0, \\
A_2 &= \psi_1(1) = \zeta(2) = \pi^2/6 = \mu_2 c^2 \quad (c \to \infty), \\
A_3 &= \psi_2(1) = -2\zeta(3) = \mu_3 c^3, \\
A_4 &= \psi_3(1) + 3[\psi_1(1)]^2 = \pi^4/15 + 3\zeta^2(2) = 3\pi^4/20 = \mu_4 c^4, \\
A_5 &= \psi_4(1) + 10\psi_1(1)\psi_2(1) = -24\zeta(5) - 10\pi^2\zeta(3)/3 = \mu_5 c^5, \\
A_6 &= \psi_5(1) + 10\psi_2^2(1) + 15\psi_1(1)\psi_3(1) + 15\psi_1^3(1) \\
&= 61\pi^6/168 + 40\zeta^2(3) = \mu_6 c^6.
\end{aligned}$$

From these we have the asymptotic moment ratios for a Weibull variate:

$$\begin{aligned}
\sqrt{\beta_1} &= \mu_3/\mu_2^{3/2} \sim -2\zeta(3)/[\zeta(2)]^{3/2} = -1.139547, \\
\beta_2 &= \mu_4/\mu_2^2 \sim 27/5, \\
\mu_5/\mu_2^{5/2} &\sim -18.566616, \\
\mu_6/\mu_2^3 &= \beta_4 \sim 91.414247.
\end{aligned}$$

For the normal itself $\sqrt{\beta_1} = 0$, $\beta_2 = 3$, $\mu_5 = 0$, and $\beta_4 = 15$. Similarly, higher order terms for the asymptotic moments could be obtained.

3 Moments of Sample Moments

3.1 Some History back to Tchouproff

In 1918 and 1919, Tchouproff produced articles of total length 55 pages in *Biometrika* on the mathematical expectation of the moments of frequency distributions. For example,

$$E(m'_r - \mu'_r)(m'_s - \mu'_s)(m'_t - \mu'_t) = (\mu'_{r+s+t} - \mu'_r\mu'_{s+t} - \mu'_s\mu'_{r+t} - \mu'_t\mu'_{r+s} + 2\mu'_r\mu'_s\mu'_t)/N^2.$$

Notice that he did not give an expression for

$$E(m_r - \mu_r)(m_s - \mu_s)(m_t - \mu_t)$$

because central moments are not linear in non-central moments. At the time generating functions were not frequently available in the literature. For non-central moments, we have

$$Ee^{\alpha(m'_r-\mu'_r)+\beta(m'_s-\mu'_s)+\gamma(m'_t-\mu'_t)} = \left\{Ee^{\frac{[\alpha(x^r-\mu'_r)+\beta(x^s-\mu'_s)+\gamma(x^t-\mu'_t)]}{N}}\right\}^N.$$

For the special case of a single moment

$$Ee^{\alpha(m'_r-\mu'_r)} = \left[Ee^{\alpha(x^r-\mu'_r)/N}\right]^N = \left(1 + \frac{\alpha^2 a_2}{2!N^2} + \frac{\alpha^3 a_3}{3!N^3} + \cdots\right)^N = A_0 + \frac{A_1\alpha}{1!} + \frac{A_2\alpha^2}{2!} + \cdots,$$

where assuming the existence of moments,

$$\left(A_1 + \frac{A_2\alpha}{1!} + \frac{A_3\alpha^2}{2!} + \cdots\right)\left(a_0 + \frac{a_1\alpha}{1!N} + \frac{a_2\alpha^2}{2!N^2} + \frac{a_3\alpha^3}{3!N^3} + \cdots\right) = \tag{10}$$
$$\left(a_1 + \frac{a_2\alpha}{1!N} + \frac{a_3\alpha^2}{2!N^2} + \cdots\right)\left(A_0 + \frac{A_1\alpha}{1!} + \frac{A_2\alpha^2}{2!} + \frac{A_3\alpha^3}{3!} + \cdots\right)$$

where $A_s = E(m'_r - \mu'_r)^s$, and $a_s = E(x^r - \mu'_r)^s$.

The equality in (10) leads to the recurrence relations

$$a_0A_1 = a_1A_0,$$
$$a_0A_2 + \frac{a_1A_1}{N} = \frac{a_2A_0}{N} + a_1A_1,$$
$$a_0A_3 + \frac{2a_1A_2}{N} + \frac{a_2A_1}{N^2} = \frac{a_3A_0}{N^2} + \frac{2a_2A_1}{N} + a_1A_2,$$

and in general

$$\sum_{s=0}^{r-1}\binom{r-1}{s}\frac{a_s A_{r-s}}{N^s}=\sum_{s=0}^{r-1}\binom{r-1}{s}\frac{A_s a_{r-s}}{N^{r-s-1}}.$$

From this (Shenton, Bowman and Sheehan, 1971; Shenton and Bowman, 1975),

$$A_{s+1}=\sum_{r=0}^{s}\binom{s}{r}a_{r-1}A_{s-r}\left(\frac{1}{N^r}-\frac{s-r}{(r+1)N^{r+1}}\right)\qquad(s=1,2,\cdots).$$

3.2 The Multivariate Case

For simplicity we confine attention to the bivariate case, defining

$$A_{r,s}=E(m'_R-\mu'_R)^r(m'_S-\mu'_S)^s,\qquad a_{r,s}=E(x^R-\mu'_R)^r(x^S-\mu'_S)^s.$$

The recursion for the coefficient of N^{-k} in $A_{s,t}$ is now defined by the two systems

$$\begin{aligned}
A^{(k)}_{s+1,t}&=\sum_{\lambda=0}^{s}\sum_{\mu=0}^{t}\binom{s}{\lambda}\binom{t}{\mu}a_{s+1-\lambda,t-u}A^{(k+\lambda+\mu-s-t)}_{\lambda,\mu}\\
&\qquad-(1-\delta_{\lambda,\mu})\sum_{\lambda=0}^{s}\sum_{\mu=0}^{t}\binom{s}{\lambda}\binom{t}{\mu}a_{\lambda,u}A^{(k-\lambda-\mu)}_{s+1-\lambda,t-\mu}\\
A^{(k)}_{s,t+1}&=\sum_{\lambda=0}^{s}\sum_{\mu=0}^{t}\binom{s}{\lambda}\binom{t}{\mu}a_{s-\lambda,t+1-\mu}A^{(k+\lambda+\mu-s-t)}_{\lambda,\mu}\\
&\qquad-(1-\delta_{\lambda,\mu})\sum_{\lambda=0}^{s}\sum_{\mu=0}^{t}\binom{s}{\lambda}\binom{t}{\mu}a_{\lambda,u}A^{(k-\lambda-\mu)}_{s-\lambda,t+1-\mu}
\end{aligned}\tag{11}$$

where δ is the Kronecker function, and

1. $\left[\frac{s+t+1}{2}\right]\le k\le s+t$,
2. $A^{(k)}_{s,t}=0$ for $k<0$ or $k\ge s+1$,
3. $[x]$ is the integer part of x, and
4. $A_{0,0}=a_{0,0}=1$; $A_{1,0}=A_{0,1}=a_{1,0}=a_{0,1}=0$.

Successive values of $A_{s,t}$ can be implemented for computer facilities. The fundamental entities are univariate expectations, such as

$$E(x-\mu_1')^r(x^2-\mu_2')^s = Ey^r(y^2-2\mu_1'y-\mu_2)^s$$
$$= \sum\sum_{0\le l+m\le s}\frac{s!p^m q^{s-l-m}}{l!m!(s-l-m)!}\mu_{r+2l+m} \quad (p=2\mu_1', q=-\mu_2).$$

After a considerable period of time Bowman and Shenton (1975) were able to extend the approach in (11) to 3 and 4 dimensional cases. For example, the ratio moments $\sqrt{b_1} = m_3/m_2^{3/2}$ and $b_2 = m_4/m_2^2$ involve m_1', m_2', m_3' and m_4', which in turn lead to fourfold summation in the fundamental non-central moment procedure. These powerful algorithms have been used to determine terms as far as those of order N^{-30}, some loss of accuracy being possible. One may refer to Bowman and Shenton (1975, 1978, 1992) and Shenton and Bowman (1967, 1970).

4 Moment Series and the Estimation of b^*/b

4.1 Series

We now pay particular attention to the 2-parameter Weibull distribution (c known) and the variate b^*/b. Series to order N^{-12} and $c = 1.1$, 2.0 and 4.0 are given in Table 1. The constant term in μ_1' is unity.

Comments:

- The N^{-12} coefficient is approximately 24! for the four moments when $c = 1.1$, but decreases in value to 12!, approximately, when $c = 4.0$.
- The sign pattern for a variance is of alternating form; there is a delay of this pattern for the variance when $c = 4$.
- As far as the computations go, the series appear to be divergent.
- Some loss of accuracy might be expected in the N^{-12} and higher coefficients.

Table 1. Moment Series for $b^*/b = \sqrt{m_2/\mu_2}$ $(a = 0,\ b = 1)$

s	μ_1'	μ_2	μ_3	μ_4
		$c = 1.1$		
1	-0.12949808D+01	0.15899616D+01	0.00000000D+00	0.00000000D+00
2	0.33541486D+01	-0.83852724D+01	0.85592997D+01	0.75839336D+01
3	-0.56619908D+02	0.12192693D+03	-0.15922945D+03	0.31042721D+02
4	0.21507737D+04	-0.44594410D+04	0.59382974D+04	-0.40771952D+04
5	-0.13880907D+06	0.28356838D+06	-0.38495160D+06	0.34140258D+06
6	0.13185520D+08	-0.26748184D+08	0.36888172D+08	-0.36652173D+08
7	-0.17017022D+10	0.34387291D+10	-0.47997698D+10	0.50863788D+10
8	0.28343473D+12	-0.57138560D+12	0.80493111D+12	-0.88910003D+12
9	-0.58790257D+14	0.11832810D+15	-0.16789751D+15	0.19088916D+15
10	0.14793076D+17	-0.29740587D+17	0.42442195D+17	-0.49291263D+17
11	-0.44258087D+19	0.88903683D+19	-0.12746590D+20	0.15046813D+20
12	0.15495262D+22	-0.31106228D+22	0.44771176D+22	-0.53535862D+22
		$c = 2.0$		
1	-0.78063616D+00	0.56127233D+00	0.00000000D+00	0.00000000D+00
2	-0.96232698D-01	-0.41692742D+00	0.51316841D+00	0.94507987D+00
3	-0.33147003D+00	0.51269461D+00	-0.87597195D+00	-0.70721799D+00
4	0.48973594D+00	-0.15062476D+01	0.24114691D+01	-0.36107931D+00
5	-0.42316661D+01	0.91641468D+01	-0.13361996D+02	0.80478231D+01
6	0.41985036D+02	-0.90592470D+02	0.13031634D+03	-0.10617071D+03
7	-0.46045208D+03	0.98596446D+03	-0.14394820D+04	0.13126743D+04
8	0.67801792D+04	-0.14274214D+05	0.20751961D+05	-0.20565287D+05
9	-0.11562712D+06	0.24178330D+06	-0.35274231D+06	0.36748559D+06
10	0.22847435D+07	-0.47490717D+07	0.69432497D+07	-0.74979549D+07
11	-0.51594909D+08	0.10673997D+09	-0.15633198D+09	0.17345727D+09
12	0.13056954D+10	-0.26915937D+10	0.39490945D+10	-0.44737757D+10
		$c = 4.0$		
1	-0.71847869D+00	0.43695738D+00	0.00000000D+00	0.00000000D+00
2	-0.29526372D+00	0.74315805D-01	0.84192689D-01	0.57279526D+00
3	-0.74615505D-01	-0.27505037D+00	0.42387706D+00	0.16476999D-01
4	0.40218228D+00	-0.99876453D+00	0.10768982D+01	-0.12693519D+01
5	0.27077063D+00	-0.76849670D-02	-0.10928083D+01	-0.54100228D+00
6	-0.91117444D+01	0.18844507D+02	-0.26371382D+02	0.27801511D+02
7	-0.29608695D+02	0.46344117D+02	-0.46076327D+02	0.81859275D+02
8	0.46472052D+03	-0.97748955D+03	0.14242622D+04	-0.15432113D+04
9	0.46478238D+04	-0.86469263D+04	0.11275708D+05	-0.14656681D+05
10	-0.27696733D+05	0.62349458D+05	-0.97731462D+05	0.10216518D+06
11	-0.86797056D+06	0.16989849D+07	-0.23721396D+07	0.29409633D+07
12	-0.15433914D+07	0.18234433D+07	-0.89768497D+06	0.36651252D+07

- The analysis of divergent series and summation techniques is considered in Baker and Hunter (1973), Baker and Gaves-morris (1981), Gaunt and Gattman (1973), Emile Borel (1928), and Bender and Wu (1969).

For the relation between series and continued fraction, a well known example relates to $\ln\Gamma(z)$. An historical account is given in Appendix D - Supplement.

5 Rational Fraction Sequences for b^*/b and a^*

5.1 Padé Sequences for b^*/b, $a = 0$, $b = 1$. Mean: $\mu_1'(b^*/b)$. $N = 15$, 30, 50

The Stieltjes p, q form (Appendix A) is

$$\mu_1'(b^*/b) = N\left(\frac{q_0}{N+}\,\frac{p_1}{1+}\,\frac{q_1}{N+}\,\frac{p_2}{1+}\,\frac{q_2}{N+\cdots}\right)$$

where N is the sample size.

If attention is paid to the p_s and q_s, there is no particular pattern but the magnitudes are in marked contrast to the series coefficients (Table 1). Nonetheless the successive "convergents" suggest convergence.

The variance of $b^*/b = \sqrt{m_2/\mu_2}$ is derived from $Var(\sqrt{m_2/\mu_2}) = 1 - 1/N - [E(\sqrt{m_2/\mu_2})]^2$.

5.2 Padé Sequence for $\mu_3(b^*/b)$, $a = 0$, $b = 1$.

$$\mu_3(b^*/b) = \frac{1}{N}\left(\frac{q_0}{N+}\,\frac{p_1}{1+}\,\frac{q_1}{N+}\,\frac{p_2}{1+}\,\frac{q_2}{N+\cdots}\right)$$

Again the convergence is satisfactory. From this and the expression (7) in §2.3, the fourth central moment $\mu_4(b^*/b)$ can be set up. The tables are excerpts from a larger tabulation which supplies information for application formulas. A similar tabulation has been set up for the moments of a^*.

Table 2a. Padé sequences for $\mu_1'(b^*/b)$, $a = 0$, $b = 1$

c	s	P_s	Q_s
1.1	0		1.00000000D+00
	1	1.29498080D+00	1.29513372D+00
	2	2.85792050D+01	1.06422041D+01
	3	1.02994696D+02	-1.66090637D+00
	4	-2.87904780D+03	3.06068568D+03
	5	4.23854877D+00	2.75310324D+02
	6	1.01771503D+02	2.93245484D+02
	7	-2.32229805D+04	0.00000000D+00

s	$N = 15$		$N = 30$		$N = 50$	
3	0.92052885	0.92638020	0.95862018	0.96026461	0.97475424	0.97537597
4	0.92264507	0.92340778	0.95947899	0.95960179	0.97515342	0.97518018
5	0.92276306	0.92275183	0.95951050	0.95950919	0.97516293	0.97516273
6	0.92276312	0.92252711	0.95951052	0.95948660	0.97516294	0.97515968
7	0.92281418	0.92243048	0.95952759	0.95947922	0.97517704	0.97515892

c	s	P_s	Q_s
2.0	0		1.00000000D+00
	1	7.80636163D-01	-9.03910875D-01
	2	-4.52941345D-01	2.23637326D+00
	3	4.49107516D+00	4.64352271D+00
	4	1.90868866D+00	5.82046739D+01
	5	-4.83205813D+01	-1.70823000D+00
	6	3.22653061D+01	-5.67876139D+00
	7	1.43189667D+03	0.00000000D+00

s	$N = 15$		$N = 30$		$N = 50$	
3	0.95053202	0.94752634	0.97463873	0.97387143	0.98462729	0.98434869
4	0.94742688	0.94744016	0.97385930	0.97386016	0.98434610	0.98434621
5	0.94743742	0.94743796	0.97386005	0.97386007	0.98434620	0.98434620
6	0.94743791	0.94743795	0.97386007	0.97386007	0.98434620	0.98434620
7	0.94743805	0.94743811	0.97386007	0.97386007	0.98434620	0.98434620

c	s	P_s	Q_s
4.0	0		1.00000000D+00
	1	7.18478691D-01	-1.12943551D+00
	2	5.75804712D-02	-8.91028987D+00
	3	8.96207683D+00	-2.41353912D+00
	4	-2.34908322D-01	1.60923060D+02
	5	-1.65834052D+02	4.58700790D-01
	6	-6.66251476D+00	1.47674034D+01
	7	4.53666946D+01	0.00000000D+00

s	$N = 15$		$N = 30$		$N = 50$	
3	0.95429083	0.95075217	0.97661086	0.97571808	0.98583399	0.98551134
4	0.95076675	0.95078786	0.97571986	0.97572061	0.98551172	0.98551180
5	0.95077532	0.95077444	0.97572038	0.97572037	0.98551179	0.98551179
6	0.95077443	0.95077444	0.97572037	0.97572037	0.98551179	0.98551179
7	0.95077462	0.95077457	0.97572037	0.97572037	0.98551179	0.98551179

Table 2b. Padé sequences for $\mu_3(b^*/b)$, $a = 0$, $b = 1$.

c	s	P_s	Q_s
1.1	0		8.55929972D+00
	1	1.86030928D+01	1.86908718D+01
	2	5.49332713D+01	4.55912542D+01
	3	1.02475174D+02	7.89604697D+01
	4	1.62301982D+02	1.17496665D+02
	5	2.36679906D+02	1.58970019D+02
	6	-4.16283017D+04	-7.16916918D-01

s	$N = 15$		$N = 30$		$N = 50$	
3	0.01698117	0.02450848	0.00587020	0.00688125	0.00249531	0.00269410
4	0.01922594	0.02173754	0.00630552	0.00653324	0.00260199	0.00263225
5	0.01977390	0.02082356	0.00637983	0.00645071	0.00261472	0.00262172
6	0.01994779	0.02044241	0.00639795	0.00642435	0.00261710	0.00261915

c	s	P_s	Q_s
2.0	0		5.13168408D-01
	1	1.70698729D+00	1.04591943D+00
	2	7.33843657D+00	3.81997487D+00
	3	-2.55005908D+00	-6.83083518D+01
	4	8.31581940D+01	-4.95512295D-01
	5	-5.61303587D+01	7.95455170D+01
	6	-1.31790983D+02	1.39028461D+00

s	$N = 15$		$N = 30$		$N = 50$	
3	0.00204772	0.00206145	0.00053949	0.00054047	0.00019849	0.00019863
4	0.00205712	0.00205776	0.00054028	0.00054030	0.00019861	0.00019861
5	0.00205787	0.00205774	0.00054030	0.00054030	0.00019861	0.00019861
6	0.00205835	0.00205828	0.00054030	0.00054030	0.00019861	0.00019861

c	s	P_s	Q_s
4.0	0		8.41926895D-02
	1	-5.03460646D+00	2.49401567D+00
	2	-3.62176045D+00	-2.09826701D-04
	3	1.20132751D+05	-1.20139305D+05
	4	5.05276796D-04	-6.61668057D+00
	5	1.04376010D+01	-2.41700973D+01
	6	6.18334032D+01	-1.59117949D+00

s	$N = 15$		$N = 30$		$N = 50$	
3	0.00056323	0.00052539	0.00011241	0.00011070	0.00003745	0.00003725
4	0.00051634	0.00051634	0.00011049	0.00011049	0.00003724	0.00003724
5	0.00051634	0.00051813	0.00011049	0.00011050	0.00003724	0.00003724
6	0.00051763	0.00051740	0.00011050	0.00011050	0.00003724	0.00003724

Note that the Padé approach has been used to assess the first four moments of b^*/b. The equalities mentioned for the variance and fourth central moment series as checks and are referred to in the sequel.

5.3 Four Moment Approximating Distributions

If we have 4 moments $(m_1', m_2, \sqrt{b_1}, b_2)$ for a statistic, then a 4 moment approximating distribution may be set up. Useful choices are the Pearson system (Elderton and Johnson, 1969) and the Johnson translation system (Johnson, 1949).

- The Pearson system: This is based on the differential equation

$$\frac{1}{y}\frac{dy}{dx} = \frac{a+bx}{Ax^2+Bx+C},$$

  where y is the density. An algorithm (Bowman and Shenton, 1979a, 1979b) is available to set up the percentage points; 1%, 2.5%, 5%, 10%, 25%, 50%, 75%, 90%, 95%, 97.5%, 99%. There is a guide to the parameter limitations and also the error involved.

- The Johnson translation system: This is described in Bowman and Shenton (1980, 1981, 1988a, 1989b). The two systems are

$$S_U: \quad z = \gamma + \delta \sinh^{-1}\left(\frac{x-\zeta}{\lambda}\right) \quad [z \epsilon N(0,1)], \text{ and}$$

$$S_B: \quad z = \gamma + \delta \ln y, \quad y = \left(\frac{x-\zeta}{\zeta+\lambda-x}\right) \quad (\zeta \le x \le \zeta+\lambda, \zeta = \mu_1'(x) - \lambda\mu_1'(y)).$$

  The reader is reminded that in the S_U paper (Bowman and Shenton, 1980) the equation for ω^* should read

$$\omega^* = \sqrt{\sqrt{2\beta_2 - 2\beta_1\psi^*(\beta_2, \beta_1; \omega) - 2} - 1}.$$

  The algorithms supplied are readily set up for computer implementation.

A comparison of assessments by simulation and Padé for a^* and b^* is given in Table 3; some percentage points are also included.

The agreement between the Padé and simulation assessments is most satisfactory, especially for $N = 50$.

- Note that a^* is positively biased and b^* is negatively biased.
- Note also that moments have been set up under the assumption that $a = 0$, $b = 1$. These may be converted to $a = a_0$, $b = b_0$ as follows:

  for the mean

  $$\mu_1'(a^*|a_0, b_0) = a_0 + b_0\mu_1'(a^*|0, 1)$$

  and for the variance

  $$\mu_2(a^*|a_0, b_0) = b_0^2\mu_2(a^*|0, 1).$$

  Similarly

  $$\mu_1'(b^*|a_0, b_0) = b_0\mu_1'(b^*|0, 1)$$

  and

  $$\mu_2(b^*|a_0, b_0) = b_0^2\mu_2(b^*|0, 1).$$

Note that the skewness and kurtosis are location and scale free.

Table 3a. Padé approximation of moments and percentage points of a^* when $c = 2.1$, $b = 1.0$, $a = 0$.

N		μ_1'	σ	$\sqrt{\beta_1}$	β_2	5%	25%	50%	75%	95%
10	Padé	0.069	0.196	-0.011	3.185	-0.25	-0.06	0.07	0.20	0.39
	MC	0.070	0.196	-0.000	3.205					
11	Padé	0.063	0.187	-0.016	3.174	-0.24	-0.06	0.06	0.19	0.37
	MC	0.063	0.186	-0.030	3.139					
12	Padé	0.058	0.179	-0.019	3.164	-0.24	-0.06	0.06	0.18	0.35
	MC	0.058	0.179	-0.017	3.144					
13	Padé	0.053	0.172	-0.022	3.155	-0.23	-0.06	0.05	0.17	0.33
	MC	0.054	0.172	-0.019	3.138					
14	Padé	0.049	0.166	-0.024	3.146	-0.22	-0.06	0.05	0.16	0.32
	MC	0.050	0.166	-0.023	3.106					
15	Padé	0.046	0.160	-0.026	3.139	-0.22	-0.06	0.05	0.15	0.31
	MC	0.046	0.161	-0.022	3.122					
20	Padé	0.034	0.139	-0.031	3.110	-0.20	-0.06	0.03	0.13	0.26
	MC	0.035	0.139	-0.028	3.099					
30	Padé	0.023	0.114	-0.032	3.077	-0.17	-0.05	0.02	0.10	0.21
	MC	0.024	0.114	-0.029	3.104					
40	Padé	0.017	0.099	-0.031	3.059	-0.15	-0.05	0.02	0.08	0.18
	MC	0.018	0.099	-0.041	3.057					
50	Padé	0.014	0.088	-0.029	3.048	-0.13	-0.05	0.01	0.07	0.16
	MC	0.014	0.089	-0.029	3.076					

Table 3b. Padé approximation of moments and percentage points of b^* when $c = 2.1$, $b = 1.0$, $a = 0$.

N		μ_1'	σ	$\sqrt{\beta_1}$	β_2	5%	25%	50%	75%	95%
10	Padé	0.922	0.225	0.335	3.141	0.58	0.76	0.91	1.07	1.31
	MC	0.921	0.224	0.327	3.122					
11	Padé	0.929	0.215	0.320	3.130	0.60	0.78	0.92	1.07	1.30
	MC	0.929	0.215	0.330	3.113					
12	Padé	0.935	0.206	0.307	3.121	0.62	0.79	0.92	1.07	1.29
	MC	0.934	0.206	0.302	3.085					
13	Padé	0.940	0.198	0.295	3.112	0.63	0.80	0.93	1.07	1.28
	MC	0.939	0.199	0.296	3.118					
14	Padé	0.944	0.191	0.285	3.105	0.65	0.81	0.94	1.07	1.27
	MC	0.944	0.192	0.285	3.091					
15	Padé	0.948	0.185	0.275	3.099	0.66	0.82	0.94	1.07	1.27
	MC	0.948	0.186	0.285	3.124					
20	Padé	0.961	0.161	0.240	3.076	0.71	0.85	0.95	1.07	1.24
	MC	0.960	0.161	0.236	3.068					
30	Padé	0.974	0.132	0.197	3.052	0.76	0.88	0.97	1.06	1.20
	MC	0.973	0.132	0.193	3.061					
40	Padé	0.981	0.115	0.171	3.039	0.80	0.90	0.98	1.06	1.17
	MC	0.980	0.115	0.194	3.070					
50	Padé	0.985	0.103	0.153	3.032	0.82	0.91	0.98	1.05	1.16
	MC	0.984	0.103	0.157	3.057					

6 A Collection of Simple Formulas for the Moments and Moment Ratios

6.1 Means

Using the Padé results for $(1.1 \leq c \leq 4.0)$ and $(10 \leq N \leq 100)$ we have the algorithm

$$\frac{E(b^*)}{b} \sim 1 + \frac{A_1}{N} + \frac{A_2}{N^2}$$

where

$$A_1 = -0.827043 + \frac{0.806668}{c} - \frac{1.423234}{c^2}$$
$$A_2 = 0.436183 - \frac{3.990936}{c} + \frac{5.658460}{c^2},$$

with absolute error less than 0.1% except at $c = 1.1$ and $N = 10$ for which the error is 0.175%. The formula given in (4) for $E(\sqrt{m_2/\mu_2})$ is derived from its series development in terms of the random variate $[m_2 - E(m_2)]$; the error for $(1.1 \leq c \leq 4.0)$ and $(13 \leq N \leq 100)$ is less than 1%.

Note that we now have the important result that

$$b^{**} = \frac{b^*}{1 + A_1/N + A_2/N^2}$$

is almost unbiased for b.

For the location parameter a, the moment estimator is

$$a^* = m_1' - b^*\Gamma(1 + 1/c) \qquad (c \text{ known}),$$

and

$$E(a^{**}) = m_1' - b^{**}\Gamma(1 + 1/c)$$

is almost unbiased for the location parameter a.

6.2 Variances

From (5), $\sigma(b^*/b) = \sqrt{1 - 1/N - [E(b^*/b)]^2}$, and this can be set up from $E(b_2^*/b)$ or the Padé form for $Var(b_2^*/b)$.

6.3 Skewness and Kurtosis

The formula for $\sqrt{\beta_1(b^*/b)}$ is

$$\sqrt{\beta_1\left(\frac{b^*}{b}\right)} = \sqrt{\beta_1(b^*)} \sim \frac{1}{\sqrt{N}}\left(B_1 + \frac{B_2}{N}\right)$$

where

$$B_1 = -0.600783 + \frac{1.964495}{c} + \frac{3.330215}{c^2}$$
$$B_2 = -0.847900 + \frac{13.437573}{c} - \frac{25.060284}{c^2}$$

with for $1.1 < c \leq 3.0$ and $10 \leq N \leq 100$ the maximum error is less than 5%. For $c > 3.0$, $10 \leq N \leq 100$, $\sqrt{\beta_1} < 0.15$.

The formula for the $\beta_2(b^*/b)$ is

$$\beta_2\left(\frac{b^*}{b}\right) = \beta_2(b^*) \sim 3 + \left(\frac{C_1}{N} + \frac{C_2}{N^2}\right)$$

where

$$C_1 = 21.924414 - \frac{102.464711}{c} + \frac{125.090738}{c^2}$$
$$C_2 = -242.161370 + \frac{995.457126}{c} - \frac{1025.128798}{c^2},$$

for values $1.1 \leq c \leq 3.2$ and $12 < N < 100$ with maximum errors less than 2%. For $c > 3.2$ the kurtosis β_2 is approximately 3.

7 Conclusion

The approximate distribution of a function of sample moments (m_1', m_2', m_3', m_4') using computer oriented extended Taylor series has been successful especially for moment ratios such as $\sqrt{b_1} = m_3/m_2^{3/2}$ and $b_2 = m_4/m_2^2$ (Shenton and Bowman, 1977; Bowman and Shenton, 1978, 1988b, 1989a). In general the series for the first four moments turn out to be divergent as far as can be judged from the pattern exhibited in the first 12 to 20 or so terms (in power of N^{-1}). In most cases the general term (N^{-s})

in the series can only be given by approximations such as $ck^s\Gamma(as+b)$, where a and b are at worst positive half-integers. The Padé approach is most likely to succeed if $a = \frac{1}{2}$, 1, $\frac{3}{2}$ or 2; for larger values of a the Padé Borel transformation (Bowman and Shenton, 1978, pp110-111; Shenton and Bowman, 1977) may be used.

Padé sequences point to a best assessment when successive terms in the sequences are nearly the same; it is possible for this to occur suggesting to a false assessment. Checks on the assessments, for the most part, rely on simulation studies and in the present study the reader is referred to Tables 3a and 3b. In addition we mention that since the 2 parameter case of b^* refers to the moments of $\sqrt{m_2/\mu_2}$ in sampling from a gamma density $cy^{c-1}e^{-y^c}$ with $c = 1$, we can compare the Weibull case with a segment of the study Bowman and Shenton (1990), which treats the Padé approximants to the moments of $\sqrt{m_2}$, $\sqrt{b_1}$, and b_2 for various values of the shape parameter and sample sizes $N = 10, 15, \cdots, 200$. The comparisons are given in Tables 4 and 5. The agreement is quite satisfactory. Note that the derivation of the moments in the two cases take different routes. For the gamma there is a recursion scheme for the rth central moment where-as the Weibull density uses the integral defined in equation (8).

A comprehensive account of Padé methods is given in Brezinskie (1980a) and the bibliography (1978, 1980b).

Table 4. Checks and Balances for moments of $E(\sqrt{m_2/\mu_2})$ and $\sigma(\sqrt{m_2/\mu_2})$

N		10	15	30	50	75	100
				$c = 1.1$			
μ_1'	Padé	0.8863	0.9222	0.9595	0.9752	0.9832	0.9873
	Eq(4)	0.8033	0.8832	0.9491	0.9713	0.9815	0.9863
σ	Padé	0.3362	0.2876	0.2147	0.1705	0.1411	0.1231
	Eq(5)	0.5197	0.3968	0.2577	0.1916	0.1529	0.1309
				$c = 2.0$			
μ_1'	Padé	0.9207	0.9474	0.9739	0.9843	0.9896	0.9922
	Eq(4)	0.9081	0.9417	0.9724	0.9838	0.9893	0.9920
σ	Padé	0.2288	0.1889	0.1351	0.1052	0.0861	0.0746
	Eq(5)	0.2763	0.2164	0.1455	0.1101	0.0888	0.0764
				$c = 4.0$			
μ_1'	Padé	0.9252	0.9508	0.9757	0.9855	0.9904	0.9928
	Eq(4)	0.9185	0.9477	0.9749	0.9852	0.9902	0.9927
σ	Padé	0.2100	0.1714	0.1210	0.0936	0.0764	0.0662
	Eq(5)	0.2386	0.1879	0.1272	0.0966	0.0780	0.0672

Table 5. Comparison of the Distribution of $\sqrt{m_2/\mu_2}$ from Weibull and gamma distribution

N		Mean	s.d.	$\sqrt{\beta_1}$	β_2
10	G Padé	0.8784	0.3639	1.12	5.25
	G MC	0.8754	0.3621	1.11	5.27
	W	0.8776	0.3634	1.128	5.293
20	G Padé	0.9334	0.2798	0.88	4.47
	G MC	0.9334	0.2792	0.87	4.47
	W	0.9338	0.2797	0.877	4.477
50	G Padé	0.9718	0.1887	0.63	3.82
	G MC	0.9711	0.1888	0.64	3.95
	W	0.9718	0.1887	0.625	3.818

W= Weibull distribution, G=Gamma distribution (Bowman and Shenton, 1990). For the Weibull distribution, $c = 1$, $a = 0$, and $b = 1$. For the gamma distribution, $\rho = 1$, $a = 1$, density $e^{-x/a}(x/a)^{\rho-1}/[a\Gamma(\rho)]$.

A Series and Continued Fractions: Stieltjes and Hardy

A.1 The Gamma Function and its Continued Fraction Component

The usual asymptotic series is

$$\ln\Gamma(z) \sim \left(z-\frac{1}{2}\right)\ln(z)-z+\frac{1}{2}\ln(2\pi)+\frac{1}{12z}-\frac{1}{360z^3}+\frac{1}{1260z^5}-\frac{1}{1680z^7}+\cdots \quad (|\arg\ z|<\pi). \tag{A1}$$

The general term in the series is

$$\frac{B_{2s}}{2s(2s-1)}\frac{1}{z^{2s-1}},$$

where B_s is a Bernoulli number and $B_0 = 1$, $B_1 = -1/2$, $B_2 = 1/6$, $B_4 = -1/30$, and for large s

$$\frac{2\cdot(2s)!}{(2\pi)^s}\left(\frac{1}{1-2^{1-2s}}\right) > (-1)^{s+1}B_{2s} > \frac{2(2s)!}{2\pi)^{2s}}.$$

(See Handbook of Mathematical Functions, 1967)

This series has intrigued many students. G.H. Hardy (1949) gave the expression

$$\log n! = \sum_1^n \log(m) = \left(n+\frac{1}{2}\right)\log(n)-n+C+\frac{B_1}{1\cdot 2n}-\frac{B_2}{3\cdot 4n^3}+\frac{B_3}{5\cdot 6n^5}-\cdots \tag{13.73}$$

with

$$C = 1-\frac{B_1}{1\cdot 2}+\frac{B_2}{3\cdot 4}-\frac{B_3}{5\cdot 6}+\frac{B_4}{7\cdot 8}-\cdots$$

Hardy remarks "The series are semi-convergent, and can be used to calculate $\log n!$ and C. We shall see later that $C = \frac{1}{2}\ln(2\pi)$.

We cannot calculate C with great accuracy from (13.73) because $n = 1$ is too small. The least term is that last written, which is 0.0054, and we can calculate

$C = .919\cdots$ to 3 places, by stopping there. This value of C, used in (13.73), would then give a fairly accurate value for $\ln n!$ for large n."

The coefficients in the series part of (A1), although decreasing in value initially, ultimately steadily increase in value to ∞. Nonetheless it can be proved for z real, and positive, that the magnitude of the error committed at a particular term in the series is less than the magnitude of the first term omitted. Actually,

$$\ln\Gamma(z) = \left(z - \frac{1}{2}\right)\ln(z) - z + \frac{1}{2}\ln(2\pi) + J(z)$$

where

$$\begin{aligned} J(z) &= \frac{1}{\pi}\int_0^\infty \ln\left(\frac{1}{1-e^{-2\pi\mu}}\right)\frac{z\,du}{z^2+\mu^2} \qquad (\Re(z) > 0) \\ &= \cfrac{1/12}{z + \cfrac{1/30}{z + \cfrac{53/280}{z + \cfrac{195/371}{z + \cfrac{2992/2273}{z + \cdots}}}}} \end{aligned}$$

as given by Wall (1948). The continued fraction was given by Stieltjes in a letter he sent to Hermite (1889). One may find it in 'Correspondence D'Hermite et de Stieltjes' (1905, pp348-352). We quote an excerpt which portrays Stieltjes as the ardent numerical fan.

> et cotte fraction continue remplace avec grand avantage la série de Stirling. Pour $x = 1$, $J(1) == 0,081061$.

La série.		La fraction continue.	
Val.app.	Corr	Val.app.	Corr
0,083 333	0,002 272	0,083 333	0,002 272
0,080 556	0,000 505	0,080 645	0,000 416
0,081 349	0,000 288	0,081 173	0,000 112
0,080 764	0,000 307	0,081 016	0,000 045
		0,081 081	0,000 020

> Si une fraction continue telle que(2) ou tous les a_i, b_i sont positifs est convergente pour $x = p > 0$, alors elle est toujours convergente tant que $x > 0$. Mais je dois réfléchir encore beaucoups sur la question diffieile que j'ai indiquée tout à l'heure. Votre tout dévoué.

A.2 Series to Continued Fractions

Stieltjes (1918) in his collected works (Vol II) on 'Sur une Applications des Fractions Continues' (p394) considers the series

$$c_0 - c_1 z + c_2 z^2 - c_3 z^3 + \cdots$$

and expresses it as the continued fraction

$$\frac{b_0}{1-}\,\frac{b_1 z}{1-}\,\frac{b_2 z}{1-}\,\frac{b_3 z}{1-\cdots} = \cfrac{b_0}{1-\cfrac{b_1 z}{1-\cfrac{b_2 z}{1-\cfrac{b_3 z}{1-\cfrac{b_4 z}{1-\cdots}}}}},$$

where

$$A_n = \begin{vmatrix} c_0 & c_1 & \cdots & c_{n-1} \\ c_1 & c_2 & \cdots & c_n \\ \cdots & \cdots & \cdots & \cdots \\ c_{n-1} & c_n & \cdots & c_{2n-2} \end{vmatrix},$$

$$B_n = \begin{vmatrix} c_1 & c_2 & \cdots & c_n \\ c_2 & c_3 & \cdots & c_{n+1} \\ \cdots & \cdots & \cdots & \cdots \\ c_n & c_{n+1} & \cdots & c_{2n-1} \end{vmatrix}, \quad (n = 1, 2, \cdots)$$

$$b_0 = A_1 = c_0, \quad A_0 = B_0 = 1,$$

$$b_{2n-1} = \frac{A_{n-1}}{A_n} \cdot \frac{B_n}{B_{n-1}}, \qquad b_{2n} = \frac{A_{n+1}}{A_n} \cdot \frac{B_{n-1}}{B_n}.$$

In connection with the problem of moments, Stieltjes preferred the form

$$\frac{1}{\alpha_0 z+}\,\frac{1}{\alpha_1+}\,\frac{1}{\alpha_2 z+}\,\frac{1}{\alpha_3+}\,\frac{1}{\alpha_4 z+\cdots}$$

in which $\alpha_0, \alpha_1, \cdots > 0$ and $\sum \alpha = \infty$ for the moment problem to have a unique solution (see Shohat and Tamarkin, 1948). The moment problem referred to here is a mechanical problem and at the time had little to do with statistics or probability.

In the application to the series for the random variate b^*/b the form preferred is

$$N\left(\frac{q_0}{N+}\,\frac{p_1}{1+}\,\frac{q_1}{N+}\,\frac{p_2}{1+}\,\frac{q_2}{N+\cdots}\right).$$

For this case N is a sample size and positive; if in addition q_0, p_1, $q_1, \cdots$ are positive, then the odd convergents form a decreasing set of upper bounds, where-as the even convergents form a set of increasing lower bounds; if there is convergence these limiting bounds will be equal. However, this theoretical case rarely happens in practice. In general the partial numerators are of a much lower order of magnitude than the series coefficients, and it is this characteristic which makes the approach useful and powerful. Note:

- Series may be truncated in an orderly pattern and continued fractions set up for the truncated components.
- Similarly, the same holds for the inverted series.
- The above constitute the Padé table of approximation sequences.

A.3 The Baker-Gammel Conjecture

There is an interesting conjecture given in Baker (1975). It is called the Baker-Gammel-Wills-conjecture (1961). Briefly, under certain conditions for a regular power series, there is a sequence of approximants in the Padé table which converges (Baker, pp188-189). There are other possibilities. For example, there is the surprising formula

$$\frac{(n-1)\Gamma(\frac{1}{2}n)}{\sqrt{2n}\Gamma(\frac{1}{2}n+\frac{1}{2})} = \left(1-\frac{1}{n}\right)\sqrt{1+\frac{2}{4n-1+}\,\frac{1}{\frac{4n}{3}+}\,\frac{1}{\frac{4n}{5}+}\,\frac{1}{\frac{4n}{7}+\cdots}} \quad (n>0),$$

and in fact the left hand side is $E(\sqrt{m_2})$ for the normal density $N(0,1)$ when $n = 1, 2, 3, \cdots$.

There are further examples which do not seem to fit into the Padé scheme. For example (Rogers, 1907a, 1907b) gives

$$\exp\left(\int_0^\infty \frac{\sinh t}{t} e^{-t/x} dt\right) = \frac{1}{1-x+}\,\frac{x^2}{2(1-x)+}\,\frac{3x^2}{2(1-x)+\cdots}$$

$$\exp\left[\int_0^\infty \left(1-\frac{\cosh 2at}{\cosh 2t}\right)\right]\frac{e^{-t/x}}{t}dt = 1+\frac{2(1-a^2)x^2}{1+}\,\frac{(3^2-a^2)x^2}{1+}\,\frac{(5^2-a^2)x^2}{1+\cdot}$$

(see Rogers 1907a and 1907b; also Bowman and Shenton, 1989, p157).

Applications of continued fractions in physics are many; see 'The Padé Approximation and its Physical applications' by J.L. Basdevant (1971).

For computer extensions of series in applied mathematics there are interesting examples and comments in Van Dyke (1975). He quotes the case of the 19th century French astronomer Delaunay who spent a lifetime in extending a series in five variables up to and including the ninth order.

Further information on the Padé table is given in Brezinski (1980), which includes programs for various algorithms related to continued fractions. A useful algorithm is also given in Wall (1948, Chapter IX). A classical treatise on continued fractions is given in Oskar Perron (1957).

BIBLIOGRAPHY

Abramowitz, M and Stegam, I.A. (1967), *Handbook of Mathematical Functions with Formulas, Graphs, and Mathematical Tables*, National Bureau of Standards Applied Mathematical Series 55.

Baker, G.A.Jr (1975), *Essentials of Padé Approximants*, Academic Press, New York.

Baker, G.A.Jr, Gammel, J.L. and Willis, J.G. (1961), An Investigation of the Applicability of the Padé Approximants Method, *J. Math. Anal. Appl.*, 2, 405-418.

Baker, G.A.Jr and Graves-Morris, P.R. (1981), *Padé Approximants: Part i, Basic Theory, Part ii: Extensions and Applications*, Addison-Wesley.

Baker, G.A.Jr and Hunter, D.L. (1973), Methods of Series Analysis II. Generalized and Extended Methods with Application to the Ising Model, *Physical Review B*, 7(7), 3377-3392.

Basdevant, J.L. (1971), The Padé Approximation and its Physical Application, TH. 1441-CERN, 17 December. (Article was to be published in *Fortschritte der Physik.*

Bender, C.M. and Wu, T.T. (1969), Anharmonic Oscillator, *Physical Review*, 184(5), 1231-1260.

Borel, Émile. (1928), *Lecons sur les Séries Divergntes*, Gauthier-Villars, Paris. (Translated by Charles L. Critchfield and Anna Vaker (1975), Los Alamos Scientific Laboratory.

Bowman, K.O. and Shenton, L.R. (1975) *Tables of Moments of the Skewness and Kurtosis Statistics in Nonnormal Sampling*, UCCND-CSD-8, Oak Ridge National Laboratory.

Bowman, K.O. and Shenton, L.R. (1978), Asymptotic Series and Stieltjes Continued Fractions for a Gamma Function Ratio, *Journal of Computation and Applied Mathematics*, 4, 105-111.

Bowman, K.O. and Shenton, L.R. (1979a), Approximate Percentage Points for Pearson Distributions, *Biometrika*, 66, 147-151.

Bowman, K.O. and Shenton, L.R. (1979b), Further Approximate Pearson Percentage Points and Cornish-Fisher, *Comm. Stat. Simula. Computa.*, B(8), 231-244.

Bowman, K.O. and Shenton, L.R. (1980), Evaluation of the Parameters of S_U by Rational Fractions, *Comm. Stat. Part B, Simulation and Computation*, B(9), 127-132.

Bowman, K.O., Serbin, C.A. and Shenton, L.R. (1981), Explicit Approximate Solutions for S_B, *Comm. Stat. Part B, Simulation and Computation*, B(10), 1-15.

Bowman, K.O. and Shenton, L.R. (1988a), Solutions to Johnson's S_B and S_U, *Commun. Statist. -Simula. Computa.*, 17(2), 343-348.

Bowman, K.O. and Shenton, L.R. (1988b), *Properties of Estimators for the Gamma Distribution*, Marcel Dekker, Inc.

Bowman, K.O. and Shenton, L.R. (1989a), *Continued Fractions in Statistical Applications*, Marcel Dekker, Inc.

Bowman, K.O. and Shenton, L.R. (1989b), S_B and S_U Distributions fitted by Percentiles: A General Criterion, *Commun. Statist. -Simula. Computa.*, 18(1), 1-13.

Bowman, K.O. and Shenton, L. R. (1990). The Approximate Distribution of Four Moment Statistics from Type III Distributions, *Commun. Statist. Theory & Methods*, 19(4), 1511-1579.

Bowman, K.O. and Shenton, L.R. (1992), Parameter Estimation for the Beta Distribution, *Journal of Statistical Computation and Simulation*, 43, 217-228.

Bowman, K.O. and Shenton, L. R. (1998). Asymptotic Skewness and the Distribution of Maximum Likelihood Estimators, *Commun. Statist. Theory and Method*, 27(11), 2743-2760.

Bowman, K.O. and Shenton, L. R. (1999a). The Asymptotic Kurtosis for Maximum Likelihood Estimators, *Commun. Statist. Theory and Method*, 28(11).

Bowman, K.O. and Shenton, L. R. (1999b). Asymptotic Profile for Moments of Maximum Likelihood Estimators and the Weibull Densities, *Commun. Statist. Theory and Method*, (submitted)

Bowman, K.O. and Williams, P.T. (1999), *Technical Basis for Statistical Models of Extended K_{ic} and K_{Ia} Fracture Toughness Databases for RPV Steels*, ORNL/NRC/LTR-99/27, Oak Ridge National Laboratory.

Brezinski, C (1978), *A Bibliography on Padé Approximation and Related Subjects, Addendum 1.*

Brezinski, C (1980a), *A Bibliography on Padé Approximation and Related Subjects, Addendum 2.*

Brezinski, C (1980b), *Padé Type Approximation and General Orthogonal Polynomials*, Birkhäuser Verlag.

David, F.N., Kendall, M.G. and Barton, D.E. (1966), *Symmetric Functions and Allied Tables*, Cambridge University Press, London, England.

Elderton, W.P. and Johnson, N.L. (1969), *System of Frequency Curves*, Cambridge University Press, London, England.

Gaunt,D.S. and Guttman, A.J. (1973), Series Expansions: Analysis of Coefficients, Chapter in Phase Transitions and Critical Phenomena, 3, C. Domb and M.S. Green, Eds., Academic Press, New York and London.

Hardy, G.H. (1949), *Divergent Series*, Oxford, at the Clarendon Press.

Johnson, N.L. (1949), Systems of frequency curves generated by methods of translation, *Biometrika*, 36, 149-176.

Kotz, S., Johnson, N.L. and Read, C.B. (1988) *Encyclopedia of Statistical Sciences, Vol 9*, John Wiley & Sons, New York. (by C.E. Antle and L.J. Bain)

MacMahon, P.A. (1960), *Combinatory Analysis*, Chelsea, New York.

Perron, O (1957), *Die Lehre von den Kettenbrüchen*, Teubner, Stuttgart.

Rogers, L.J. (1907a), On the Representation of Certain Asymptotic Series as Continued Fractions, *Proc. Lnd. Math. Soc.*, 4(2), 393-395.

Rogers, L.J. (1907b), Supplementary Note on the Representation of Certain Asymptotic Series as Continued Fractions, *Proc. Lnd. Math. Soc.*, 4(2), 393-395.

Shenton, L.R. and Bowman, K.O. (1970), Tables of the Moments of the Maximum Likelihood Estimators of the Two Parameter Gamma Distribution, *Rep. Statist. Appl. Res., JUSE*, 17(3), 25-44.

Shenton, L.R. and Bowman, K.O. (1967), Remarks on Large Sample Estimators for Some Discrete Distributions, *Technometrics*, 9(4), 587-598.

Shenton, L.R. and Bowman, K.O. (1975), The Development of Techniques for the Evaluation of Sampling Moments, *Internat. Statist. Rev.*, 43(3), 317-334.

Shenton, L.R. and Bowman, K.O. (1977), A New Algorithm for Summing Divergent Series Part III: Application, *Journal of Computation and Applied Mathematics*, 3, 35-51.

Shenton, L.R., Bowman, K.O. and Sheehan, D. (1971), Sampling Moments of Moments Associated with Univariate Distributions, *JRSS Ser. B*, 33, 444-457.

Shohat, J.A. and Tamarkin, J.D.(1943), *The Problem of Moments.* American Mathematical Society, New York.

Stieltjes, T.J. (1905), *Correspondence D'Hermite et de Stieltjes*, Gauthier-Villars, Paris.

Stieltjes, T.J. (1918), *Oeuvres Complétes*, Tome 2, P. Noordhoff, Groningen.

Tchouproff, A.A. (1918), On the Mathematical Expectation of the Moments of Frequency Distributions. *Biometrika*, XII, 140-169.

Tchouproff, A.A. (1919), On the Mathematical Expectation of the Moments of Frequency Distributions. *Biometrika*, XII, 185-210.

VanDyke, M (1975), Computer Extension of Perturbation Series in Fluid Mechanics, *SIAM. J. Appl. Math.*, 28(3), 720-734.

Wall, H.S. (1948), *Analytic Theory of Continued Fractions*, Chelsea Publishing Company, Bronx, New York.

Internal Distribution

1-5 B. R. Bass
6-10 K. O. Bowman
11 W. G. Craddick
12 K. W. Childs
13 T. L. Dickson
14 D. M. Hetrick
15 S. K. Iskander
16 W. J. McAfee
17 P. W. McGrady
18 R. K. Nanstad
19-20 C. E. Pugh
21 J. J. Simpson
22 M. A. Sokolov
23-27 P. T. Williams
28 D. A. Wolf
29 Laboratory Records

External Distribution

30 W. H. Bateman, NRR, U.S. Nuclear Regulatory Commission, MS O7 D4, Washington, D.C. 20555-0001
31 R. H. Dodds, 3140 Newmark Laboratory, 205 North Matthews, Urbana, IL 61801
32 C. J. Fairbanks, RES/DET/MEB, U.S. Nuclear Regulatory Commission, MS T-10 E10, Washington, D.C. 20555-0001
33 E. M. Hackett, RES/DET/MEB, U.S. Nuclear Regulatory Commission, MS T-10 E10, Washington, D.C. 20555-0001
34 J. A. Joyce, U.S. Naval Academy, Mechanical Engineering Department, MS 11C, 590 Hollway Road, Annapolis, MD 21402
35-39 M. T. Kirk, RES/DET/MEB, U.S. Nuclear Regulatory Commission, MS T-10 E10, Washington, D.C. 20555-0001
40 R. E. Link, U.S. Naval Academy, Mechanical Engineering Department, MS 11C, 590 Hollway Road, Annapolis, MD 21402
41-42 S. N. Malik, RES/DET/MEB, U.S. Nuclear Regulatory Commission, MS T-10 E10, Washington, D.C. 20555-0001
43 M. E. Mayfield, RES/DET, U.S. Nuclear Regulatory Commission, MS T-10 E10, Washington, D.C. 20555-0001
44 M. A. Mitchell, NRR, U.S. Nuclear Regulatory Commission, MS O7 D4, Washington, D.C. 20555-0001
45 M. Modarres, University of Maryland, Center for Reliability Engineering, College Park, MD 20742
46 A. Mosleh, Materials and Nuclear Engineering Dept., University of Maryland, 2100A Marie Mount Hall, College Park, MD 20742-7531
47 M. E. Natishan, Materials Characterization Laboratory, A. J. Clarke School of Engineering, University of Maryland, College Park, MD 20742
48 C. G. Santos, RES/DET/MEB, U.S. Nuclear Regulatory Commission, MS T-10 E10, Washington, D.C. 20555-0001
49 R. L. Tregoning, Fatigue and Fracture Branch, Carderock Division, Naval Surface Warfare Center, 9500 McArthur Blvd., West Bethesda, MD 20817-5700
50 K. R. Wichman, NRR, U.S. Nuclear Regulatory Commission, MS O7 D4, Washington, D.C. .20555-0001